Microtubule-depolymerizing Agents Potentiate Anti-tumor Immunity by Stimulation of Dendritic Cells

Inauguraldissertation

zur
Erlangung der Würde eines Doktors der Philosophie
vorgelegt der
Philosophisch-Naturwissenschaftlichen Fakultät
der Universität Basel

von

Kea Simone Martin

aus Istein, Deutschland

Basel, 2015

Genehmigt von der Philosophisch-Naturwissenschaftlichen Fakultät

auf Antrag von

Dissertationsleiter:	Prof. Dr. Alfred Zippelius
Fakultätsvertreter:	Prof. Dr. Jean Pieters
Korreferent:	Prof. Dr. Daniela Finke

Basel, den 23.06.2015

Prof. Dr. Jörg Schibler (Dekan)

This PhD-Thesis was conducted under the supervision of Prof. Dr. Alfred Zippelius from January 2012 until July 2015 at the University Hospital Basel, Department of Biomedicine, Laboratory of Cancer immunology, Basel, Switzerland.

Parts of this thesis have been submitted, published, and presented at national and international congresses.

Peer-reviewed articles:

Müller, Kreuzaler, Khan, **Martin**, Glatz, Savic, Harbeck, Kreipe, Reddy, Christgen, Zippelius. "T-DM1 reinstates anti-tumor immunity in HER2-positive breast cancer". *Sci Transl Med.* **2015** Nov 25;7(315):315

Martin*, Schreiner*, Zippelius. "Modulation of APC function and anti-tumor immunity by anti-cancer drugs". *Front. Immunol.* **2015** Sep 29;6:501

Martin*, Müller* *et al.* "Microtubule-depolymerizing agents used in antibody-drug conjugates induce antitumor immunity by stimulation of dendritic cells". *Cancer Immunol Res.* **2014** Aug; 2(8): 741.

Martin*, Müller* *et al.* "The microtubule-depolymerizing agent ansamitocin P3 programs dendritic cells toward enhanced anti-tumor immunity". *Cancer Immunol Immunother*. **2014** Sep; 63(9): 925.

Müller, **Martin**, Theurich, von Bergwelt-Baildon, Zippelius. "Cancer chemotherapy targets intratumoral dendritic cells to potentiate anti-tumor immunity". *OncoImmunology*, **2014** Aug 3;3(8):e954460

* Authors contributed equally

Conference presentations (oral and poster):

Martin *et al.* "Microtubule-depolymerizing agents used in antibody-drug-conjugates induce anti-tumor immunity by stimulation of dendritic cells". *Immunotherapy of Cancer Conference*, München, **2014**

Martin *et al.* "Stimulation of dendritic cells significantly contributes to the anti-cancer effect of dolastatin derivatives". *World Immune Regulation Meeting – VII*, Davos, **2013**

Martin *et al.* "Stimulation of dendritic cells significantly contributes to the anti-cancer effect of dolastatin derivatives". *European Cancer Center*, Freiburg, **2012**

Contents

1 Summary

Dendritic cells (DC) are unique players in the initiation and regulation of anti-tumor immune responses. Yet, the immunosuppressive tumor microenvironment may hamper the maturation stage and antigen-processing capacity of tumor-residing DCs. Thus, in an optimal setting, anti-cancer drugs have the power to reduce tumor size and, at the same time, modulate DC function towards efficient priming of antigen-specific effector T cells. With this in mind, we screened a small library of classical chemotherapeutics with distinct pharmacological mechanisms for their DC-stimulatory potential. As a result we discovered a previously unrecognized immunostimulatory profile of microtubule-destabilizing agents (MDAs), including dolastatins and maytansines, which so far have been described exclusively for their tumor cell cytotoxicity. Intriguingly, distinct compounds of this class potently provoked phenotypic and functional maturation of murine as well as human dendritic cells, resulting in an enhanced capacity to prime naïve T cells. Local administration of MDAs triggered *in situ* maturation of skin Langerhans cells and efficiently promoted antigen uptake and migration of tumor-resident DCs to tumor-draining lymph nodes in murine tumor models.

Underlining the requirement of an intact host immune system for the full therapeutic benefit of specific MDAs, the antitumor effect was far less pronounced in immunocompromised mice. Moreover, substantial therapeutic synergies were observed when combining MDAs with immunotherapy such as tumor-antigen-specific vaccination or blockade of the cytotoxic T-lymphocyte antigen 4 (CTLA-4) or programmed cell death ligand 1 (PD-L1) co-inhibitory pathways. Of note, combined T cell checkpoint inhibition and MDA treatment resulted in an increased intratumoral effector T cell to regulatory T cell ratio that is associated with beneficial prognosis in multiple tumor entities. Importantly, synthetic analogues of dolastatins and maytansines are currently used as cytotoxic payloads of the two recently approved antibody-drug conjugates (ADC) brentuximab vedotin and trastuzumab-emtansine (T-DM1), respectively. Treatment with ADCs coupled to microtubule-destabilizing agents induced DC homing in murine models and activated cellular antitumor immune responses in patients, thereby demonstrating the immune-modulating potential of these ADCs.

Ultimately, these data shed light on the MDA-triggered molecular pathways that, when activated in DCs, result in inflammatory responses. We here propose that MDA-mediated microtubule disassembly triggers the release of the microtubule-associated nucleotide exchange factor GEF-H1 from its cytoskeletal anchor. Subsequent induction the small GTPase RhoA results in activation of mitogen-activated protein kinases (MAPKs) including the c-Jun N terminal kinases (JNK). Phenotypic and functional DC maturation is then mediated by JNK-dependent phosphorylation of the transcription factor c-Jun, leading to activator protein -1 (AP-1) target gene expression.

Hence, by providing the molecular basis that links microtubule disruption with triggering of innate immune responses that translate into adaptive anti-tumor immunity, we reveal a novel mechanism of action for MDAs and provide a strong rationale for clinical treatment regimens combining MDA-based therapies with immune-based therapies.

2 Graphical Abstract

Microtubule-depolymerizing agents potentiate anti-tumor immunity by stimulation of dendritic cells

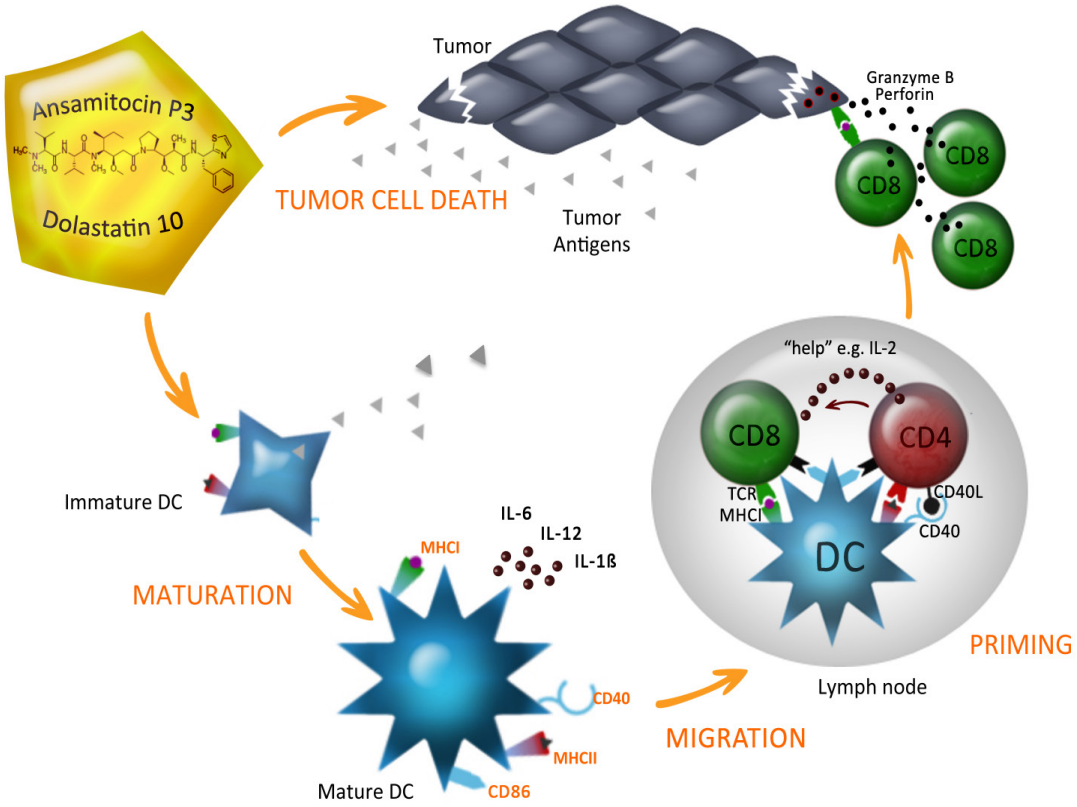

The cytotoxic compounds dolastatin 10 and ansamitocin P_3 do not only induce tumor cell death and subsequent antigen release from dying cancer cells but are capable of directly promoting dendritic cell differentiation and maturation. Tumor-derived antigens are taken up by immature DCs at the tumor site that, upon MDA-induced maturation, up-regulate costimulatory molecules such as the B7 family members CD80 and CD86, as well as CD_{40} and MHC molecules. Upon migration to the tumor-draining lymph nodes (LNs) these antigen-loaded DCs prime antigen-specific CD_4^+ and $CD8^+$ T cells. Ultimately, expanded and activated T cells infiltrate the lesion where they recognize and attack antigen-expressing cancer cells.

3 Abbreviations

A	
ADC	Antibody-Drug-Conjugate
ADCC	Antibody-dependent Cellular Cytotoxicity
ADCP	Antibody-dependent Cellular Phagocytosis
AIDS	Acquired Immune Deficiency Syndrome
AIM2	Absent in Melanoma2
ALCL	Anaplastic Large Cell Lymphoma
ALL	Acute Lymphocytic Leukemia
ALR	AIM2-like Receptor
AP-1	Activator Protein 1
APC	Antigen-presenting Cells
APC	Allophycocyanin
ASC	Apoptosis-associated Speck-like Protein Containing a CARD
ASK1	Apoptosis Signal-regulating Kinase1
ATP	Adenosin Triphosphat

B	
BCA	Bicinchoninic Acid
BCG	Bacillus Calmette–Guerin
Bcl	B-cell lymphoma/leukemia-10
BDCA	Blood Dendritic Cell Antigen
BiTe	Bi-specific T cell Engager
BMDC	Bone Marrow-derived Dendritic Cell
BSA	Bovine Serum Albumin
BTLA-4	B- and T-lymphocyte Attenuator 4

C	
CAR	Chimeric Antigen Receptors
CARD	Caspase Recruitment Domain
CARDIAK	CARD-containing ICE Associated Kinase
CCR	C-C chemokine receptor
CD	Cluster of Diffrentiation
CDC	Complement Dependent Cytotoxicity
cIAP	Cellular Inhibitor of Apoptosis Protein
CHOP	CCAAT/-enhancer-binding Protein Homologous protein
CLA	Cutaneous Lymphocyte-associated Antigen
CLL	Chronic Lymphocytic Leukemia
CLR	C-type Lectin Receptor
COX	Cyclooxigenase
CpG DNA	DNA containing unmethylated CpG motifs
CR	Complement Receptor
CRT	Calreticulin
C/T Antigen	Cancer/Testis Antigen
CTL	Cytotoxic T-Lymphocyte
CTLA-4	Cytotoxic T-lymphocyte Antigen 4
CTLD	C-type Lectin Domain

D	
DAMP	Damage-associated Molecular Pattern Molecules
DC	Dendritic Cell
DMEM	Dulbecco's Modified Eagle's Medium
DMXAA	5,6-Dimethylxanthenone-4-acetic Acid
DNA	Deoxyribonucleic Acid
DSMO	Dimethylsulfoxid

E	
EDTA	Ethylendiamin-tetraacetatic Acid
EGTA	Ethyleneglycol-tetraacetic Acid
ELISA	Enzyme-linked Immunosorbent Assay
EpCAM	Ephitelial Cell Adhesion Molecule
ER	Endoplasmatic Reticulum
ERK	Extracellular Signal-regulated Kinases
ES	Embryonic Stem Cell

F	
FACS	Fluorescence Activated Cell Sorting
FAP	Fibroblast Activation Protein
Fc	Fragment, crystallizable
FCM	Flow Cytometry
FCS	Fetal Calf Serum
FDA	Food and Drug Administration
FITC	Fluorescein-Isothiocyanat
FoxP3	Forkhead box P3
FSC	Forward Scatter
5-FU	5-Fluorouracil

G	
Gr-1	Gamma Response 1
GTP	Guanosin Triphosphate
Gp	Glycoprotein

GEF-H1	Guanine Nucleotide Exchange Factor H1
GITR	Glucocorticoid-induced TNFR Family Related Gene
GM-CSF	Granulocyte Macrophage Colony-stimulating Factor

H

H&E	Hematoxylin and Eosin
HEPES	4-(2-Hydroxyethyl)-1-piperazinethansulfonsäure
HER2	Human Epidermal Growth Factor Receptor 2
HeLa	Henrietta Lacks (Tumor Cell Line; Donor)
HL	Hodgkin Lymphoma
HLA-DR	Human Leukocyte Antigen (subunit combination DR)
HMGB1	High-mobility Group Box1
HS	Human Serum
Hsp	Heat Shock Protein

I

ICD	Immunogenic Cell Death
IDO	Indoleamine2,3-dioxygenase
Ig	Immunoglobulin
IF	Immunofluorescence
IFN	Interferon
IHC	Immunohistochemistry
IKK	IκB Kinase
IMDM	Iscove's Modified Dulbecco's Medium
i-NOS	Inducible Nitric Oxide Synthase
IL	Interleukin
IPC	Interferon Producing Cells
IPS1	Interferon-β Promoter Stimulator 1 (MAVS)
IRAK	Interleukin-1 Receptor-Associated Kinases
IRF	Interferon-regulatory Factor

J

JNK	c-Jun N-Terminal Kinases

K

kDA	Kilodalton
Ko	Knockout

L

LAG-3	Lymphocyte-Activation Gene 3
LC	Langerhans Cell
L/D	Live/Dead (stain)
3LL	Lewis Lung Carcinoma
LN	Lymph Node
LPS	Lipopolysaccharide
LRR	Leucin-rich Repeat
LT	Lymphoid Tissue
Ly6C	lymphocyte Antigen 6C

M

mAB	Monoclonal Antibody
MACS	Magnetic-Activated Cell Sorting
MAGE	Human Melanoma Antigen
Mal	MyD88-adapter-like
MALT-1	Mucosa-associated Lymphoid Tissue Lymphoma Translocation Protein-1
MAM	Mitochondrial-associated ER Membranes
MAPK	Mitogen-activated Protein Kinase
MAP2K	Mitogen-activated Protein Kinase Kinases
MAP3K	Mitogen-activated Protein Kinase Kinase Kinases
MART-1	Melanoma Antigen Recognized by T cells
MAVS	Mitochondrial Antiviral Signaling Protein (IPS-1)
MCA	3-Methylcholanthrene
MDA-5	Melanoma Differentiation-associated Gene-5
M-CSF	Macrophage colony-stimulating factor
MDA	Microtubule-depolymerizing agent
MDSC	Myeloid-derived suppressor cell
MDP	Muramyl Dipeptide
MFI	Mean Fluorescence Intensity
MHC	Major Histocompatibility Complex
MICA/B	MHC Class I Chain-related Genes
MIIC	MHC Class II-rich Compartments
MIP	Macrophage Inflammatory Protein
MLK	Mixed-Lineage Kinase
MMAE	Monomethylauristatin E
moDC	monocyte-derived dendritic cell
MT	Microtubule
MTOC	Microtubule-organizing Center
MWCO	Molecular Weight Cut Off
MyD88	Myeloid differentiation primary response 88

N

NACHT	Neuronal Apoptosis Inhibitor Protein (NAIP)
$NaHCO_3$	Sodium Hydrogen Carbonate

NALP3	NACHT, LRR and PYD domains-containing protein3
NCI	National Cancer Institute
NEMO	NF-κB Essential Modulator
NFAT	Nuclear Factor of Activated T cells
NF-κB	Nuclear Factor κ-light-chain-enhancer of activated B cells
NHL	Non-Hodgkin Lymphoma
NK cell	Natural Killer Cell
NKG2D	Killer cell lectin-like receptor subfamily K, member 1
NKT cell	Natural Killer T Cell
NLR	NOD-like receptor
NLT	Non-lymphoid Tissue
NOD	Nucleotide-binding Oligomerization Domain

O

OD	Optic Density
OVA	Ovalbumin

P

PAMP	Pathogen-associated Molecular Patterns
PAP	Prostatic Acid Phosphatase
PBS	Phosphat Buffered Saline
PBMC	Peripheral Blood Mononuclear Cell
PCR	Polymerase Chain Reaction
pDC	Plasmacytoid Dendritic Cell
PD-1	Programmed Cell Death 1
PD-L1	Programmed Cell Death- Ligand 1
PDGF	Platelet-derived Growth Factor
PE	Phycoerythrin
PET-CT	Positron emission tomography–computed tomography
Pfu	Plaque-forming unit
PGE_2	Prostaglandin E_2
PI	Propidiumiodid
PMSF	Phenylmethanesulfonyl-Fluoride
PMT	Post-translational Modifications
Poly I:C	Polyinosinic:polycytidylic Acid
PPR	Pattern-recognition Receptors
PYD	Pyrin Domain

Q

qPCR	Quantitative Real Time PCR

R

RAE-1	Retinoic Acid Early Transcript-1
RAG2	Recombination Activation Gene 2
RhoA	Ras homolog gene family, member A
RIG-I	Retinoic Acid-inducible Gene 1
RLR	RIG-I-like Receptor
RICK	RIP-like Interacting CLARP Kinase
RIP2	Receptor-interacting protein 2
RIPA	Radioimmunoprecipitation Assay
RNA	Ribonucleic Acid
ROCK	RhoA-associated Kinase
ROS	Reactive Oxygen Species
rpm	Revolutions per Minute
RPMI	Roswell Park Memorial Institute
RT	Room Temperature

S

SAPK	Stress-activated Protein Kinase
scFv	Single Chain Variable Fragments
SDS	Sodium Dodecyl Sulfate
Ser	Serine
Siglec	Sialic-Acid Binding Immunoglobulin-like Lectin
SLC	Secondary Lymphoid-Tissue Chemokine
SMOC	Supramolecular Organizing Centers
SSC	Side Scatter
STAT	Signal Transducers and Activators of Transcription
STING	Stimulator of Interferon Genes

T

TAA	Tumor-Associated Antigen
Tab.	Table
TAK1	Transforming Growth Factor β-activated Kinase1
TBK1	Tank-binding Kinase 1
TCR	T Cell Receptor
Teff	Effector T cell
TGF	Transforming Growth Factor
T_H	T Helper Cell
Thy1.1	Thymocyte Antigen 1.1
TIL	Tumor-infiltrating Lymphocytes
Tim-3	T cell Immunoglobulin Mucin-3
TIRAP	Toll-interleukin-1 receptor (TIR) domain containing adaptor protein
TLR	Toll-like Receptor
Tlp2	Tumor Progression Locus2
TRAF	TNF receptor Associated Factors
TRAIL	TNF-related Apoptosis-inducing Ligand
TRAM	TRIF-related adaptor molecule

TRANCE	TNF-related Activation-induced Cytokine
Treg	Regulatory T cell
TRIF	TIR-domain-containing adapter-inducing interferon-β
TRIS	Tris(hydroxymethyl)-aminomethane
TRUCK	T cells Redirected for Universal Cytokine-mediated Killing
TSA	Tumor-specific Antigen
Tyr/Thr	Tyrosine/Threonine
V	
VBL	Vinblastine
VEGF	Vascular Endothelial Growth Factor
W	
WT	Wild Type

4 Introduction

4.1 Cancer Immunology

The immune system protects its host from pathogens by adequately differentiating between "self" and "non-self" antigenic structures. To this end, innate pattern recognition and genetic recombination of lymphocytic antigen receptors enable recognition of an immense diversity of foreign antigens, while appropriate regulation of immunity ensures tolerance to normal tissues. Cancer cells pose a challenge to the immune system by being pathogenic, but "self". Nevertheless, genetic instability of cancer cells such as mutations, translocations, or other genetic abnormalities lead to expression of neo- or tumor-associated antigens, which may be recognized as "altered self" and therefore initiate an anti-tumor immune response [1, 2]. An increasing understanding of naturally occurring anti-tumor immune responses as well as of the mechanisms employed by tumors to suppress immunity have led to the development of various successful immunotherapy approaches during the last decades [3]. Currently, the most commonly accepted view on the interaction of the immune system and tumors are described by the concepts of *Cancer Immunosurveillance* and *Cancer Immunoediting* [4].

4.1.1 Concept of Immunosurveillance & Immunoediting

Cancer immunotherapy aims at using the body's own protective mechanisms to actively fight emerging neoplastic cells. In 1909 Paul Ehrlich already stated that there must be mechanisms by which the immune system is able to protect the host against primary tumors, as if not, they would occur at much higher frequency. Therefore, tumors must express antigens that distinguish them from normal cells [5]. And indeed, with the first demonstration of tumor antigens, fifty years later the idea of the immune system controlling cancer outgrowth emerged again. Hence, in the 1960s Burnet and Thomas defined the concept of *Immunosurveillance* as the ability of the immune system to recognize and destroy tumor cells [6-8]. Meanwhile, various tumor antigens have been identified, with them often being products of mutated genes, aberrantly expressed normal genes, or genes encoding viral proteins. Human tumor antigens include differentiation antigens (e.g., melanocyte differentiation antigens MelanA/melanoma antigen recognized by T cells (MART)-1, tyrosinase and gp-100), mutational antigens (e.g., abnormal forms p53), overexpressed cellular antigens (e.g., survivin, telomerase, or human epidermal growth factor receptor 2 (HER2)/neu), viral antigens (e.g., human papillomavirus proteins), and cancer/testis (CT) antigens (e.g., Human Melanoma Antigen (MAGE) and NY-ESO1) [1, 9]. Further evidence for the hypothesis of *Immunosurveillance* appeared years later with the generation of the first molecularly defined immunodeficient mouse models. These models were generated, for example, by deletion of the recombination activation gene 2 (RAG2), which leads to a deficiency in peripheral αβ T cells, B cells, Natural Killer T (NKT) cells and γδ T cells [10, 11]. Using $RAG2^{-/-}$ mice, Shankaran and colleagues were able to demonstrate for the first time that tumors induced by the carcinogen 3-methylcholanthrene

(MCA) occurred at higher frequency in immunodeficient mice when compared to strain-matched WT mice [10].

The relationship between tumor and immune system, however, is considered to be much more complex as initially believed, which is why, over the last decades the concept has been extended. The so-called *Immunoediting* hypothesis takes into account that the immune system not only protects the host from developing tumors, but also shapes tumor immunogenicity. It describes a tumor-immune-system-interaction that consists of three phases, namely *Elimination*, *Equilibrium* and *Escape* (Figure 4-1) [4, 12].

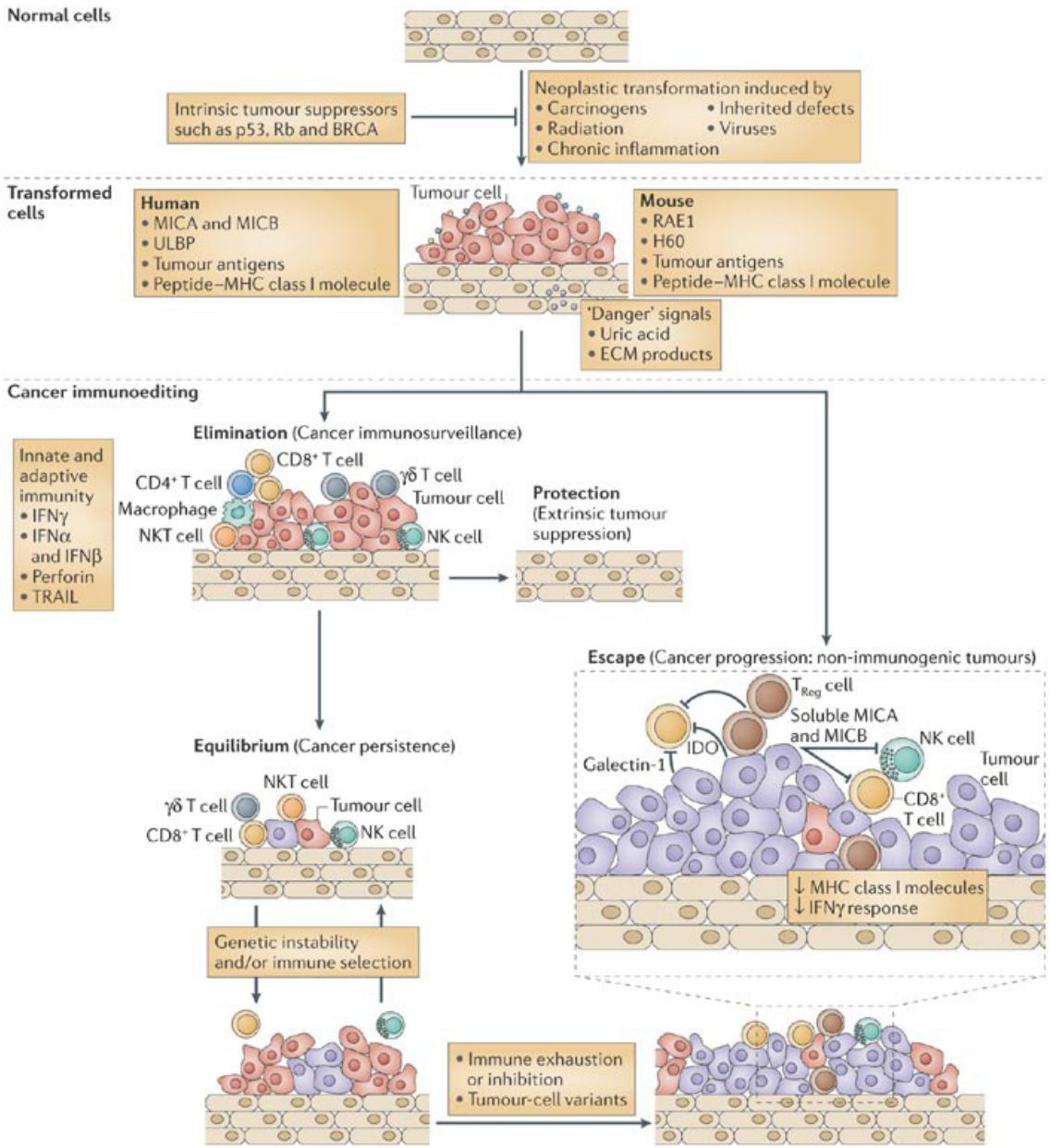

Figure 4-1 ***The Cancer Immunoediting concept.*** In case of transformation of normal tissue cells and failure of intrinsic tumor suppressor mechanisms, a clinically detectable tumor may grow out. The immune system may either eliminate a developing tumor (Elimination phase) or, if elimination is incomplete, maintain it in a dormant or equilibrium state (Equilibrium phase). Constant immunosurveillance in combination with genetic instability of tumor cells, however, may promote tumor cell variants with low immunogenicity. These may elaborate additional immunosuppressive molecules and cells and ultimately escape from the extrinsic tumor suppressor actions of immunity (Escape phase). Adapted from Dunn GP. Interferons, immunity and cancer immunoediting. Reprinted with permission from Nature Publishing Group © 2006 [12].

4.1.1.1 Elimination

During the initial elimination, or *immunosurveillance* phase the immune system is able to recognize and destroy an emerging tumor before it becomes clinically visible. $CD4^+$ and $CD8^+$ effector T cells activated and expanded by recognition of relevant tumor antigens are primarily required to mount an effective

immunosurveillance response [4, 10, 13]. But nevertheless, both innate and adaptive immunity act in concert to promote the elimination process and together with $CD4^+$ and $CD8^+$ T cells, NK and NKT cells as part of the innate response are major contributors to host antitumor defense mechanisms [14]. On a molecular level, cytokines such as interleukin (IL)-12 and IFN-γ as mediator of effector functions, as well as type I interferons (IFN-α/β), play major roles in antitumor immunity [12]. IFN-γ has been shown to be especially important for the establishment of host protection by acting on both the immune system-, as well as on the tumor cell-side [15, 16]. Type I IFNs may possibly activate antigen-presenting cells (APCs) and enhance cross-priming of tumor-associated antigens [17]. Damage-associated molecular pattern molecules (DAMPs) directly released by dying tumor cells or damaged tissue as a result of progressive tumor growth are considered as further APC-activating signals [18, 19]. In this line, a recent study determined tumor cell aneuploidy, in particular tetraploidization, as immunogenicity-increasing factor leading to enhanced immune elimination of tumor cells. Hyperploid cells displayed endoplasmic reticulum stress responses that induced increased surface expression of the danger signal calreticulin (CRT), which activated APCs at the tumor site [20]. Importantly, this study confirmed $CD4^+$ and $CD8^+$ T cells, IFN-γ and the IFN-γ receptor as major determinants of the elimination process. Also, stress ligands such as the human MHC class I chain-related genes MICA/B (mouse Retinoic acid early transcript; RAE-1 and MHC class I-related glycoprotein H60) are frequently expressed on tumors. These bind to activating receptors (e.g., Killer cell lectin-like receptor subfamily K, member 1; NKG2D receptor) on innate cells, thereby inducing release of pro-inflammatory and immunomodulatory cytokines that establish a favorable microenvironment for adaptive antitumor mechanisms [21]. Furthermore, studies have shown that mice lacking the cytotoxic T and NK cell effector molecule perforin develop carcinogen-induced and spontaneous tumors at a higher incidence as their wild type counterparts [22]. In summary, a balanced action of various cell types, signaling, and effector molecules of both innate and adaptive immunity is necessary for the elimination of transformed cells; a process that may not always be achieved in a complete fashion.

4.1.1.2 Equilibrium

The equilibrium phase has been characterized as a state of tumor cell dormancy that is induced, at least to some extent, by constant immunosurveillance. Few tumor cells may survive the elimination phase, but are usually not able to grow out to form recurrent primary tumors or metastases. In this case, the adaptive immune system maintains residual cancer cells in a state of dormancy, thus, specifically controls and limits cancer progression [21]. Hence, both tumor and immune cells enter the state of equilibrium, which may possibly last for decades. The mechanisms underlying the equilibrium process are still largely unknown due to the difficulty in isolating dormant tumor cells from patients. Evidence for this state comes mainly from clinical observations of breast cancer, melanoma and renal carcinoma, indicating that tumor growth is not continuous but may undergo long periods of subclinical dormancy [20]. Experimental evidence is provided by studies using mouse models of spontaneous tumor development. In this line, immune-competent mice treated with low-dose MCA remained apparently

tumor free, but at all times harbored transformed cells as upon depletion of adaptive immunity such as $CD4^+$ and $CD8^+$ T cells and/or blocking of IFN-γ and IL-12p40 by administration of antibodies, tumors rapidly grew out at the site of original MCA injection in 50% of the mice [23]. Interestingly, depletion of NK cells, their cell recognition (anti-NKG2D) or their effector functions (anti-TNF-related apoptosis-inducing ligand; TRAIL) did not induce tumor outgrowth, implicating that the adaptive immune system exclusively maintains the equilibrium phase and thus, contrasts to the need of an interplay of both innate and adaptive immune system to protect hosts in the elimination phase. Also, the recognition of the type and frequency of tumor-infiltrating lymphocytes (TILs) as prognostic factor for different types of cancer has been steadily increasing over the last decade [24]. Consistent with this, Wu *et al*. discovered enhanced infiltration of $CD3^+$ T cells as well as an increased ratio of $CD8^+$ T cells to regulatory T cells (Treg) in the tumor microenvironment of dormant sarcomas when compared to progressively growing tumors. The authors further describe that a high proportion of intratumoral effector cells such as cytotoxic T Lymphocytes (CTLs), NK cells, and γδ T cells together with a low proportion of regulatory cells such as MDSCs and Tregs maintains dormancy, hence favors the state of equilibrium and ultimately, the overall-survival [25]. In contrast to the previous study, which indicated no role for innate effectors such as NK cells in inhibiting tumor outgrowth [23], this study demonstrates that NK cells make up an important proportion of TILs in equilibrium phase tumors, which indicates a more prominent role for NK cells than previously appreciated [25]. The role of IL-12p40 as T_H1 cytokine in supporting the process of elimination has been previously described extensively by Koebel and colleagues [23]. In a following study, the same group demonstrated that the IL-12 cytokine family member IL-23 may counteract the function of IL-12p40 by promoting tumor cell resistance [26]. It is becoming increasingly evident that the balance of pro-and anti-tumoral immune effectors plays an important role in maintaining tumors in the equilibrium phase. Apart from inducing tumor cell dormancy, adaptive immunity has furthermore been ascribed responsible for the process of immunoediting [10, 27]. Selective pressure exerted by immunological defense mechanisms may help to shape tumor cells that are less immunogenic and therefore, may evade recognition until some of these cells eventually enter the escape phase. The concept of immunoediting has emerged in 2001, when Shankaran and colleagues observed that tumors formed in immunodeficient mice were in general more immunogenic than those formed in immunocompetent mice [10].

4.1.1.3 Escape

Cancer cells entering the escape phase mean failure of the immune system to eliminate or control transformed cells and therefore, allowing them to grow in an unrestricted manner. These tumor cells are highly instable and rapidly undergo genetic and epigenetic modifications to bypass immunological defenses. The immune system contributes to a Darwinian selection process by killing of antigen-positive tumor cells and hence, by leaving behind only the more aggressive and less immunogenic cancer cell variants [4, 28]. There is a long list of mechanisms, which tumors may evolve in order to avoid immunological destruction. Apart from the ability to induce central or peripheral T cell tolerance,

tumors may acquire defects in antigen-processing or -presenting pathways by means of MHC class I down-regulation or the development of IFN-γ or IFN-α/β insensitivity, which prevents T cell-mediated elimination. Tumor cells with impaired IFN-γ signaling are not able to produce the intracellular machinery needed for antigen-presentation [15]. The before mentioned genetic instability of tumor cells may lead to complete loss of tumor-specific antigens (TSAs), and in a similar way, cancer cells may lose ligands for recognition by innate immune cells (such as NKG2D-ligands). Even if effector T cells recognize tumor cells, they may still evade destruction by the expression of impaired death receptors, such as mutated, inactive forms of TRAIL [29]. A rather active way to circumvent immunological defenses is the expression of immune-inhibitory ligands, such as PD-L1, on the surface of transformed cells [30]. A tumor may generate an immunosuppressive tumor-microenvironment by the secretion of factors that directly inhibit cells of both the adaptive and the innate immune system, or by inducing regulatory immune cells [4, 31].

Furthermore, dendritic cell function is crucial for the priming of T cells and initiation of immunity. Tumors may secrete sterol metabolites to suppress the expression of the C-C chemokine receptor type 7 (CCR7) on DCs, thereby impeding their migration capacity [32]. In addition, many cancers express vascular endothelial growth factor (VEGF), which supports one of the characteristic mechanisms of tumors, angiogenesis, and also may prevent endogenous DC function [32]. A study from Gabrilovich in 1999 demonstrated that monoclonal antibodies targeting VEGF can increase DC function *in vivo*, and therefore improve overall success of tumor immunotherapy [33]. Furthermore, the release of immune-suppressive cytokines such as transforming growth factor (TGF)-β inhibits DC activation as well as T and NK cell function [34-36]. The role of IL-10 is not yet clear, as it has been found to suppress DC function and to affect T cell responses, but also may enhance immunological destruction of tumor cells [37]. Ultimately, cancer cells protect themselves by the expression of enzymes that metabolize amino acids in the tumor microenvironment. Indoleamine 2,3-dioxygenase (IDO), for example, metabolizes tryptophan, which leads to inhibition of T cell proliferation by starvation or through toxic metabolites [38].

Additionally, tumors may recruit regulatory immune cells such as $CD4^+CD25^+FoxP3^+$ regulatory T cells (Tregs) or myeloid-derived suppressor cells (MDSC). Tregs are known to suppress CTL function by various mechanisms, including a) expression of suppressive cytokines such as TGF-β, IL-35 or IL-10, b) direct killing of effector T cells via granzymeA/B (cytolysis), c) by consumption of IL-2, which is required for effector T cell homeostasis, as well as expansion and d) by interfering with APC activation leading to insufficient T cell costimulation [39, 40]. MDSCs expand and accumulate in tumors due to expression of granulocyte macrophage colony-stimulating factor (GM-CSF), IL-1β, VEGF or prostaglandin E_2 (PGE_2). Cells of this heterogeneous group of myeloid progenitors and immature myeloid cells produce immunosuppressive cytokines, [41, 42]. An immunosuppressive microenvironment further attracts M2 macrophages into the tumor mass. These cells, in contrast to M1-polarized macrophages, are able to

inhibit T cell function *via* the expression of TGF-β and IL-10 or promote stromal development and angiogenesis *via* the expression of platelet-derived growth factor (PDGF) [43]. All together, the complex mixture of an immunosuppressive milieu that directly inhibits effector cells or recruits regulatory immune cells in combination with the high genetic variation of cancer cells enables them to hide from immunological recognition and makes it difficult for an organism to fight cancer.

4.1.1.4 Immunoediting in human cancer

Indication for immunosurveillance in human patients is reported in studies associating the occurrence of tumor-infiltrating lymphocytes (as in quantity, quality, and localization) with the survival of the corresponding patients [44]. Presence of $CD4^+$ T helper (T_H) cells and $CD8^+$ CTLs within tumors, in addition to cytokines such as tumor necrosis factor (TNF)-α or IFN-γ that promote tumor control, has been shown to improve the prognosis of patients with various cancers such as ovarian and colorectal cancers, non-small cell lung cancer or breast cancer [21, 44]. In this line, spontaneous antibody and T cell responses against tumor-associated antigens (TAAs) have been detected in cancer patients, demonstrating active immunosurveillance mechanisms. Further data supporting the concept of *immunosurveillance* in human cancers arises from immunodeficient individuals, such as acquired immune-deficiency syndrome (AIDS) patients or transplant recipients, which demonstrate an increased risk to develop cancers [45-48]. These cancers are mainly of viral origin, but some clinical studies show an increased incidence of colon, lung, pancreas, kidney, head, and neck as well as non-melanoma skin cancers [21]. In a special case of organ transplantation, both recipients of kidneys from the same donor developed malignant melanoma, which originated in the donor's tissue. Sixteen years before transplantation, the donor was successfully treated against melanoma [15]. Hence, the donor's immune system was able to keep the tumor cells in a dormant state (as supposed to be found in the equilibrium phase), while the immunosuppressed recipients were not able to control tumor outgrowth. Together, these observations support the hypothesis that new malignancies only arise in the permissive environment of a compromised immune system, which cannot sustain an elimination or equilibrium phase [44].

4.2 Therapeutic options in cancer

4.2.1 Immunotherapy

4.2.1.1 Cancer vaccines

Active immunotherapy includes cancer vaccines designed to prime and expand a pool of tumor reactive T cells by delivering a specific antigen in a surrounding supportive for T cell activation. Thus, vaccination relies on APCs and, in most cases, on concomitant administration of adjuvants, such as Freund`s adjuvant, Bacillus Calmette–Guerin (BCG), montanide, alum, or Toll-like receptor (TLR) agonists such as CpG-DNA for their optimal stimulation [49]. Possible preparations of tumor antigen-

dependent cancer vaccines include a) recombinant short peptides that directly bind MHC molecules on the surface of APCs or full-length proteins, which rely on the uptake and processing by APCs, b) TAA-containing whole tumor cells or lysates, alone or complexed with chaperones, c) TAA-encoding nucleic acids in the form of naked DNA or RNA or delivered by viral entities (adeno-, or lentivirus) and d) DC-based vaccines [3]. The latter include autologous DCs loaded with TAAs *ex vivo* as well as fusion proteins and TAA-linked antibodies directed against a DC surface receptor, such as DEC205, which both allow selective delivery of TAAs to DCs *in vivo* [50, 51]. Apart from the two multivalent prophylactic vaccines Cervarix® and Gardasil®, that have been approved against HPV-infection-related cervical cancer, only one therapeutic vaccine has been approved recently; the cell-based vaccine sipuleucel-T (Provenge®). It is made of autologous peripheral blood mononuclear cells (PBMCs) loaded *ex vivo* with a fusion protein containing the TAA prostatic acid phosphatase (PAP) and the APC-stimulating cytokine GM-CSF, and has been clinically approved for the treatment of patients with metastatic hormone-refractory prostate cancer in 2010 [3, 52]. Multiple peptide- or protein-based cancer vaccines are currently under evaluation in phase I-III clinical trials [3]. Yet, further approvals are still rare as most cancer vaccines struggle to demonstrate improved survival or quality of life. Poor antigenicity or heterogeneous expression of the tumor antigen, ineffective adjuvants, and the immunosuppressive nature of the tumor microenvironment include reasons for constant failure or low efficacy of therapeutic vaccines. Thus, extensive research is ongoing to overcome these limitations. Importantly, vaccines targeting DCs *in vivo* with TAA-encoding mRNA, as well as *ex vivo* modification of DCs are considered save and have been demonstrated to induce potent CD_4 and CD8 T cell responses [53, 54]. To improve CD_4 help and memory formation, DCs may be targeted by viruses that encode for co-stimulatory molecules or T_H1 polarizing cytokines in addition to the TAA. *Ex vivo* modified autologous DC-based vaccines may further be improved in regard to the DC subset used [55], optimal *ex vivo* or *in vivo* DC activation including concomitant administration of immunostimulatory chemotherapeutics or radiotherapy [56], pre-conditioning of the vaccine site with recall antigens [57], or appropriate routes of DC re-infusion [3]. Finally, tumor cells can be targeted with oncolytic viruses that selectively infect and kill tumor cells and additionally may be modified to express immune-attracting cytokines such as GM-CSF [58].

4.2.1.2 Adoptive cell therapy: TILs, CARs & TRUCKs

Further approaches engaging the hosts' immune system include adoptive transfer of *ex vivo* expanded tumor-infiltrating lymphocytes (TILs) or chimeric antigen receptor-bearing autologous T cells (CAR-engineered T cells). Although expansion of autologous TILs with IL-2 produced remarkable responses in metastatic melanoma, the protocols for *ex vivo* T cell activation and expansion are constantly being improved [59, 60]. T cells engineered to express a TCR of defined antigen-specificity or chimeric antigen receptors (CARs) overcome the hurdles that pose the isolation of sufficient TILs from patients and the unknown specificity of those T cells. A CAR is composed of one polypeptide chain with an extracellular antigen-binding domain derived from an antibody and an intracellular signaling chain,

which is frequently the TCR-derived CD3ζ chain. Importantly, the antibody domain recognizes a specific ligand independent of MHC molecules, while signals are transduced by TCR-associated downstream kinases [61]. Second and third generation CARs additionally incorporate one or two co-stimulatory signaling domains into the cytoplasmic CAR tail in order to prolong and fine-tune T cell responses [62]. Indeed, second-generation CARs directed against CD19 are evaluated in clinical trials for treatment of chronic lymphocytic leukemia (CLL), acute lymphocytic leukemia (ALL,) and non-Hodgkin lymphomas (NHL) with encouraging results [63-65], similar to TCR engineered T cells in melanoma [66], and $CD4^+$ TIL infusions in metastatic epithelial cancer [67]. CAR efficacy may further be enhanced by introduction of chemokine- or cytokine-encoding sequences, resulting in "T cells redirected for universal cytokine-mediated killing" (TRUCKs). The additional cytokine expression in the tumor microenvironment is believed to enhance anti-tumor immunity to those tumor cells that are not recognized by a specific CAR [61]. Drawbacks of T cells transduced with modified TCRs, CARs, or TRUCKs are autoimmune side effects due to limited control of T cell activation. Hence, attempts have been made to include inducible molecular "safety switches" in order to remove inappropriately activated CAR T cells in case of severe autoimmune symptoms [68].

4.2.1.3 Monoclonal antibodies, bispecifics and BiTes

Monoclonal antibodies (mAb) are widely used for cancer therapy. These may either directly trigger adaptive immunity, or target tumor cells for both immune-mediated or -independent triggering of tumor cell death by a) blockade of receptors involved in tumor cell growth and survival (i.e., anti-HER2; trastuzumab), b) depletion of tumor-associated stroma and vasculature to support disruption of the microenvironment (i.e., anti-fibroblast activation protein (FAP) and anti-tenascin or anti-VEGF; bevacizumab), or c) the selective delivery of cytokines into the tumor in form of immunoconjugates. Tumor-targeted mAbs often additionally activate innate immune cells *via* their Fc (fragment, crystallizable) portion by complement-dependent cytotoxicity (CDC), antibody-dependent cellular cytotoxicity (ADCC), or antibody-dependent cellular phagocytosis (ADCP), thereby increasing tumor cell killing (i.e., anti-CD20; rituximab, as well as trastuzumab) [69]. Bispecific antibody constructs are engineered to recognize a specific tumor-associated or stromal antigen with one arm and CD3 with the other. T cells are thereby brought into close proximity of tumor cells, while triggering of CD3 results in T cell activation, degranulation and tumor cell killing independent of TCR specificity, MHC expression and peptide presentation [70]. The so-called TriomAb catumaxomab was designed to target the tumor antigen epithelial cell adhesion molecule (EpCAM) as well as CD3 on T cells, while additionally engaging Fc receptors on innate cells [71]. Its approval for the treatment of malignant ascites by the European Commission in 2009 was granted due to efficient triggering of tumor cell death as well as protective immunity. Bi-specific T cell engager (BiTe) molecules recognizing CD19 [72], CD33 or EpCAM are currently tested in several phase I/II trials for treatment of non-Hodgkin lymphomas (NHL), acute myeloid leukemia (AML) and metastatic colorectal, gastric or lung cancer, respectively [72, 73]. BiTes function similar to bispecific mAbs, but instead of assembling a complete antibody, these molecules

directly combine two single chain variable fragments (scFv) recognizing a tumor- or stromal antigen and CD3. Interestingly, BiTes seem, at least in cell culture experiments, to better overcome mutations in signaling pathways that classically lead to tumor cell resistance [74]. In essence, multiple forms (diabodies, minibodies, complete IgG) and fragments (scFvs) of antibodies are engineered in order to improve antigen-binding, tumor-targeting, and T cell activating properties of the constructs [69].

4.2.1.4 T cell checkpoint blockade

In contrast to the above-described tumor antigen-dependent approaches, monoclonal antibodies targeting activating receptors or immune-regulatory checkpoints on T cells aim at non-specific prolongation of endogenous T cell responses. Agonistic antibodies have been developed against the TNF-receptor family related activating receptors CD137 (4-1BB), OX40, glucocorticoid-induced TNFR family related gene (GITR), and CD27 on T cells or against CD40 on APCs [75]. Inhibitory T cell receptors such as the checkpoint receptors CTLA-4, programmed cell death 1 (PD-1), T cell immunoglobulin mucin-3 (Tim-3), lymphocyte-activation gene 3 (LAG-3), or B- and T-lymphocyte attenuator 4 (BTLA-4) are expressed either constitutively or upon activation and function to dampen T cell responses in order to prevent autoimmunity in healthy individuals. Tumors, however, adopt these mechanisms in order to promote their growth and survival by circumventing immunosurveillance. Blockade of inhibitory receptors results in enhanced T cell proliferation and effector activity, although specific mechanisms may differ amongst distinct receptor-ligand pairs. The CTLA-4 blocking antibody ipilimumab was the first of its class to be approved for metastatic melanoma in 2011 and has since demonstrated impressive clinical success including long-term protective immunity in responding patients [52, 76]. Mechanistically, CTLA-4 outcompetes the activating T cell receptor CD28 for its ligands on APCs, i.e., CD80 (B7-1) and CD86 (B7-2), with a 10-100 fold higher affinity, which is one way to suppress T cell function. Furthermore, CTLA-4 transduces negative signals in effector T cells through phosphatases and directly controls activation of $CD4^+$ Tregs, which constitutively express CTLA-4 [77]. Known ligands for PD-1 include PD-L1 (B7-H1) and PD-L2 (B7-DC), which are expressed on APCs, but also on non-hematopoietic cells including stromal cells at the tumor site and tumor cells themselves, and of which at least PD-L1 is inducible by IFN-γ [78]. While CTLA-4 acts to diminish T cell responses during the process of priming, PD-1 signaling is thought to be crucial for limiting effector T cell responses in tissues, hence at the tumor site. Thus, combinatorial blockade of distinct checkpoints has demonstrated to be synergistic and is thoroughly evaluated in pre-clinical as well as clinical trials [77]. In fact, about 70% of currently (January 2015) registered clinical trials for melanomas evaluate safety and/or efficacy of ipilimumab in combination with radiotherapy, surgery, or other monoclonal antibodies [52]. Also, T cell checkpoint blockade has become attractive for treatment of multiple other solid tumor entities. The PD-1 blocking mAb nivolumab received FDA approval in March 2015 for squamous non–small cell lung cancer, but also demonstrated potent clinical activity in renal cell carcinoma, colon carcinoma, and melanoma and is evaluated in a number of additional entities in phase I-III clinical trials [77]. Of note, blockade of the IFN-γ inducible PD-L1, has shown equally promising

therapeutic activity [77]. Interestingly, patients that had progressed under anti-CTLA-4 treatment responded to anti-PD-1 treatment, thus demonstrating their distinct modes of action [79]. Despite of all successes, a major limitation of checkpoint inhibition is the low response rate, while the factors determining responsiveness remain unknown. Seven recent articles, however, refine our understanding of a) potential cancer types that respond to those therapies [80], b) biomarkers that can predict the success of checkpoint inhibition, such as high numbers of pre-existing $CD8^+$, $PD1^+$ and $PD\text{-}L1^+$ T cells in the tumor microenvironment [81-83], and c) the effect of the number, as well as the nature of additional somatic mutations on the response rates [84-86]. As an example, patients responding best to inhibition of CTLA-4 had mutations leading to neoantigens similar to viral or bacterial antigens [86]. Also, Minn and colleagues recently demonstrated synergy of CTLA-4 blockade and radiotherapy in melanoma patients, although 64% of patients were resistant to treatment [87]. Using the B16 mouse model of melanoma, the group subsequently highlighted the failure to increase the intratumoral ratio of $CD8^+CD44^+$ effector T cells to Treg cells (CD8/Treg ratio) as predictor of immunological resistance. Importantly, resistance correlated with PD-L1 expression on insensitive melanoma cells and was overcome with additional blockade of the PD-1/PD-L1 signaling axis [87]. These data highlight the need for additional biomarkers that predict the outcome of T cell checkpoint blockade. In the same line, further investigations will ultimately help determining effective combinations with additional checkpoint blocking antibodies, agonistic antibodies, such as anti-CD40 or anti-41BB (CD137), or even with immune-modulatory chemo- and radiotherapy approaches.

4.2.2 Immunostimulatory chemotherapeutics

In light of the recent success of novel immunotherapy approaches, future therapeutic efforts will ultimately focus on the development of effective combination strategies that exert complementary pressure on tumors *via* immune activation and additional direct toxicity. Of note, accumulating evidence reveals previously unrecognized immune-modulatory features of chemo- and radiotherapy [88, 89]. In addition to reducing the primary tumor burden, and thereby, at least in part, reverting the immunosuppressive microenvironment, specific compound classes can also induce DC maturation, enhance antigen cross-presentation, selectively eliminate immunosuppressive cells, or induce immunogenic tumor cell death (ICD) [90, 91]. Chemotherapeutics may additionally increase tumor cell immunogenicity by triggering upregulation of tumor antigen and MHC expression, enhanced co-stimulation *via* B7-1, or decreased expression of co-inhibitory molecules, such as PD-L1 [91, 92]. Further agents render tumor cells more sensitive to T cell–mediated lysis through fas-, perforin-, and granzyme B–dependent mechanisms [93]. Anthracyclines [94], oxaliplatin [95], and cyclophosphamide [96], as well as irradiation [94] have been reported to induce ICD, which, in distinction to non-immunogenic apoptosis, is characterized by the induction of endoplasmatic reticulum (ER) stress and autophagy [97, 98]. Hallmarks of ICD include the pre-apoptotic exposure of calreticulin (CRT) on the cell surface, the secretion of adenosine triphosphate (ATP), and the post-apoptotic release of the chromatin-binding protein high-mobility group box 1 (HMGB1). Importantly, the suppression of each of these APC-

activating signals abolishes the immunogenicity of cell death, demonstrating the non-redundancy of each of these pathways [79, 94, 99]. Several cytotoxic agents are able to target suppressive subsets, such as Tregs or MDSCs and thereby promote adaptive anti-tumor immunity. One of the first drugs reported to interfere with Tregs was cyclophosphamide, which at low doses depletes Tregs and inhibits their effector functions as well as homeostatic proliferation [100-103]. Similar, doxorubicin, 5-azacytidine, 5-fluorouracil (5-FU), and gemcitabine substantially reduce the numbers of MDSCs by induction of apoptosis [104-107]. In contrast, low, non-cytotoxic doses of paclitaxel stimulate the differentiation of MDSCs into functional DCs expressing MHCII and costimulatory molecules [108, 109]. These functional DCs have lost their suppressive capacity and contribute to the induction of T cell responses. Similarly, docetaxel treatment polarizes MDSCs towards an M1 phenotype with loss of suppressive effects, higher levels of MHCII and CD80 expression, and a shift from IL-10 to IL-12 secretion [110]. Triggering of direct DC maturation by chemotherapeutics has been reported for topoisomerase I inhibitors, although with conflicting results [111-113], for camptothecin, lenalidomide, and docetaxel [113], as well as for paclitaxel and other compounds at low, non-cytotoxic concentrations [114-117]. Along the same line, microtubule-destabilizing agents (MDAs), such as the *vinca*-alkaloids have been demonstrated to directly affect DC maturation at clinically relevant doses [118, 119]. Early studies indicated that microtubule disruption by colchicine, vinblastine, and vincristine induced marked expression of IL-1 in monocytes [120]. Yet, the mechanisms for the induction of DC maturation remain elusive.

Thus, a detailed characterization of the immunostimulatory effects of currently used chemotherapeutic agents may guide the way for rational combinations with immunotherapeutic approaches.

4.3 Dendritic cell biology

DCs were first described by Steinman and Cohn in 1973 as large stellate cells with distinct properties from the formerly known cell types, such as mononuclear macrophages, granulocytes, or lymphocytes [121]. They function as sentinel cells seeking out foreign invaders throughout the body, whether these are bacteria, viruses, or toxins. Upon encounter with endogenous or exogenous antigens, DCs capture and process these antigens for the subsequent presentation to T cells, thereby initiating an adaptive immune response. DCs possess highly specialized mechanisms for antigen uptake and processing, the capacity to migrate to defined sites in lymphoid organs, such as the T cell areas, and most important, the capacity to provide costimulation necessary for activation of effector cells. DCs rapidly differentiate or mature in response to a variety of stimuli ranging from pathogen-associated molecular patterns (PAMPs) to many other non-microbial factors, such as DAMPs, cytokines, innate lymphocytes or immune complexes. But other than the exclusive display of antigens, DCs may also alert other immune cells to the presence of injury or infection at a specific site. With these functions, DCs play a major role in the connection of innate and adaptive immunity [122, 123].

4.3.1 Dendritic cell subsets

One striking feature of dendritic cells is their short life cycle and rapid turnover. Although originally isolated from lymphoid tissues, it is known today that all lymphoid and most non-lymphoid tissues possess their own DC populations [124]. The heterogeneity in body localization, developmental stages, and functional properties makes a clear definition of sub populations rather difficult. Generally, DCs may belong to lymphoid tissue (LT)-resident DCs or non-lymphoid tissue (NLT) migratory DCs that migrate to lymph nodes (LNs) via the lymphatics. To date DCs are categorized in four main subsets: conventional DCs (cDCs), plasmacytoid DCs (pDCs), Langerhans Cells (LCs), and inflammatory DCs (iDCs) (Figure 4-2) [125].

In mice, CD11c expressing conventional DCs in lymphoid tissues can be divided in two subgroups with largely complementary functions based on expression of CD4 or CD8α. CD8α$^+$ DCs are generally recognized for their highly efficient cross-presentation of exogenous antigens *via* MHCI molecules to CD8$^+$ T cells, whereas CD4$^+$ DCs are specialized in priming CD4$^+$ T cells by presentation of MHCII-restricted antigens. Counterparts of CD8α$^+$ DCs in peripheral non-lymphoid tissues have been described to express CD103, whereas peripheral equivalents to lymphoid tissue CD4$^+$ DCs express high amounts of CD11b [126, 127].

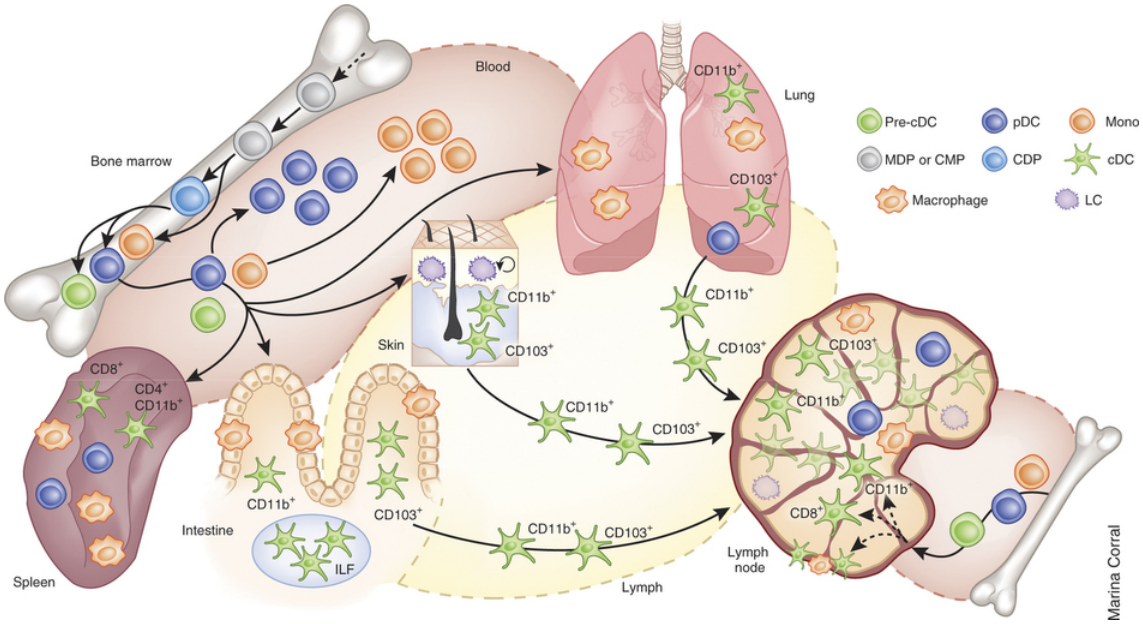

Figure 4-2 ***Development, migration and tissue residency of distinct DC subsets***. "cDCs, pDCs and monocytes (Mono) derive from bone marrow progenitors. Pre-cDCs, pDCs and monocytes transit through the blood and seed peripheral organs, where pre-cDCs complete their differentiation into CD8$^+$ (or CD103$^+$) cDCs or CD4$^+$ (or CD11b$^+$) cDCs. Monocytes can migrate into tissues and differentiate into macrophages. In the intestine, cDCs and macrophages populate the villi; cDCs are also present in intestinal lymphoid follicles (ILF). In the skin, dermal DCs consist of both CD11b$^+$ and CD103$^+$ cDC subsets. LCs populate the epidermis and self-renew locally. Macrophages, pDCs and both cDC subsets reside in the lung. A hallmark characteristic of cDCs is their ability to migrate from tissues to draining lymph nodes after encountering antigen, to prime T cell responses. In contrast, macrophages

mostly remain at the site of differentiation". Adapted from Satpathy AT. Re(de)fining the dendritic cell lineage. Reprinted with permission from Macmillan Publishers Limited. Copyright © 2012 [125].

In humans three major types of conventional DCs are found and classified based on the expression of CD141 (blood dendritic cell antigen; BDCA-3), CD1c (BDCA-1) and CD14. $CD141^+$ DCs may be both migratory and resident, are found in human blood, tonsils and LNs as well as in some NLTs and resemble mouse $CD8^+/CD103^+$ DCs in their capacity to cross-present antigens to $CD8^+$ T cells [128]. $CD1c^+$ DCs are mainly found in blood, LNs, spleen and NLTs such as the skin, express CD11c and CD11b and display a phenotype comparable to that of mouse $CD11b^+$ DCs. Their major function is thought to include the modulation of mucosal T cell responses and initiation of immunity towards extracellular antigens [129]. $CD14^+$ DCs are unique to the human system as murine counterparts are still unknown. This subset has been shown to potently induce follicular helper T cells (T_{FH}) and antibody-secreting B cells and phenotypically resemble monocytes as well as macrophages [128].

Plasmacytoid DCs, skin resident LCs, and inflammatory DCs have been described both in humans and mice. It has been proposed that LCs and dermal (interstitial) DCs originate from a myeloid precursor, whereas plasmacytoid DCs may develop from a lymphoid precursor. However, this hypothesis is still under discussion [130]. Conventional DCs (here: other than pDCs) predominantly express the leukocyte integrin CD11c/CD18 (CD11c) or complement receptor 4 (CR4). pDCs only weakly express CD11c and have been identified by expression of BDCA-2 in humans and sialic-acid binding immunoglobulin-like lectin H (Siglec-H) in mice. In contrast, macrophages and monocytes express mainly CD11b/CD18 (CD11b) [131]. LCs and interstitial DCs share the ability to both activate $CD4^+$ and $CD8^+$ naïve T cells and secrete IL-12. However, only interstitial DCs are capable of inducing naïve B cells to differentiate into immunoglobulin (Ig)-secreting plasma cells. Plasmacytoid DCs (also: interferon-producing cells; IPC) were named after their resemblance to Ig-producing plasma cells and are unique in their ability to produce large amounts of type I IFNs upon viral stimulation. pDCs express the toll-like receptors TLR7 and TLR9, which provide sensitivity to single-stranded RNA viruses as well as to the non-methylated CpG-residues associated with many DNA viruses. It has been shown that type I IFNs stimulate a rapid antiviral response in uninfected somatic cells, while also influencing the development and maturation of DCs from blood monocytes [131, 132]. However, pDCs are less efficient in antigen capture and presentation as they express fewer MHCII and costimulatory molecules as conventional DCs do. Nevertheless, they may support a sustained production of IL-12 by conventional DCs *via* CD40 signaling, as TLR9 stimulation induces CD40ligand (CD40L) expression on pDCs. Epidermal LCs display a typical immature phenotype, are highly phagocytic and contain large granules called Birbeck granules. In contrast to other DC subsets, LCs develop from embryonic precursors, mainly fetal liver monocytes. LCs promote peripheral tolerance by constantly migrating to skin-draining LNs to present dermal and epidermal antigens to $CD4^+$ T cells, which induces anergy due to their immature phenotype. In some cases of viral infections, however, LCs in the skin may capture antigens and travel to the lymph

nodes to transfer them to resident $CD8^+$ DCs *via* cross-presentation, which seem to be responsible to prime naïve $CD8^+$ T cells [129].

Tissue inflammation, e.g., upon infection, may induce DCs of monocytic origin expressing CD11b and CD11c across species as well as CD64, FcγRε, and lymphocyte antigen 6C (Ly6C) in mice and CD1a, CD206, CD1c as well as CD14 in humans. So-called inflammatory DCs or TipDCs (due to expression of TNFα and i-NOS) migrate to tissue-draining LNs while expressing IL-12 and IL-23 to induce T_H1 or T_H17 responses, depending on the type of activation stimulus [133, 134]. Further known DC populations are splenic marginal DCs, interdigitating DCs in T cell-rich zones in secondary lymphoid tissues, germinal center (follicular) DCs, thymic DCs, liver DCs, and peripheral blood DCs [135]. Efforts are done to define an alignment of human and murine DC subsets and their respective functions (Figure 4-3). In this line, analysis of transcription factors seems to define lineages more accurately as compared to cell surface antigens [129].

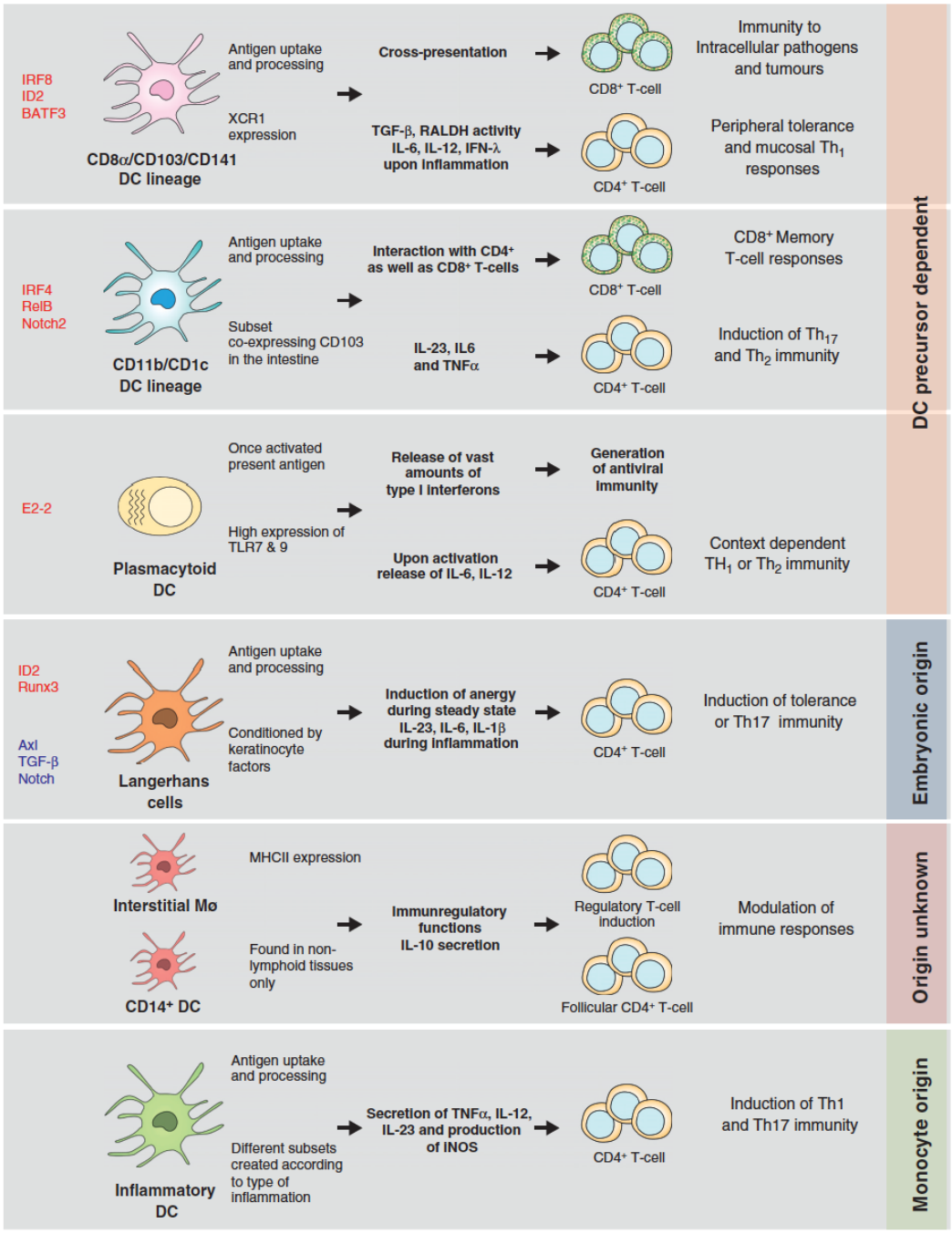

Figure 4-3 ***Different DC subsets shape different immune responses.*** Transcription factors that define DC lines are highlighted (mouse: red, human: blue). Adapted from Schlitzer A, Ginhoux F. Organization of the mouse and human DC network. Reprinted with permission from Elsevier Ltd. Copyright © 2014 [129].

4.3.1.1 DC subsets and cell lines used in this study

Human monocyte-derived DCs. Generation of large amounts of immature dendritic cells *in vitro* by culture of $CD14^+$ blood monocytes in presence of GM-CSF and IL-4 have first been described by Lanzavecchia and colleagues in 1994 [136]. Monocyte-derived DCs (moDCs) display efficient antigen-presentation capacity accompanied by the ability to induce activation of naïve T cells. Meanwhile, many studies have been performed using monocyte-derived DCs and thereby evaluated the use of this *in vitro* culture system for the assessment of DC biology [137].

Murine bone marrow-derived DCs and SP37A3 DC-cell line. For the study of murine DC activation, both bone marrow-derived DCs (BMDCs), generated by differentiation of bone marrow cells in the presence of GM-CSF (first described in) [138], and the DC cell line SP37A3 were used. SP37A3 DCs were established by growth-factor dependent long-term culture of splenic DCs as described by Winzler *et al*. [139]. SP37A3 DCs express CD11b and CD11c, low levels of CD205, but no CD8α. Properties of this DC cell line have been described extensively by Bros *et al.* [140].

4.3.2 Dendritic cell activation & initiation of T cell immunity

In most tissues DCs are present in an immature state. They possess low capacity to stimulate naïve T cells but are very well equipped for antigen capture and processing. Pathways for antigen (Ag) capture include macropinocytosis, receptor-mediated endocytosis *via* C-type lectin receptors (mannose receptor, DEC205), or Fcγ receptor types I (CD64) and II (CD32) as well as phagocytosis of particles, fragments from apoptotic and necrotic cells, viruses or bacteria [141]. Furthermore, DCs are able to internalize peptide-loaded heat shock proteins glycoprotein 96 (gp96) and heat shock protein 70 (Hsp70) [123]. Capture of an antigen itself may provide a first signal for activation of the DC, whereas signaling through the receptors CD40, TNF-R, and IL-1R may furthermore trigger activation of DCs [141]. Additionally, the danger model suggests that signals indicating inflammation or tissue damage such as cytokines, heat shock proteins, HMGB1, uric acid, or extracellular ATP may be necessary for the activation of Ag-bearing DCs to induce their full maturation [18, 19, 142]. After activation, DCs change phenotypically as well as functionally from Ag-capturing cells to antigen presenting cells. They rapidly lose their Ag-capturing capacities, as at this stage the processing of antigens as well as the assembly of peptide-MHC class II complexes is of most importance. The antigen enters the cell and is directed to MHC class II-rich compartments (MIIC), which are abundant in immature DCs. Within these compartments, peptide binding to MHCII molecules is edited and enhanced. During maturation, MIICs convert to vesicles that release their MHC-peptide complexes at the cell surface where they remain stable for days (Figure 4-4) [123].

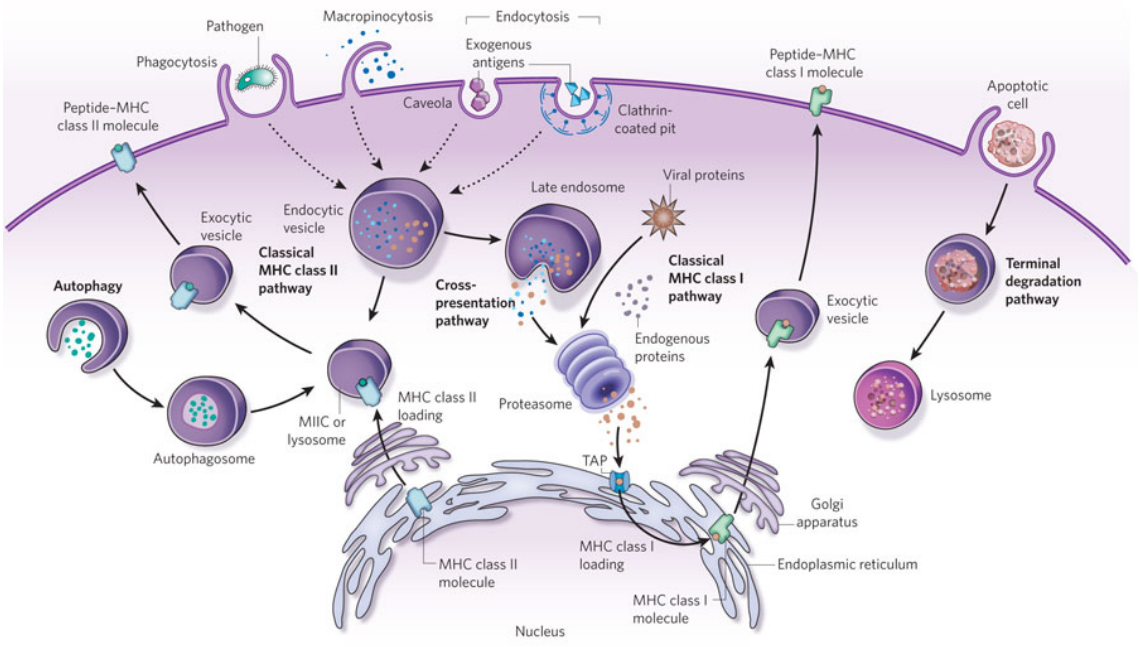

Figure 4-4 ***Antigen presentation pathways in dendritic cells***. Phagocytosis, macropinocytosis, and endocytosis mediate uptake of exogenous particles, proteins or pathogens into the cell. Antigens are then processed in endocytic vesicles (phagosomes, endosomes, lysosomes and/or endolysosomes) and loaded onto MHCII molecules in a lysosome or MHCII compartment (MIIC) before antigen-MHC complexes are moved to the cell surface. MHCII loading of endogenous antigen provided by autophagy may occur in stress situations. Antigens are loaded onto MHCI either through the classical pathway or by cross-presentation. Endogenous or viral proteins in the cytosol are processed through the proteasome, transported into the endoplasmic reticulum, passed through the Golgi and finally transported to the cell surface *via* the classical pathway. In addition, exogenous antigens that have been phagocytosed, macropinocytosed or endocytosed can be cross-presented on MHCI molecules by specific DC subsets. Here, antigen is loaded in endocytic compartments or may escape endosomes and arrive in the cytosol, where it is processed through the proteasome as usual, loaded onto MHC class I molecules and transported to the surface. Adapted from Hubbell YA. Materials engineering for immunomodulation. Reprinted with permission from Macmillan Publishers Limited. Copyright © 2015 [143].

For generation of CTLs, DCs present antigenic peptides in the context of MHCI molecules. Peptides from self and intracellular pathogens are loaded *via* the endogenous pathway, whereas peptides originating from extracellular Ags or immune complexes captured by FcγR are processed *via* the exogenous pathway. Endogenous, cytosolic proteins are degraded and loaded onto newly synthesized MHCI molecules in the ER. Extracellular antigens that are taken up with phagocytosed particles, exosomes or dead (dying) cells may escape the endocytic pathway and enter the ER to be loaded onto MHCI molecules for presentation to $CD8^+$ CTLs [130]. The later has been termed cross-presentation and is an important process in the generation of immunity against tumors or viruses that do not infect the APC itself. Cross priming denotes the activation of CTLs *via* this pathway. In case specific self-antigens (auto-antigens) are presented to $CD8^+$ T cells, the process leads to elimination of auto-reactive T cells and has been termed cross-tolerance. Furthermore, the family of MHC-related CD1 molecules has been identified as non-classical Ag-presentation molecules that present microbial lipids and glycolipid-containing antigens [123].

DC maturation is a continuous process that is initiated with Ag-capture and DC activation in the periphery and is not completed until the mature DC interacts with T cells in secondary lymphoid organs (Figure 4-5). Hence, migration of DCs occurs simultaneously to the maturation process. Various molecules such as Lipopolysaccharide (LPS) from bacterial cell walls, bacterial DNA, and double-stranded RNA, as well as T cell-derived signals are known to influence maturation. In addition, the balance between pro- and anti-inflammatory signals in the local microenvironment plays an important role. Apart from the loss of receptors for phagocytosis or endocytosis and the change in MIICs, the up-regulation of co-stimulatory molecules such as CD40, CD58, CD80 (B7.1), and CD86 (B7.2) as well as morphological changes, such as a loss of adhesive structures, and cytoskeleton reorganization are accompanying and enabling maturation and migration [123]. DCs migrate from the periphery to T cell areas in lymphoid organs *via* afferent lymph, which is triggered by chemokines as well as cytokines such as IL-1. During maturation, DCs up-regulate CCR7, which binds to and is activated by macrophage inflammatory protein-3 beta (MIP-3β) and secondary lymphoid-tissue chemokine (SLC, also known as 6Ckine) from which the latter is expressed on lymphatic vessels. Mature DCs enter draining lymph nodes and migrate to the T cell area in response to MIP-3β and/or 6Ckine. DCs themselves may be able to produce these chemokines to enhance and stabilize the signal. Expression of both MIP-3β and 6Ckine is necessary to attract naïve T and B cells and therefore, these chemokines may support the encounter of mature Ag-bearing DCs with antigen-specific lymphocytes [144]. Once DCs are interacting with T cells *via* the TCR, they receive additional maturation signals from the T cell, such as CD40L or TNF-related activation-induced cytokine (TRANCE). To sum up, in lymph nodes DCs complete maturation, attract T and B cells by the release of chemokines and maintain the viability of re-circulating T cells [141].

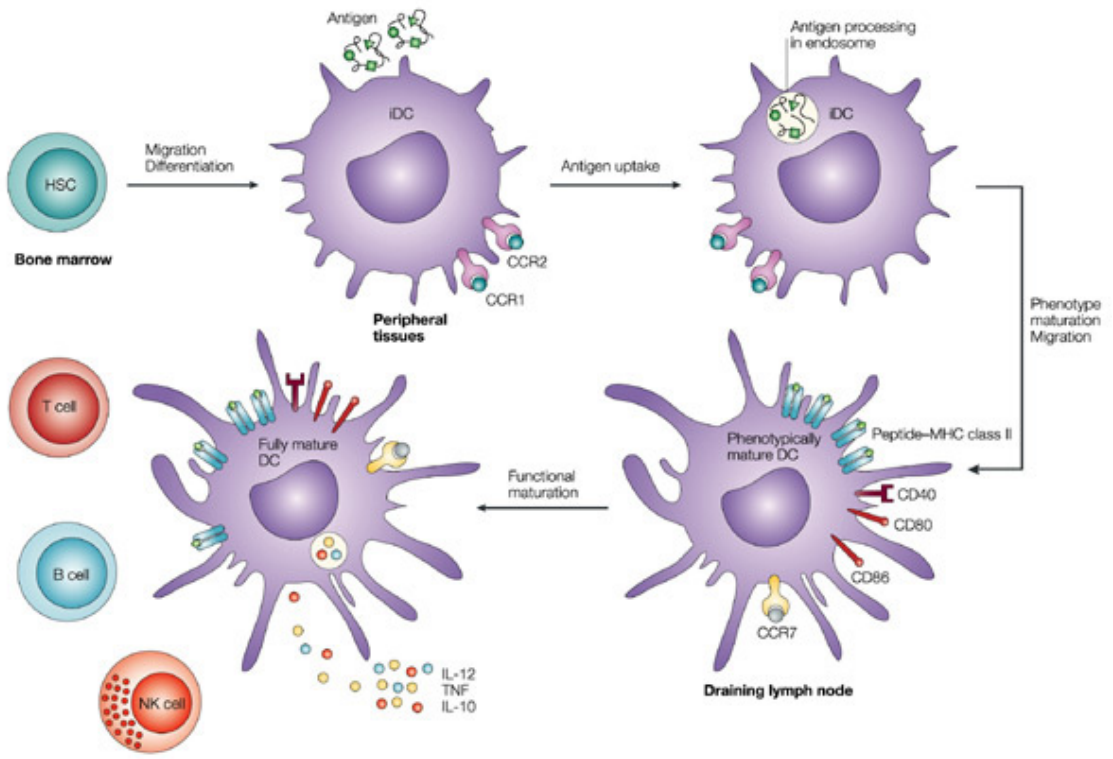

Figure 4-5 The DC maturation process. "Hematopoietic stem cells (HSCs) differentiate into immature dendritic cells (iDCs) that are recruited to peripheral tissues, where they continuously internalize and process antigens. After antigen capture and depending on the nature of the antigen, DCs migrate to the draining lymphoid tissue and mature phenotypically, which results in upregulation of CD40, CD80, CD86, MHCII and CCR7. In the draining lymphoid tissue, they present peptide–MHC complexes, interact with antigen-specific lymphocytes and mature functionally. Mature DCs activate T cells, B cells and NK cells and produce pro-inflammatory cytokines, such as IL-12 and TNF". Adapted from Hackstein H, Thomson W. Dendritic cells: emerging pharmacological targets of immunosuppressive drugs. Reprinted with permission from Macmillan Publishers Limited. Copyright © 2015 [145].

4.3.2.1 Dendritic cell signaling pathways & PRR

As key initiators and regulators of adaptive immunity, dendritic cells respond to a broad variety of conserved molecular patterns derived from infectious pathogens (i.e., PAMPs), as well as host-derived molecules from damaged or transformed self-tissues (i.e., DAMPs). Endogenous DAMPs may be identified as dangerous in case of aberrant localization or as part of abnormal (immune-) complexes that arise as a consequence of infection, inflammation or other types of cellular stress [146]. For recognition of either alarm signal, a broad variety of cells including DCs, macrophages, monocytes, B cells, neutrophils, or epithelial cells express the germ-line encoded pattern recognition receptors (PRRs). By differential triggering of a plethora of extra- and intracellular PRRs, not only the type, but also the duration and timing of encountered stimuli define the outcome of any immune activation. Hence, fine-tuning of innate signaling by PRRs determines tailor-made immune responses to distinct molecular patterns by directing T helper cell differentiation *via* DC-mediated cytokine secretion and expression of costimulatory molecules [147].

PRRs can be classified in five sub families: Toll-like receptors (TLRs), C-type lectin receptors (CLRs), nucleotide-binding domain, leucine-rich repeat (LRR)-containing (or NOD-like) receptors (NLRs), RIG-I-like receptors (RLRs), and AIM2-like receptors (ALRs) [148]. Of those, TLRs and CLRs are membrane-bound receptors located either on the cell surface or in endocytic compartments for recognition of extracellular or endosomal antigens, respectively. NLRs, RLRs and ALRs are located in the cytoplasm and recognize intracellular antigens. Upon activation, PPRs oligomerize and, by recruiting specific adaptor proteins and kinases, form multi-subunit complexes that transduce signals for initiation of both transcriptional and non-transcriptional responses. Major transcriptional response is the induction of leukocyte-recruiting chemokines, as well as pro-inflammatory cytokines and type I IFNs for initiation of innate as well as adaptive immune responses. Non-transcriptional responses include autophagy, phagocytosis and the processing of cytokines. Also, signaling *via* the IL-1 and IL-18 receptors is closely related to TLR signaling due the shared Toll/interleukin-1 receptor (TIR) homology domain, which mediates interaction with adaptor proteins. Importantly, IL-1 and TNF-α play outstanding roles in pathogen clearance by amplifying inflammatory responses induced by PAMPs or DAMPs [149].

TLRs. To date 13 TLRs have been described, from which TLR1-9 are conserved between humans and mice, while TLR10 is expressed in humans and TLR11-13 are expressed in mice. TLRs are type I transmembrane receptors that recognize PAMPs *via* leucine-rich repeats (LRRs), while their cytoplasmic TIR domain interacts with a set of adaptor proteins that is composed of TIR-containing adaptor protein (TIRAP), myeloid differentiation primary response 88 (MyD88), TIR domain–containing adaptor-inducing IFN-β (TRIF), and TRIF-related adaptor molecule (TRAM). Adaptor proteins transducing signals from PPRs play a crucial role in simultaneous detection of divers ligands as they integrate signals from more than one receptor. Signal transduction from the receptors to the adaptors depends on the cytoplasmic TIR domain that serves as the docking site for the TIR-containing cytoplasmic adaptor proteins [149]. All TLRs except for the endosomal TLR3 engage MyD88 either directly or in combination with the adaptor TIRAP/Mal, whereas TLR4 uniquely engages either MyD88 or TRIF for downstream activation of signaling cascades. TLR4 can either undergo trafficking to specialized sites on the cell membrane to induce MyD88-dependent pro-inflammatory cytokine production, or it is endocytosed and mediates production of IFNs *via* TRIF-dependent endosomal signaling [150]. Recruitment of adaptors subsequently initiates formation of larger signaling complexes composed of serine/threonine kinases (such as interleukin-1 receptor-associated kinases (IRAK)-1,-2,-4), ubiquitin E3 ligases (such as TNF receptor associated factors (TRAF)-3,-6 and cellular inhibitor of apoptosis proteins (cIAP)-1,-2), as well as the regulatory subunit of the IκB kinase (IKK) complex, NF-κB essential modulator (NEMO; also called IKKγ). They induce activation of mitogen-activated kinases (MAPKs) and the transcription factor families nuclear factor κ-light-chain-enhancer of activated B cells (NF-κB), activator protein 1 (AP-1), or interferon regulating factors (IRFs) for production of pro-inflammatory cytokines and type I IFNs (Figure 4-6) [151].

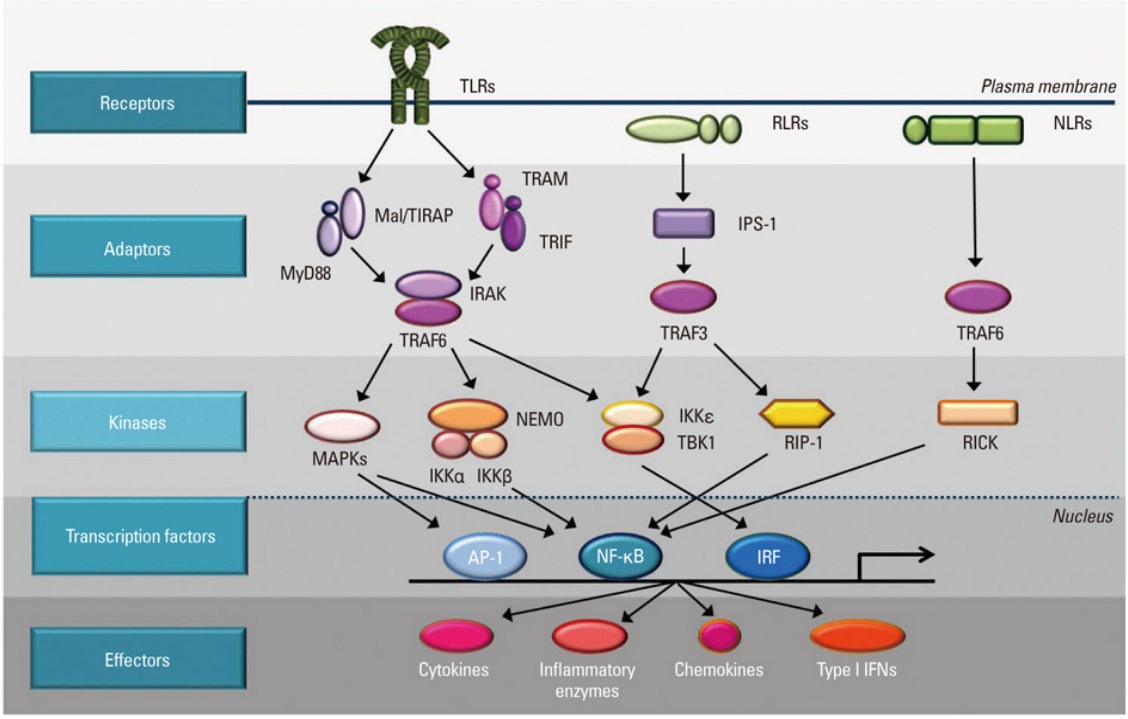

Figure 4-6 ***Multiple levels of intracellular signaling pathways downstream of pattern-recognition receptors.*** **"**Signaling is initiated by cell surface or intracellular receptors and transduced *via* adaptor proteins and kinases that mediate activation of transcription factors followed by subsequent transcription of effector molecules. Adapted from Eunshil Jeong and Yoo Young Lee. Intrinsic and Extrinsic Regulation of Innate Immune Receptors." Reprinted with permission from Creative Commons Attribution (CC BY) license (open access article) [151].

RLRs. The group of antiviral RLRs includes retinoic acid-inducible gene I (RIG-I), melanoma differentiation-associated gene-5 (MDA-5), and laboratory of genetics and physiology 2 (LGP2), which use the mitochondrial antiviral signaling protein (MAVS, also known as IPS-1, Cardif or VISA) as common adaptor protein. RLRs recognize intracellular viral and bacterial nucleic acids based on differences in structure and localization. Upon RLR triggering, MAVS forms a complex with caspase recruitment domain 9 (CARD9) and B-cell lymphoma/leukemia-10 (Bcl-10) to induce pro-inflammatory cytokines *via* activation of MAPKs and NF-κB transcriptional activation, whereas induction of type I IFNs requires TRAF3 and the kinases TBK1 and IKKε that activate IRF3 and IRF7 [149]. Similar to the MyD88-TIRAP-IRAKs-cluster, which has been termed "myddosome", MAVS forms so-called "supramolecular organizing centers (SMOC)" with RIG-I or MDA-5 in combination with TRAFs in order to facilitate enzymatic activation of signaling components and to provide spatial specificity [152]. Also, subcellular localization of receptors and adaptors is an important determinant of innate recognition of, and responses to PAMPs and DAMPs. As an example, viruses require cytoplasmic organelle-like replication complexes in order to transcribe their genome. These complexes contain host-derived membranes originating from the ER, the Golgi apparatus, mitochondria, or lysosomes, and indeed, MAVS is situated at mitochondria, peroxisomes, and mitochondrial-associated ER membranes (MAM).

Interestingly, MAVS situated on mitochondria and MAVS situated on peroxisomes induce different types of IFNs [153].

While RLRs recognize viral RNA species, sensing of pathogenic DNA is accomplished either by TLR9 in case of unmethylated CpG-DNA, or *via* the stimulator of interferon genes (STING) pathway. STING is localized at the ER from where, upon activation, it moves to the Golgi, leaves the Golgi and associates with TBK1 on still not well defined "IFN-inducing vesicles" to induce IRF3 and NF-κB-mediated cytokine expression. To date the only viral DNA receptor that has been shown to activate STING is called cGas and recognizes B-type cytoplasmic DNA [154, 155].

CLRs. CLRs form a heterogeneous group of hundreds of receptors that all contain the so-called C-type lectin domain (CTLD) and have meanwhile been divided in 17 subgroups based on their structure. Most CLRs function as opsonins that lack the ability to directly induce pro-inflammatory responses. Specific subgroups such as the dectins, however, can induce the NF-κB signaling cascade *via* a complex composed of CARD9, Bcl-10, and mucosa-associated lymphoid tissue lymphoma translocation protein-1 (MALT-1). Furthermore, Dectin-1 signaling initiates phagocytosis of microbes upon binding to particulate ligands [148].

NLRs. The family of intracellular NOD-like receptors is divided into four subfamilies based on different N-terminal effector domains. Similar to other PRR-associated proteins, NLRs nucleate large signaling complexes (SMOCs), which either form the caspase-1 dependent "inflammasomes", activate MAPK and NF-κB pathways in caspase-1 independent fashion, or act in the nucleus as transcriptional regulators [156]. Within the NLRC (formerly known as NOD) subfamily, NOD1 and NOD2 are best described. They recognize different components of bacterial peptidoglycan [NOD1: D-γ-glutamyl-meso-DAP dipeptide (iE-DAP); NOD2: muramyl dipeptide (MDP)], and upon activation undergo oligomerization, which enables interaction with the kinase receptor-interacting protein 2 (RIP2; also known as CARDIAK or RICK). Further recruitment of a kinases as well as ubiquitin ligases and NEMO mediate activation of NF-κB and MAPKs. Both NOD1 and NOD2 may also recognize ssRNA and it has been shown that NOD2 signaling after RNA stimulation is RIP2 independent but engages MAVS to induce type I IFNs *via* IRF3. ssRNA triggering of NOD2 furthermore synergizes with previous MDP stimulation in production of pro-inflammatory cytokines [157].

Inflammasomes. Caspase-1 dependent signaling complexes termed inflammasomes perform the crucial task to produce the mature form of the pro-inflammatory cytokines IL-1β and IL-18 in response to a variety of pathogenic, but also endogenous danger-associated stimuli, such as ATP and uric acid, or crystalline structures, such as alum and silica [158]. Importantly, inflammasome activation requires two signals. Prior triggering of TLRs as first signal is necessary to induce production of pro-IL-1β, which is then processed by the inflammasome upon its activation by a second signal [159]. They are generally

composed of a sensor protein belonging to the absent in melanoma (AIM)2-like receptor (ALR)-, RLR- or NLR families, the adaptor protein apoptosis-associated speck-like protein containing a CARD (ASC) and the inactive zymogen procaspase-1. Formation of the inflammasome is enabled only after triggering of the sensing receptor, which enables sensor oligomerization and recruitment of ASC and procaspase-1. The close proximity of zymogens within the inflammasome is believed to facilitate their autocatalytic cleavage into the enzymatically active protease caspase-1, which then cleaves its substrates pro-IL-1β and pro-IL-18 into their active forms [158]. Triggering of the inflammasome furthermore provokes an extremely rapid, inflammatory form of cell death termed "pyroptosis". After this explosion-like cell death, prion-like ASC structures may serve as messengers to promote cell-to-cell communication in at least two ways: first, ASC oligomers continue to produce IL-1β in the extracellular space and second, ASC prions act as danger signals themselves, as their uptake by macrophages induces further production of IL-1β. Consequently, an initial triggering of only few sensor molecules may induce an immune response that is extensively amplified *via* polymerization of ASC-caspase-1 prions, which then expand the inflammasome response to other innate cells [158].

Multiple NLRPs (NALPs), NLRCs (NODs), and AIM2-like proteins serve as inflammasome- nucleating proteins. Of these, the best-described initiator is $NLRP_3$, which was shown to be activated in canonical or non-canonical manner, depending on the activating stimuli. The canonical pathway is induced by certain Gram-positive bacteria, viruses such as influenza virus, pore-forming toxins, as well as by a row of endogenous ligands, such as ATP and crystalline substances such as alum or silica. Rather than recognizing such a divers set of ligands, it is now accepted that $NLRP_3$ responds to stress-induced signaling pathways including potassium efflux, the generation of mitochondrial reactive oxygen species (ROS), cathepsin release as a result of phagolysosomal membrane destabilization, release of mitochondrial DNA, or translocation of $NLRP_3$ to mitochondria through the adaptor molecule MAVS [158]. Non-canonical activation has been proposed to occur by direct recognition of cytoplasmic LPS by caspase-11. Direct activation of caspase-11, however, seems to be against former paradigms, as it has never been shown that caspases bind PAMPs directly and it was believed that the scaffolding by a multiprotein complex is crucial for caspase activation. Therefore, caspase-11 seems to be an exception to the rule, as triggering by cytoplasmic LPS leads to self-oligomerization inducing subsequent caspase-1 maturation downstream of the $NLRP_3$ inflammasome well as cell death by pyroptosis, although the underlying mechanisms remain unknown. Since caspase-11 is only expressed in mice, it is believed that the caspases 4 and 5 are the respective homologues that perform non-canonical inflammasome activation in humans [160]. All together, the field of innate pattern-recognition, and especially regarding the induction of inflammasomes and other novel SMOCs, is constantly moving. It is to expect that various paradigms will have to be re-considered upon new insights.

Signaling effectors: MAPKs, NF-κB, IRFs and AP-1. MAPKs are ubiquitously expressed and respond to a variety of stimuli including growth factors, hormones, cytokines, agents that signal through G

protein-coupled receptors, or are related to TGF-β, and environmental stresses [161]. Thus, multiple cellular processes involve activation of MAPKs, which is not limited to innate immunity. Hence, MAPKs may promote tumor cell apoptosis in response to cytotoxic agents and at the same time, activate innate immunity as a result of inflammation or PRR-triggering. A complex network of distinct intermediate signaling components thus regulates specific responses. MAPK initiation in innate immunity involves simultaneous or subsequent induction of the NF-κB, AP-1 or IRF transcription factors. Importantly, while NF-κB and AP-1 mediate induction of proinflammatory responses, IRFs are essential for production of IFNs (Figure 4-7).

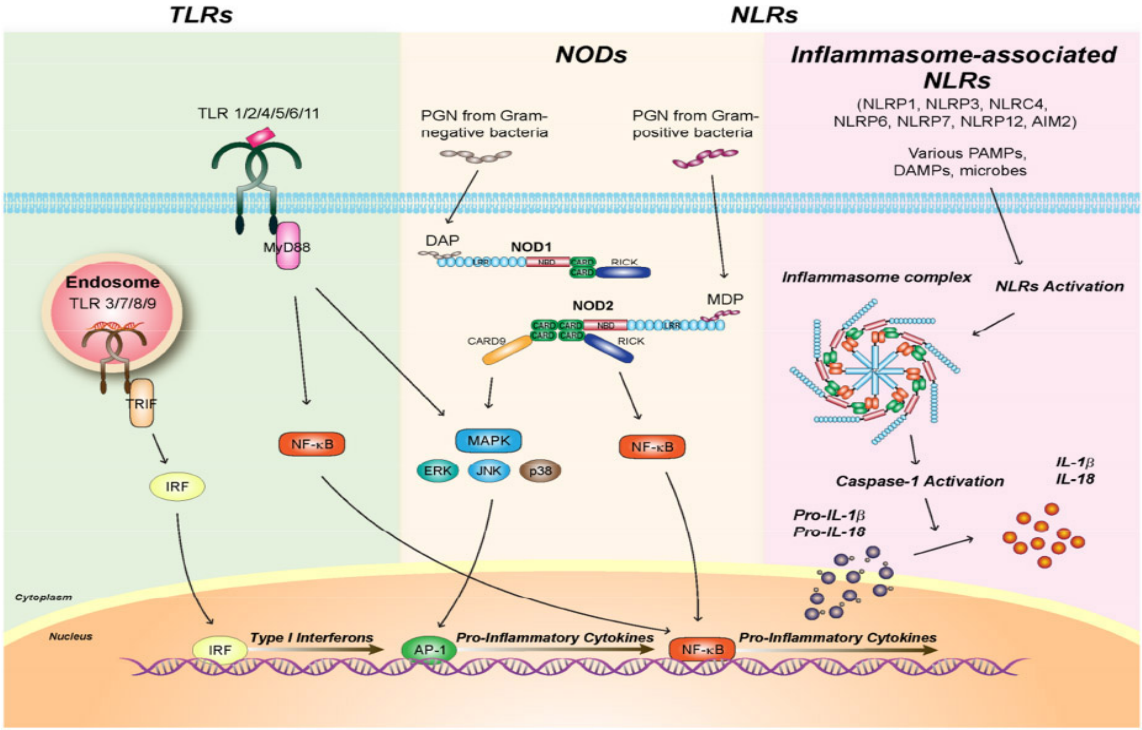

Figure 4-7 ***Innate signaling pathways: induction of MAPKs, NF-κB, AP-1 and IRFs***. "TLRs located in plasma membrane (TLR1, 2, 4, 5, 6, 11) activate the NF-κB and MAPK (JNK, ERK, p38) signaling pathways *via* MyD88. Nucleic acid recognition by endosomal TLRs (TLR3, 7, 8, 9) induces production of type I interferon and proinflammatory cytokines *via* TRIF-IRF3 and MyD88-NF-κB signaling pathways, respectively (left). NOD1 and NOD2 recognize i.e.-DAP and MDP from bacterial cell wall components, respectively, while NOD-induced proinflammatory responses require MAPK and NF-κB activation through the recruitment of adaptor molecule CARD9 and RICK/RIP2. Members of NLRs participate in the activation of inflammasome complex consisting of NLRs, procaspase-1 and ASC in the cytosol". Adapted from Hyo Sun Jin, Jeong-Kyu Park and Eun-Kyeong Jo. Toll-like Receptors and NOD-like Receptors in Innate Immune Defense during Pathogenic Infection. Reprinted with permission from Creative Commons Attribution (CC BY) license (open access article) [162].

MAPKs themselves are activated by phosphorylation within a three-tiered signaling cascade in which upstream kinases phosphorylate downstream kinases. Hence, MAPKs are initiated via tyrosine/threonine (Tyr/Thr) phosphorylation by dual-specificity MAPK kinases (MAP2Ks, also called MEKs or MKKs). These MAP2Ks are activated by serine-threonine (Ser/Thr) phosphorylation mediated by upstream MAPK kinase kinases (MAP3Ks), while MAP3Ks are typically activated by interactions with a small GTPase and/or phosphorylation by protein kinases downstream from cell surface receptors

[163]. 14 MAPKs are known in mammalian cells, including the classical MAPKs extracellular signal-regulated kinase 1 (ERK1) and ERK2, the p38 MAPK family, which comprises four isoforms (p38α, p38β, p38γ and p38δ), and the Jun N-terminal kinase (JNK) family, consisting of three isoforms (the constitutively expressed JNK1 and JNK2, as well as the tissue-specific JNK3, which is mainly expressed in the brain). ERK1/2 are activated by the MAP2Ks MKK1 or MKK2 and p38 is activated by the MKK3 and MKK6, while JNKs are phosphorylated preferentially by MKK4 and MKK7. MAP3Ks for the JNK module include MEKK1 and MEKK4, MLK2 and MLK3, ASK1, TAK1, and Tpl2. MAPKs can either induce activation of downstream kinases or transcription factors such as CCAAT/-enhancer-binding protein homologous protein (CHOP), nuclear factor of activated T cells (NFAT) or AP-1 [161].

4.4 Microtubule function

The eukaryotic cytoskeleton is composed of three types of filamentous structures: i.e., intermediate filaments, actin filaments and microtubules, of which all are linked with each other. The long and tubular-structured microtubules (MTs) are formed by polymerization of α- and β-tubulin subunits that associate to heterodimers. MTs orchestrate numerous cellular activities such as organizing cytoplasmic organelles, directing intracellular transport, supporting cell proliferation, inducing cellular motility as well as maintaining cell shape and polarization [164-166]. Polymerization of MTs occurs *via* the nucleation-elongation mechanism, in which a short microtubule nucleus is formed prior to rapid elongation at the ends of the MTs by non-covalent addition of tubulin dimers. Polymerization and depolymerization processes are highly dynamic as microtubules switch stochastically between states of consecutive growing and shortening, a process that is crucial to the cellular functions of MTs and that is called "dynamic instability". Transitions during this process are called "catastrophes" (from growth to shrinkage) and "rescues" (change to assembly of MTs) [167]. As these dynamics are not only equilibrium-driven, energy is provided by the hydrolysis of GTP at the time that tubulin with bound GTP adds to the microtubule ends (Figure 4-8). MTs are polar structures having a fast growing (+) end exposing β-tubulin subunits and a slow growing (-) end exposing α-tubulin subunits. This polarity is an important factor for directing movement along MTs. Secondly, microtubules undergo "treadmilling", a dynamic behavior in which tubulin molecules bound to GDP dissociate from one end and are replaced by the addition of tubulin molecules bound to GTP at the opposite end of the same MT [168, 169].

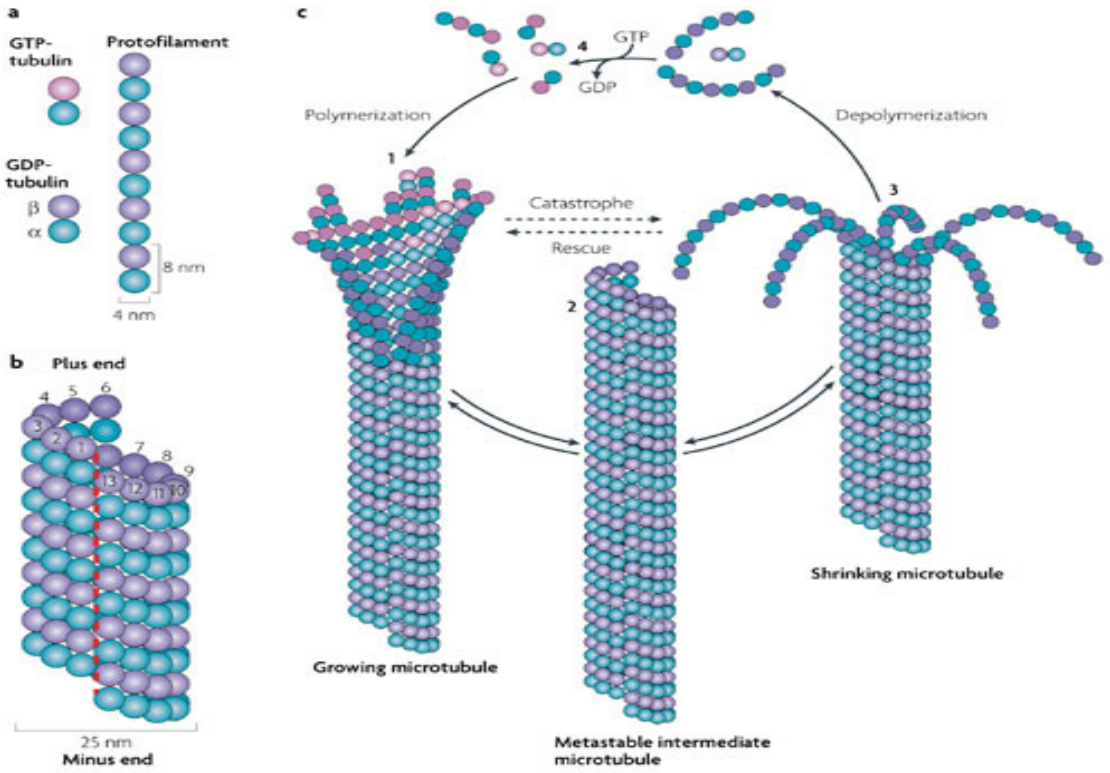

Figure 4-8 ***Microtubule structure***. (A) α- and β-tubulin molecules combine to form heterodimers. 13 of these vertically-stacked tubulin heterodimers form the protofilaments, which are arranged side-by-side to form a hollow, cylindrical microtubule. (B) The minus end final subunits are α-tubulin (blue), whereas the plus end final subunits are β-tubulin (purple). The red dashed line along the length of the microtubule indicates the seam formed by two adjacent protofilaments. MTs are usually nucleated by a complex containing γ-tubulin as well capping proteins at the minus end (not shown). (C) GTP bound to tubulin subunits (lighter color) at the plus end loose one phosphate with time, resulting in GDP-bound tubulin subunits within the MT. Adapted from Anna Akhmanova and Michel O. Steinmetz. Tracking the ends: a dynamic protein network controls the fate of microtubule tips. Reprinted with permission from Nature Publishing Group © 2015 [170].

MTs in most cells grow out from a microtubule-organizing center (MTOC), in which the minus ends of microtubules are anchored. In eukaryotic cells the centrosome takes over the role of the MTOC and is located near the nucleus in non-dividing interphase cells. Importantly, during mitosis duplicated centrosomes are the starting point for outward growing MTs to form the mitotic spindle [167].

4.4.1 Microtubule-binding anti-cancer agents

Due to their major contribution to important cellular processes such as the precise segregation of chromosomes during cell division, the transport of cellular cargos, or the positioning and movement of intracellular organelles, MTs have been extensively explored as target for anti-cancer therapeutics [165, 169, 171]. Inhibition of microtubule function leads to cell cycle arrest at G2/M phase and subsequent cell death. Microtubule-targeted drugs at relatively high concentrations either inhibit microtubule polymerization, destabilize microtubules and decrease microtubule polymer mass, or promote microtubule polymerization, stabilize microtubules and increase the polymer mass. By suppressing the dynamic instability of microtubules, these compounds induce mitotic arrest leading to subsequent

inhibition of cell proliferation and induction of apoptosis. Most microtubule-targeted antimitotic drugs have originally been isolated from a large range of plants (i.e., algae) and animals (i.e., sea hares), with the earliest discovery being the *vinca*-alkaloids that have been isolated over 40 years ago and are meanwhile widely used for treatment of mainly hematologic, but also solid cancers [169, 172]. Based on their effect on MTs, these compounds are usually classified into two main groups (Table 4-1):

Microtubule-destabilizing agents stimulate depolymerization of microtubules at high doses. Compounds of this class include the *vinca*-alkaloids (vinblastine, vincristine, vinorelbine, vindesine and vinflunine), nocodazol, colchicine, dolastatins, maytansines (mertansines), combretastatins and others (cryptophycins, halichondrins, estramustine, noscapine, rhizoxin, spongistatins, podophyllotoxin, steganacins and curacins).

Microtubule-stabilizing agents stimulate microtubule polymerization and include taxol (paclitaxel), docetaxel (taxotere), the epothilones, discodermolide, the eleutherobins, sarcodictyins, laulimalide, rhazinalam, and certain steroids and polyisoprenyl benzophenones.

Of note, both classes, although increasing or decreasing microtubule polymerization at high concentrations (e.g., 10-100 nM for vinblastine in HeLa cells), powerfully suppress microtubule dynamics at 10–100-fold lower concentrations and, therefore, kinetically stabilize microtubules without changing the microtubule-polymer mass. In other words, the effects of the drugs on dynamics are often more pronounced than their effects on polymer mass [169].

Table 4-1 ***Microtubule-binding agents currently in clinical practice or in development in clinical trials.*** Abbreviations: ADC, antibody–drug conjugate; ALL, acute lymphoblastic leukemia; NSCLC, non-small-cell lung cancer; GBM, glioblastoma multiforme; nab, nanoparticle albumin-bound; T-DM1, trastuzumab emtansine. Adapted from Herbert H Loong, Winnie Yeo. Microtubule-targeting agents in oncology and therapeutic potential in hepatocellular carcinoma. Reprinted with permission from Dove Medical Press © 2015 [173].

Mechanism of action	Type of microtubule-binding agent	Family	Compound	Clinical applications/pertinent active clinical trials
Microtubule destabilizing	Vinca-domain binder	Vincas	Vincristine	ALL, lymphomas, various solid tumors
			Vindesine	ALL, lymphomas, lung cancer
			Vinorelbine	Breast cancer, NSCLC
			Vinblastine	Lymphomas, various solid tumors
			Vinflunine	Bladder cancer, NSCLC, breast cancer
		Halichondrin	Eribulin	Breast cancer
		Maytansinoids	Mertansine ADCs	T-DM1 approved for breast cancer
		Dolastatins	Brentuximab vedotin	Hodgkin's lymphoma
	Colchicine-domain binder	Combretastatins	Fosbretabulin	Phase I/II trials in GBM, lung, thyroid, and sarcomas
			Verubulin	
			Crinobulin	
			Ombrabulin	
Microtubule stabilizing	Taxol-domain binder	Taxanes	Paclitaxel	Ovarian cancer, breast cancer, NSCLC
			Docetaxel	NSCLC, breast cancer, prostate cancer, stomach cancer, head and neck cancer
			Cabazitaxel	Prostate cancer
			Nab-paclitaxel	Breast cancer, pancreas cancer
		Epothilones	Ixabepilone	Breast cancer
			Patupilone	Clinical trials for brain metastases in breast and ovarian cancers, melanoma, and other solid tumors
			Sagopilone	Clinical trials in GBM, prostate, and lung cancers
			KOS-1584 (epothilone D analog)	Phase II trials in NSCLC
Others	Estramustine – binds to microtubule-associated protein			Prostate cancer; clinical trials with taxanes, vincas, and ixabepilone for prostate cancer

4.4.1.1 Dolastatins

Dolastatin 10, described as one of the most potent antineoplastic agents, was originally isolated from the Indian Ocean sea hare *Dolabella auricularia* by George Pettit (Figure 4-9) [174]. The five-subunit penta-peptide potently inhibits microtubule assembly by interacting with tubulin at the "peptide sub-site" of tubulin's "*vinca* domain" (Table 4-1). The binding site is in close physical proximity to vinblastine, with dolastatins acting as non-competitive inhibitors of vinblastine binding to tubulin [175]. Dolastatin 15 has very similar properties and although only slightly differing in structure, it is nine times less potent than dolastatin 10, but both are more potent than vinblastine [176]. Meanwhile, a range of synthetic analogues, the auristatins, have been synthesized and although dolastatin 10 failed in a phase II clinical trial with advanced breast cancer patients due to high toxicity when administered systemically [177], further auristatins have been developed for use in antibody-drug conjugates (ADC) [178]. In terms of hydrophobicity, stability and potency, monomethylauristatin E (MMAE) was the most successful compound and is now used as cytotoxic payload of the ADC brentuximab vedotin, developed by Seattle Genetics and approved for treatment of relapsed Hodgkin lymphomas (HL) and systemic anaplastic large cell lymphomas (ALCL) [179].

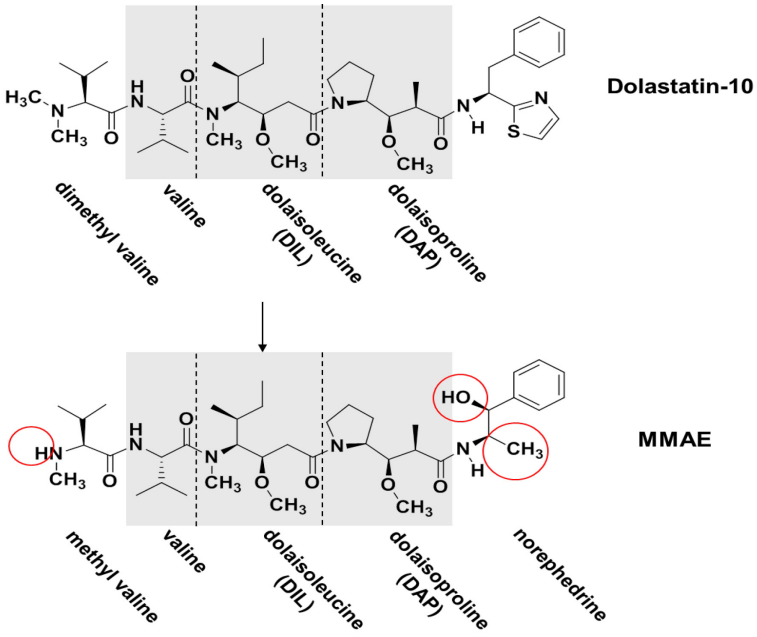

Figure 4-9 ***Chemical structures of dolastatin 10 and MMAE.*** Image courtesy of Robert Lyon, Seattle Genetics.

4.4.1.2 Maytansinoids

Maytansine, a natural product originally derived from the bark of the African shrub *Maytenus ovatus*, has been known to exert its antimitotic activity by inhibiting the assembly of microtubules and blocking the cells at mitosis. Its structural analogue ansamitocin P_3 binds to tubulin in a competitive manner with vinblastine and rhizoxin suggesting that it partially overlaps the vinblastine binding site (Figure 4-10; Table 4-1) [180-182]. Treatment of MCF-7 breast cancer cells with ansamitocin P_3 resulted in severe disruption of interphase and mitotic microtubules. The affected cells were blocked in mitosis and accumulated p53 and its downstream partner p21 in the nucleus, which activated apoptotic cell death in these cells [183]. Similar to dolastatin 10, systemic administration of free maytansinoids has demonstrated substantial toxicity. The extraordinary cell-killing potency, though, has led to the exploration of maytansine derivatives as cytotoxic payloads of antibody-drug conjugates [184]. In addition, synthetic derivatives of maytansine have been developed that possess a 100- to 1000-fold higher cytotoxic potency than clinically used anticancer drugs, such as the *vinca* alkaloids [185]. Amongst those, DM1 has been developed for conjugation to the α-HER2 antibody trastuzumab (Herceptin®), which has been approved for treatment of HER2-overexpressing metastatic breast cancer in 1998 [186]. The resulting trastuzumab-emtansine (T-DM1) has recently been approved in HER2-positive breast cancer while further maytansinoid-conjugated antibodies, such as BT062 (α-CD138-DM4), SAR3419 (α-CD19-DM4), BAY94-9343 (α-mesothelin-DM4), and IMGN529 (α-CD37-DM1) are currently under clinical evaluation in phase I/II protocols [187].

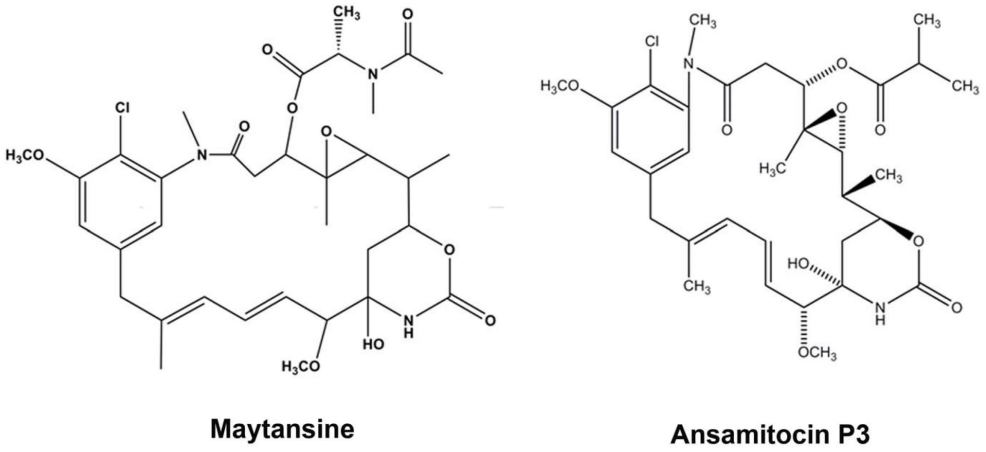

Figure 4-10 ***Chemical structures of maytansine and its analogue ansamitocin P3.*** Adapted from Venghateri JB. Ansamitocin P3 depolymerizes microtubules and induces apoptosis by binding to tubulin at the vinblastine site. Reprinted with permission from Creative Commons Attribution (CC BY) license (open access article) [183].

4.4.2 Regulation and sensing of MT structure

The functional heterogeneity of MTs is largely mediated by a variety of microtubule-associated proteins (MAPs), such as motor-proteins or microtubule plus end-tracking proteins (+ Tips), by expression of different tubulin isotypes, or by post-translational modifications (PTMs) [188, 189]. Similarly, small Rho-GTPases, which belong to the Ras superfamily of GTPases, have been described as major regulators of cytoskeleton function [190]. The Ras homolog gene (Rho) family of small GTPases compromises at least 20 members, from which Rac, RhoA/B/C, and Cdc42 have been best characterized. The so-called "molecular switches" constantly cycle between their active, GTP-bound and inactive, GDP-bound state and have been implicated in controlling MAPK signaling pathways as well as cell cycle-associated processes [191]. They are themselves carefully regulated by a large amount of activators and inhibitors. A large variety of guanine nucleotide exchange factors (GEF) mediate activation by catalyzing GDP exchange with GTP, whereas the group of GTPase-activating proteins (GAPs) induce deactivation *via* GTP hydrolysis [190]. Finally, RhoGTPases are regulated by guanine nucleotide exchange inhibitors (GDIs) that extract inactive Rho proteins from membranes and sequester them in the cytosol [192]. Functionally, Rho is known to be responsible for the assembly of contractile actin and myosin filaments (stress fibers), Rac mediates the assembly of actin-rich surface protrusions (lamellipodia), and Cdc42 was shown to promote the formation of actin-rich, finger-like membrane extensions (filopodia) [190].

4.4.3 Linking microtubule-disruption with DC maturation

In the context of signal transmission in response to microtubule destabilization, GEF-H1, a guanine nucleotide exchange factor for Rho (first characterized by Ren and colleagues) [193], is particularly interesting. Only two GEFs are currently known to co-localize with MTs, namely p190Rho-GEF and

GEF-H1 (as well as its murine homologue lfc). However, of those only GEF-H1 may sense MT depolymerization [194]. Moreover, Krendel *et al*. provide experimental evidence that GEF-H1 is responsible for regulating Rho activity in response to microtubule depolymerization and that microtubule disassembly results in the activation of RhoA (Figure 4-11) [195-197]. Also, it has been shown that GEF-H1 preferentially activates RhoA when compared to Rac1 or Cdc42 [195]. Importantly, MT depolymerization in response to the MDA nocodazol disrupted the phosphorylated, hence inhibited GEF-H1 complex, resulting in potent activation of GEF-H1 [198]. Interestingly RhoA activation by the MDA vinblastine has previously been shown for tumor cells as well as for DCs [199, 200]. Due to the localization of GEF-H1 on MTs and its specificity for RhoA, it seems that during MT depolymerization, RhoA might be an important molecular mediator of downstream signaling. Importantly RhoGTPases have been shown to induce MAPK signaling cascades *via* interaction with MAP3K family proteins or Rho-associated kinase (ROCK) [201, 202]. Both MAP3Ks as well as ROCK have been known to induce activation of the stress-activated protein kinases JNK and p38, which in turn induce AP-1 and NF-κB dependent gene transcription [202, 203]. Therefore, Rho-mediated MAP kinase activation might possibly be involved in linking microtubule disassembly with activation of pro-inflammatory molecules in innate immune cells.

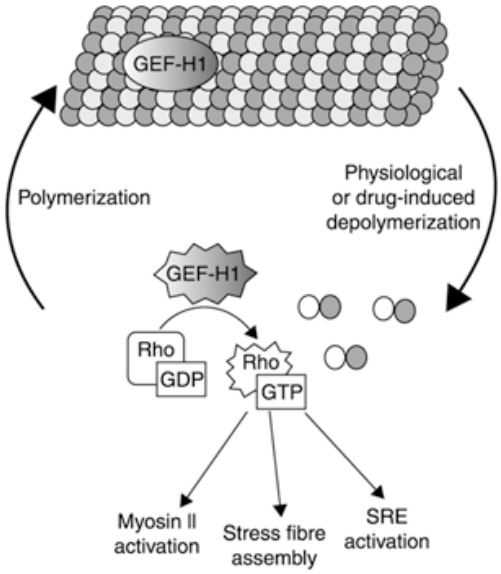

Figure 4-11 ***A model for the regulation of GEF-H1 activity by microtubules***. "Inactive GEF-H1 is bound to MTs and released upon disruption of those. Release induces activation of GEF-H1, which in turn catalyzes GTP binding to RhoA. Active RhoA may then induce formation of actin stress fibers, increase myosin II contractibility or induce serum-responsive element (SRE)-dependent gene expression". Adapted from Krendel M. Nucleotide exchange factor GEF-H1 mediates cross-talk between microtubules and the actin cytoskeleton. Reprinted with permission from Nature Publishing Group © 2015 [198].

5 Aim of the thesis

Efficient therapeutic options for patients suffering from cancer are still limited. Cytotoxic or targeted therapies display high toxicity, and although these therapies are often initially successful, most tumors ultimately relapse. On the other hand, recent advances in understanding the anti-tumor immune response have led to major improvements in the field of cancer immunotherapy [204]. In particular, blocking immune checkpoints with monoclonal antibodies such as anti-CTLA-4 and anti-PD-1 has emerged as promising strategy that mediates clinically significant responses in a broad variety of cancer types [205, 206]. Nevertheless, only a fraction of patients respond and many responders eventually relapse. Possible explanations include immune effector cell exhaustion at the tumor site mediated by the immunosuppressive tumor microenvironment [207]. In this line, the physical reduction of the primary tumor burden by ionizing radiation, targeted therapies or chemotherapy may relieve the suppressive pressure exerted on the immune system and at the same time, release tumor-associated antigens for priming of *de novo* T cell responses. Furthermore, it has recently become evident that specific chemotherapeutic agents and molecular targeted therapies display formerly unrecognized immunomodulatory features, and thus mediate therapeutic effects by promoting anti-tumor immune responses [88, 89, 208]. Therefore, the combination of selected chemotherapy partners with immunotherapies has great clinical potential, but requires a deeper understanding of the immune-promoting nature of these agents.

In order to provide the basis for rational development of chemo-immunotherapy regimens, we formulated the following aims to be addressed in this thesis:

I. *To screen classical chemotherapeutic agents with distinct pharmacological mechanisms for their capacity to trigger DC maturation.*

II. *To provide a detailed description of the nature of the anti-tumor immune response initiated by DC-stimulatory compounds.*

III. *To characterize the interplay of immune effector cells with those agents and to define the impact of host immunity on the compounds' anti-tumor efficacy.*

IV. *To characterize potentially synergistic treatment regimens that combine immunostimulatory chemotherapeutics with immunotherapy, including a description of the immunological basis of synergistic regimens.*

V. *To translate important findings into the human setting and to put observations in a clinically relevant perspective.*

VI. *To identify the molecular pathways that mediate activation of dendritic cells upon drug-treatment.*

6 Methods

For a listing of materials and mammalian cell lines, please refer to chapter 10 (Attachments).

6.1 Cell culture methods

All work concerning mammalian cell culture was done under sterile conditions. Cells, buffers, media and reagents were handled under a laminar flow bench that guarantees a particle-free environment inside the hood by constantly passing the air though filters with a size of 0.2 µm. All fluids were either purchased sterile, autoclaved or passed though filters with 0.2 µm pore size. Incubation of cells took place in respective incubators with 37 °C in saturated steam atmosphere and 5-10% CO_2. The media was exchanged every 3-4 days. In case cells of one flask reached confluency, they were detached with PBS + 2 mM EDTA, centrifuged and resuspended in fresh medium to be expanded onto two or more culture flasks.

SP37A3 DCs were grown in SP-culture medium (IMDM + 10% FCS, 1 mM Na-pyruvat, 10 mM non-essential amino acids, 100 U penicillin / 0.1 mg/ml streptomycin, 50 µM β-mercaptoethanol and 2 mM glutamin) supplemented with 20 ng/mL murine GM-CSF and 20 ng/mL M-CSF. DC stimulation with was performed in IMDM complete supplemented with 20 ng/mL GM-CSF only.

Murine and human tumor cell lines were grown in DMEM complete medium (DMEM + 10% FCS, 1 mM Na-pyruvat, 10 mM non-essential amino acids, 100 U penicillin / 0.1 mg/ml streptomycin, 50 µM β-mercaptoethanol and 2 mM glutamin).

Cell counting

The cell number was determined using a Neubauer hemocytometer. 10 µL of a homogeneous cell suspension were mixed with trypan blue solution 1:1 and pipetted under the microscope slide of the hemocytometer. Viable cells, i.e., cells that were not stained by the blue dye, present in 16 small squares were counted 4 times (upper left, upper right, lower right and lower left quadrant). The number of cells per mL was then calculated as follows: average number of cells in 16 small squares x 2 x 10^4.

Cryoconservation and defreezing of cells

For long-term storage in liquid nitrogen, cells were frozen in FCS + 10% DMSO (freezing medium) in cryovials. To this end, cells were detached, counted and resuspended in freezing medium at a density of $1x10^6$ - $5x10^6$ cells/mL, with 1 mL per vial. The vials were then transferred into a cryo freezing container and stored at -70 °C for at least two days before transferring the vials into a liquid nitrogen tank.

For a quick defreezing of cells, the vials were thawed in the water bath at 37 °C until only a small amount of frozen material was left. By carefully pipetting up and down, the cell suspension was thawed

completely, added to 10 mL pre-warmed culture medium and centrifuged at 300xg for 5 minutes. Finally, cells were resuspended in 5-10 mL culture medium and transferred into an appropriate cell culture flask.

6.1.1 Generation of murine bone marrow-derived DCs

Bone marrow cells from C57Bl/6 WT, TRIF$^{-/-}$, TLR4$^{-/-}$, MyD88$^{-/}$, RIP2$^{-/-}$ and NALP3$^{-/-}$ mice were prepared as previously described [209]. Briefly, bone marrow cells were flushed from femurs and tibias with pre-warmed culture medium, washed, depleted of red blood cells and washed again. 2x10^{6} cells in 10 mL RPMI1640 complete medium supplemented with 20 ng/mL GM-CSF were plated per 10 cm cell culture dish. 10 mL culture medium containing GM-CSF was added on day 3 and 10 mL medium was exchanged on day 6. DCs were activated on day 7 either on 10 cm culture dishes or on 96-well plates (7x10^{4} cells/well). After 24h stimulation, the phenotype was assessed by flow cytometry or DCs were used in co-culture assays.

6.1.2 Generation of human DCs from CD14^{+} monocytes

PBMCs were isolated from buffycoats from healthy blood donors (Blood Transfusion Center, University Hospital Basel) by density gradient centrifugation using Histopaque®-1077. CD14^{+} monocytes were isolated from PBMCs by either positive selection using MACS CD14-microbeads (Miltenyi Biotec) or by plastic adherence as described previously [210]. The CD14^{-} PBMC fraction was kept for subsequent isolation of T lymphocytes (see below). CD14^{+} monocytes were counted and cryo-preserved in freezing medium or cultured in RPMI1640 supplemented with 10% FCS, 50 ng/mL recombinant human GM-CSF and 250 U/mL recombinant human IL-4 on 6-well plates [137]. After 5 days of culture the surface expression of CD11b, CD11c, CD40, CD86 and HLA-DR was analyzed by flow cytometry and cells were used for subsequent assays.

6.1.3 Purification of human T cells

CD4^{+} T cells and CD8^{+} T cells were purified from the CD14^{-} PBMC fraction by positive selection using anti-CD4 or anti-CD8 Microbeads (Miltenyi Biotec), respectively, according to the manufacturer's instructions. The purity of positively selected CD4^{+} and CD8^{+} T cells was analyzed by direct staining for membrane expression of CD4 and CD8 by flow cytometry. A portion of both CD4^{+} and CD8^{+} T cells was cryopreserved for later use in T-cell priming experiments.

6.2 *In vitro* and *ex vivo* cell-based assays & flow cytometry

6.2.1 Flow cytometry

Staining of cell surface or intracellular proteins was generally conducted in 96-well round bottom plates. All washing steps were performed with 200 µL buffer per well followed by centrifugation at 300xg at 4 °C, buffer was discarded by inverting the plate quickly. Cells were harvested and washed in cold PBS prior to incubation with an Fc receptor-blocking antibody to reduce non-specific binding of the staining antibodies (50 µL/well; 1:100 in PBS) together with a fixable live/dead stain (LD-IR; 1:400) for 20 minutes on ice. The cells were washed twice with cold FACS buffer before addition of a mix of fluorescently labeled monoclonal antibodies for staining of cell surface proteins. The cells were then incubated for another 30 minutes on ice and in the dark, followed by three more washing steps. In case of intracellular staining (e.g., for detection of cytokines), the cells were fixed in IC fixation buffer (eBioscience) for 20 minutes after surface staining. Staining of intracellular proteins was performed in permeabilization buffer (Biolegend) for 45 minutes at room temperature (RT) in the dark after 3 washing steps in permeabilization buffer. Finally the cells were washed twice and resuspended in FACS buffer prior to analysis.

6.2.2 Drug screen for DC maturation

24 chemotherapeutic compounds were tested for their ability to induce DC maturation at varying doses (for a list of cytotoxic compounds please refer to the Materials section; chapter 10.1). To this end, murine SP37A3 DCs or human monocyte-derived DCs (moDCs) were tested for their maturation status prior to the experiment. Non-treated and LPS-treated (500 ng/mL) cells were stained for anti-mouse CD86-APC, anti-mouse CD40-PE and anti-mouse MHCII (I-A/I-E)-Pacific Blue or anti-human CD86-PE, anti-human CD40-APC and anti-human MHCII (HLA-DR)-Pacific Blue, respectively. Dead cell exclusion occurred in both cases by prior Live/Dead-IR staining.

Experiments determining the optimal assay plate, cell number and assay medium were performed previously. Murine SP37A3 cells were plated at $8x10^4$ cells/well in 180 µL medium supplemented with 20 ng/mL mGM-CSF in 96-well flat bottom plates. The cells were allowed to adhere overnight before the chemotherapeutic compounds were added 10-fold concentrated in 20 µL to yield final concentrations between 0.01 µM – 10 µM. Controls contained 3 wells of a) untreated cells, b) LPS-treated cells (500 ng/mL) and d) vinblastine-treated cells (0.1 µM). For determination of optimal assay conditions when performing the drug screen with human DCs, various protocols were tested. As human monocyte-derived DCs are highly sensitive to mechanical stress, $CD14^+$ monocytes were seeded onto 24-well plates ($5x10^4$ cells/well in 500 µL RPMI1640 + 10% FCS + 50 ng/mL hGM-CSF) immediately after purification and were left untouched for 5 days. On day 5 chemotherapeutics or LPS were added to the cells. Both human and murine cells were incubated with drugs or controls for 24 h, detached, washed and subsequently stained for flow cytometric analysis as described above. All assays were performed in

duplicates. Supernatants were kept and immediately frozen at -70 °C for later analysis of cytokine release by ELISA.

6.2.3 *In-vitro* stimulation of murine OVA-specific OT-I and OT-II T cells

To assess priming of antigen-specific T cells, SP37A3 DCs or day 7 BMDCs were pulsed for one hour with OVA full-length protein (0.1 mg/ml) *prior to* exposure to dolastatin 10 (0.1 µM) or LPS (500 ng/mL) for 24 hours. In case DCs were pulsed with the respective peptides, i.e., $OVA_{257-264}$ peptide (T4; SIITFEKL; low-affinity variant of SIINFEKL) or $OVA_{323-339}$ peptide (both 500 ng/mL), these were added *after* DC activation by dolastatin 10 or LPS for one hour. In both cases, activated and pulsed DCs were washed twice and counted. Meanwhile, $CD8^+$/ $CD4^+$ T cells were purified from LNs and spleen of naïve OT-I/ OT-II transgenic mice expressing a TCR specific for ovalbumin. T cells were separated from other splenocytes by negative selection using the Pan T cell Isolation Kit (Stemcell Technology) and were loaded with the proliferation dye eFluor670 (eBioscience) before seeding onto a 96-well round bottom plate at a density of $2x10^5$ cells/well. Activated DCs were added in varying cell densities to yield DC: T cell ratios ranging between 1:5 and 1:50. Proliferation of T cells was assessed after 3 days by flow cytometry.

6.2.4 Human mixed lymphocyte reaction

Human moDCs were activated with cytotoxic compounds [MMAE (1 nM), dolastatin 10 (1 nM)] or LPS (500 ng/mL) for 24h, washed twice in culture medium, counted and used for functional analysis. To this end, allogeneic $CD8^+$ T cells from healthy blood donors loaded with the proliferation dye eFluor670 were plated in sterile 96-well flat-bottom plates (10^5 cells/well) in RPMI complete medium containing 10% human serum (AB) instead of FBS. Activated DCs were added at various cell densities to yield DC to T cell ratios of 1:5 to 1:50. T cell proliferation was assessed after 4 days by flow cytometry.

6.2.5 Culture of human tumor explants

Tumor resections obtained from patients (based on signed informed consent) with different tumor entities, including non-small cell lung-, breast-, kidney- and stomach cancer, were cut into pieces of approximately 1-2 mm diameter and cultured in presence of cytotoxic compounds (0.1 µM) or LPS as positive control (500 ng/mL) for 24 h in 24-well plates. Analysis was performed using flow cytometry. For this purpose, tumor pieces were dissociated mechanically and digested enzymatically with accutase, collagenase IV, hyaluronidase, and DNAse typeIV (see recipe digestion mix). To this end, cut tumor pieces were transferred to 50 mL centrifuge tubes, 4 mL of digestion mix were added and the tubes were incubated for 1 - 1.5 h at 37 °C while shaking smoothly at 150 rpm. Cell suspensions were passed through a 70 µm nylon mesh to remove remaining tissue. Single-cell suspensions were washed once with culture medium and once with cold PBS before proceeding to the FACS staining. As

described above, cells were incubated with a FcR-blocking antibody together with the fixable near-IR Live/Dead stain in PBS and subsequently stained with anti-CD45, anti-CD11c, anti-CD11b, anti- HLA-DR, and anti-CD86 fluorescently labeled antibodies in FACS buffer.

6.2.6 Human lymphoma-DC co-culture

The $CD30^+$ lymphoma cell lines Karpas-299 and L-540 as well as the $CD30^-$ cell line Ramos were plated in 96-well plates ($5x10^4$ cells/well) in the presence of the antibody-drug conjugate brentuximab vedotin at concentrations between 0 and 10 µg/mL, or the control cytotoxic agents cisplatin, etoposide and mafosfamide at 100 µM for 3 days. On day 3, immature day 5 monocyte-derived dendritic cells (moDCs, see above) were added ($5x10^4$ cells/well) and co-cultured for another 24 h. Control DCs were left untreated or incubated with the free agent MMAE at 0.1 µM for 24 h. For analysis of moDC maturation by flow cytometry, the cells were stained for CD11c, HLA-DR and CD86. Dead cells were excluded by Live/Dead-IR staining.

6.2.7 Phenotypic characterization of patient PBMCs

PBMCs from six patients were collected before and after brentuximab vedotin administration. The patients received brentuximab vedotin 1.8 mg/kg per day every 21 days as monotherapy. The blood collection was performed before the first brentuximab infusion and just before the second application (except one patient, no. 2, from whom the follow-up blood sample was drawn after two administrations of brentuximab). PBMCs were isolated from heparinized blood samples by density gradient centrifugation using Histopaque®-1077. Multicolor flow cytometry analysis was performed to assess the frequency and activation status of T and B cells, as well as DC populations. For detection of $FoxP3^+$ regulatory T cells, intracellular staining using the FoxP3-Fix/Perm-Kit (Biolegend) was performed following the manufacturer's instructions. Dead cells were stained with Live/Dead near IR fixable dead cell stain.

6.3 Immunohistochemistry

Tumor biopsies were collected at the German Hodgkin Center, Köln (Prof. M. von Bergwelt-Baildon) from two patients with a $CD30^+$ cutaneous T cell and a $CD30^+$ Hodgkin lymphoma, respectively. The biopsies were taken before and after one and two cycles of brentuximab vedotin, respectively. Stainings were performed at the Institute of Pathology, University of Basel (Dr. S. Savic). The biopsies were fixed in 4% neutral-buffered formaldehyde and embedded in paraffin wax. All immunohistochemical stainings were performed using primary antibodies against CD30, CD_4 and CD8 (all Roche/Ventana Medical Systems) on a Benchmark XT autostainer (Roche/Ventana Medical Systems) according to the manufacturer's protocol. The biopsies were examined by 2 independent investigators. Lymphocytes expressing the above mentioned markers were quantified in an area of 10

high power fields (400x). Total numbers of lymphocytes (as determined by H&E staining), $CD30^+$ lymphoma cells, as well as $CD4^+$ and $CD8^+$ T cells were determined for pre- and post-therapy biopsies.

6.4 Cytokine detection

IL-1β, IL-6, and IL-12p40 in supernatants of murine DC cultures were detected by standard sandwich enzyme-linked immunosorbant assay (ELISA) procedures using commercially available kits, following manufacture's instructions. Furthermore, cytokine production of SP37A3 DCs or BMDCs was characterized by flow cytometric analysis. For this purpose, cells were cultured in presence of dolastatin 10, ansamitocin P_3 (both 0.01 µM) or LPS (500 ng/ml) for 20 h (IL-12p40), 15 h (IL-6) or 6 h (IL-1β). Brefeldin A was added for the whole incubation time (IL-1β and IL-6) or for the last 6 h of culture (IL-12p40). Cell surface staining of MHCII and CD11c was performed prior to fixation, permeabilization and intracellular cytokine staining.

6.5 Animal experiments

6.5.1 *In-vivo* activation of skin Langerhans cells

Dolastatin 10 (10 µg/animal), dolastatin 15 (10 µg/animal), vinblastine (17,6 µg/animal) or vehicle alone was injected intradermally (i.d.) into the ears of C57Bl/6 mice. Analysis was performed after 24 h using flow cytometry and immunofluorescence (immunofluorescence protocol described in paragraph 6.7). For flow cytometric analysis, epidermal sheets were dissociated mechanically and digested enzymatically by incubation with digestion mix for 1 h at 37 °C while shaking. Single-cell suspensions were prepared and stained with anti-CD45, anti-CD11c, anti-MHCII, and anti-CD86 antibodies. Dead cells were excluded using SytoxBlue® nucleic acid stain.

6.5.2 Analysis of DC homing to tumor-draining LNs

For detection of DC homing upon injection of free dolastatin, C57Bl/6 mice bearing subcutaneous (s.c.) E.G7 tumors were injected intratumorally (i.t.) with FITC-conjugated dextran (FITC-Dx; 100 µg/mouse) together with dolastatin 10 (10 µg/mouse) or PBS. For analysis of DC homing upon systemic administration of the anti-Thy1.1-MMAE ADC, mice bearing subcutaneous RMA-Thy1.1 tumors were injected intravenously with the anti-Thy1.1-MMAE ADC (30 mg/kg) or PBS 24 h prior to intratumoral injection of FITC-Dx (100 µg/mouse). Single cell suspensions from tumor-draining and non-draining LNs were prepared 48 h after injection of dolastatin 10 or ADC, stained for CD45, CD11c, MHCII and CD86 and analyzed by flow cytometry, while excluding dead cells from the analysis.

6.5.3 *In-vivo* stimulation of OT-I and OT-II T cells

LN and spleen cells from naïve OT-I and OT-II transgenic mice (congenic marker Ly5.2) were labeled with eFluor670 and adoptively transferred into C57Bl/6-Ly5.1 mice bearing s.c. MC38 tumors. After 24 h, mice were immunized via tail-base injection with peptides alone [25 µg/mouse $OVA_{257-264}$ peptide (T4) and 5 µg/mouse $OVA_{323-339}$ peptide], or together with dolastatin 10 (1 µg/mouse) or LPS (25 µg/mouse). Tumor-draining and non-draining inguinal LNs were dissected and single cell suspensions were prepared. Cells were stained for CD4 and CD8 and proliferation of OT-I $CD8^+$ T cells as well as OT-II $CD4^+$ T cells was assessed 4 days after adoptive transfer by flow cytometry.

6.6 Tumor challenge and therapeutic protocols

7-10 week-old C57Bl/6 mice were injected s.c. with 2.5 - $5x10^5$ tumor cells (i.e. E.G7, 3LL, MC38 or RMA-Thy1.1) in 100 µl DMEM without phenol red into the right flank. Tumors were allowed to grow until they reached a size of approximately 100 mm^3 before initiation of treatment or analysis of infiltrates. Tumor growth, determined as a function of tumor size over time, was measured every second day. Tumor volume was calculated according to the formula: $D/2*d^2$ with D and d being the longest and shortest diameter of the tumor in mm, respectively. According to animal regulations mice were euthanized when tumors reached a size of 1500 mm^3.

6.6.1 Vaccination in combination with dolastatin 10

For the dolastatin 10/vaccination treatment combination, a single dose of dolastatin 10 (0.4 mg/kg) was administered i.v. 15 days after tumor cell (3LL-OVA) injection. On days 17 and 24, mice were immunized intra muscular (i.m.) with $5x10^7$ plaque-forming units (pfu) of replication-deficient adenovirus type 5 encoding for chicken OVA (Ad-OVA).

6.6.2 Checkpoint blockade in combination with dolastatin 10

For the dolastatin 10/antibody treatment combination, two doses of dolastatin 10 (0.3 mg/kg) were administered i.v. on day 16 and 19 after tumor challenge (MC38). Treatment with four doses (250 µg per mouse and dose) of anti-CTLA-4 and anti-PD-1 [intra-peritoneal (i.p.) administration] was initiated at day 16 (without dolastatin treatment) or on day 21 (in combination with dolastatin treatment).

6.6.3 Treatment upon T cell-depletion/ IFN-γ neutralization

For T cell depletion mice were injected with anti-CD4 (clone: GK1.5) or anti-CD8 (clone: 53-6.72) antibodies at 10 mg/kg on day 14, 15, 19, 23 and 27 after tumor cell implantation. Dolastatin 10 (a single dose of 0.4 mg/kg) treatment was initiated on day 16. For IFN-γ neutralization mice were injected with anti-IFN-γ (clone: XMG1.2) at 25 mg/kg on day 14, 15, 19, 23 and 27 after tumor cell implantation.

6.6.4 Treatment in CD11c DTR/GFP mice, Rag2$^{-/-}$ mice or IFN-γ R$^{-/-}$ mice

WT C57Bl/6, Rag2$^{-/-}$, and IFN-γR$^{-/-}$ mice bearing s.c. E.G7 (or 3LL-OVA) tumors received intratumoral injections of dolastatin 10 (0.4 mg/kg) or vehicle (PBS) on day 10. WT and CD11c-DTR/GFP mice bearing s.c. MC38 tumors were treated i.v. with dolastatin 10 (0.4 mg/kg) on day 16. Diphteria toxin (DT; 4 ng/g body weight) or PBS (control) was injected i.p. on day 15.

6.6.5 Analysis of tumor infiltrating lymphocytes

7-10 week-old mice were injected s.c. with 5x10^5 MC38 tumor cells in 100 µl DMEM without phenol red into the right flank. On day 16 and 18 after tumor challenge mice were treated with dolastatin 10 (both 0.3 mg/kg) i.v., followed by three doses of anti-CTLA-4/ anti-PD-1 (250 µg each, i.p.) on day 20, 22 and 24. Mice receiving anti-CTLA-4/PD-1 only were treated on day 16, 18 and 20. On day 26 tumors were dissociated mechanically and digested using digestion mix. Cell suspensions were further enriched for immune cells by density gradient centrifugation using Histopaque®-1119 solution. After washing, single cell suspensions were stained for the indicated markers for flow cytometric analysis. For detection of IFN-γ-producing cells, single cell preparations were cultured over night in the presence of anti-CD3/CD28 (2/4 µg/mL) antibodies and monensin (2 µM).

6.7 Immunofluorescence

Skin Langerhans cells_CD86 and MHCII

Mice were treated as outlined in chapter 6.5.1 *(In-vivo activation of skin Langerhans cells)*. 24 h after injection of cytotoxic compounds or control substances, ears were harvested and epidermal sheets were separated. Epidermal sheets were prepared as previously described [211]. Epidermal sheets were stained overnight with anti-MHCII-PE (1:100) and anti-CD86-FITC (1:100) antibodies in 50 µl staining buffer (PBS + 5% FBS) at 4 °C, washed two times for 10 min with PBS + 5% FBS and mounted onto glass slides. Analysis was done using an Olympus BX61 fluorescence microscope.

SP37A3_α-Tubulin and GEF-H1

SP37A3 dendritic cells were serum-starved (IMDM w/o FCS) overnight. Two hours before treatment with ansamitocin P3 (0.1 µM) for 5 or 15 minutes, 2x10^5 cells were plated on polylysine-coated cover slips in 24-well plates in serum-free medium. After treatment, cells were washed twice with cold PBS (5 min each) on ice, fixed with IC fixation buffer for 20 min at RT, washed three times in PBS (5 min each) and permeabilized using 1x perm-buffer for 5 min. The coverslips were blocked with 10% FCS in perm-buffer for 30 minutes at RT to block nonspecific protein-binding sites. Primary antibodies (sheep anti-lfc/GEF-H1, 1:15 and rabbit anti-α-tubulin, 1:150) were added in 150 µL blocking buffer and coverslips were incubated for 1 h at RT prior to washing in perm-buffer (3x 10 min). Fluorochrom-labeled secondary antibodies (anti-sheep Alexa488, 1:200 and anti-rabbit Alexa647, 1:200) were added to the slides in 150 µL blocking buffer. After 1 h incubation at RT, coverslips were washed three times for 10

min in PBS and subsequently mounted using antifade reagent (ProLong®, Life Technologies) containing DAPI to stain nuclei. Slides were analyzed by confocal microscopy using the LSM 710 Rocky microscope (Zeiss) and Zen software (Zeiss).

6.8 Molecular biology methods

6.8.1 RNA isolation and quantitative real-time PCR (qPCR)

Total RNA was isolated from $1x10^6$ - $5x10^6$ cells using TRIzol-Reagent (Invitrogen Life Technologies) and Direct-zol™ RNA MiniPrep columns (Zymo Research) according to the manufacturer's instructions. RNA concentration and purity was determined using a Nanodrop spectrophotometer. Single-stranded cDNA was synthesized from total RNA (pretreated with DNaseI amplification grade) with the use of oligo(dT) as primer and RevertAid™ H Minus M-MuLV Reverse Transcriptase (Life Technologies) according to manufacturer's instructions.

Sequences of qPCR primers are depicted in Table 6-1. Primers were synthesized by Microsynth AG and were used for qPCR at 10 µM.

Table 6-1 ***Oligonucleotides used for qPCR***. Primer sequences are either based on previous reports or have been designed using the web-based primer design tool from Roche (Universal ProbeLibrary Assay Centre; https://lifescience.roche.com).

Gene	Sequence (5' – 3')	Source of sequence
CD80	GAAGCCGAATCAGCCTAGC CAGCGTTACTATCCCGCTCT	Roche Universal Probe Library
CD86	TCGTCTTTCACAAGTGTCTTCAG TTGCCAGTAGATTCGGTCTTC	Roche Universal Probe Library
IL-1β	CATGGAATCCGTGTCTTCCT GAGCTGTCTGCTCATTCACG	[212]
IL-6	AGTTGCCTTCTTGGGACTGA TCCACGATTTCCCAGAGAAC	[213]
IL-12p35	TGGCTACTAGAGAGACTTCTTCCACAA GCACAGGGTCATCATCAAAGAC	[214]
IL-12p40	CAGCTCGCAGCAAAGCAA GACGCCATTCCACATGTCACT	[215]
IL-23p19	TGCTGGATTGCAGAGCAGTAA GCATG CAGAGATTCCGAGAGA	[215]
IFN-α1	CCTGAGAA/GAGAAGAAACACAGCC GGCTCTCCAGAC/TTTCTGCTCTG	Roche Universal Probe Library
IFN-β	GCTCCTGGAGCAGCTGAAT CGTCATCTCCATAGGGATCTTGA	Roche Universal Probe Library
TNF-α	CTGTAGCCCACGTCGTAGC TTGAGATCCATGCCGTTG	Roche Universal Probe Library

S18RNA	AGTCAGTTCATCCGGCCTTA ATCTTCACGCACTCCTCGAT	Roche Universal Probe Library

Quantitative real-time PCR

qPCR was performed on the Applied Biosystems® Vii A7 Real-Time PCR System using the SYBR Green-based GoTaq® qPCR Master Mix (Promega). PCR reactions were performed in 40 cycles of 15 seconds at 95°C and 60 seconds at 60°C. Product was not generated in control reactions in which reverse transcriptase was omitted during cDNA synthesis. Gene expression values relative to S18RNA gene expression (internal control), and fold expression in treated samples normalized to expression in untreated DC samples was calculated by a comparative CT method according to the following formula [216]:

$2^{-\Delta\Delta C}{}_T$ = [(C_T gene of interest - C_T internal control) treated sample

- [(C_T gene of interest - C_T internal control) control sample)]

6.8.2 Western Blot

Cells ($2x10^6$ - $4x10^6$) were washed twice in ice-cold TBS prior to lysis in 100 µl ice-cold RIPA lysis buffer (10 mM Tris-Cl (pH 8.0), 1 mM EDTA, 0.5 mM EGTA, 1% Triton X-100, 0.1% sodium deoxycholate, 0.1% SDS, 140 mM NaCl, 1mM PMSF) containing a commercially available protease and phosphatase inhibitor cocktail (Thermo Scientific). Samples were cleared by centrifugation at 4 °C (10 min, 10.000xg) and a small aliquot was used for determination of protein concentration using the colorimetric Thermo Scientific Pierce BCA Protein Assay Kit according to manufacturer's instructions. Samples were mixed with 2x Laemmli buffer and reduced and denatured at 95 °C for 5 minutes. 10-30 µg total protein was separated by SDS polyacrylamide gel electrophoresis using 4-20% gradient gels (Mini-PROTEAN® TGX™ Precast Gels, Bio-Rad) and transferred onto PVDF (Immun-Blot®, 0.2 µm, Bio-Rad) or nitrocellulose (0.45 µm, Bio-Rad) membranes using a semi-dry transfer cell apparatus (Bio-Rad). The running gel, the membrane and Whatman filter papers were soaked in transfer buffer and a transfer sandwich was realized (anode - filter paper – membrane – gel - filter paper - cathode). The transfer was performed during 36 min at 25 V and 0.17 A per gel. Membranes were stained with Ponceau S solution to verify the quality of the protein transferred.

Next, membranes were blocked in ROTI-block (Roth; both total and phosphorylated proteins), 5% non-fat dry milk (total proteins) or 5% BSA (phosphorylated proteins) in TBS-T (0.1% Tween-20 in TBS) for two hours at RT before overnight incubation with primary antibodies in ROTI block, 1% non-fat dry milk or 1% BSA at 4 °C. All incubation and washing steps were performed with slight agitation on a rocking table. After washing in TBS-T (5 x 5 min), membranes were incubated with secondary HRP-conjugated antibodies for 1 hour at RT. The membranes were washed in TBS-T (4 x 5 min) and TBS (2 x 5 min) and subsequently incubated with ECL solution during 1 min. Excess substrate reagent was drained out

before the membranes were transferred into an autoradiography cassette and exposed to ECL films (Kodak).

Membrane stripping for reprobing

For reprobing, the membranes were washed twice with TBS-T for 10 minutes each to remove the remaining ECL solution prior to incubation with stripping buffer (Thermo Scientific) for 15 min at RT. After washing (TBS-T; 3 x 5 min), membranes were blocked again and immunodetection was repeated as previously described.

6.8.3 RhoA activation (G-LISA)

$2x10^6$ SP37A3 DCs were plated onto 6 cm cell culture dishes (BD Falcon) in 2 mL SP culture medium (IMDM complete + 20 ng/mL mGM-CSF and 20 ng/mL mM-CSF) and were allowed to adhere for two hours. Next, culture medium was exchanged with serum-free medium (IMDM + 20 ng/mL mGM-CSF) and cells were serum-starved overnight in order to reduce baseline RhoA activation. After overnight culture, DCs were stimulated with 0.1 µM ansamitocin P_3 for 5, 10, 15, 30 and 60 minutes and collected on ice using cell scrapers. Cells were washed once with ice-cold PBS and lysed in 90 µL cell lysis buffer provided by the kit (RhoA G-LISA; Cytoskeleton Inc.; cat: BK124). 15 µL of each cell lysate were set aside for measurement of protein concentrations using the provided Precision Red™ Advanced Protein Assay Reagent, while remaining lysates were snap-frozen in liquid nitrogen. Samples were thawed prior to analysis and volumes were adjusted to yield equal concentrations of total protein in each sample (0.5-2 mg/mL). Samples and constitutively active RhoA protein (control) were added onto the G-LISA plate in duplicates (GTP-bound RhoA from samples is bound by the immobilized Rho-GTP-binding protein) and the plate was processed according to manufacturer's instructions. Similar to the procedure of an ELISA, active RhoA bound to the plate is detected by an HRP-conjugated secondary anti-RhoA antibody. Finally, active RhoA is quantified by absorbance measurement at 490 nm.

6.9 Statistics

Statistical values were calculated using a 2-tailed paired Student's t test, if not indicated otherwise; p< 0.05*; p< 0.01**, p< 0.001***, p< 0.0001****. Kaplan Meier survival plots were analyzed using a log rank test (Mantel-Cox). $P < 0.05$ was considered significant for all biological tests.

6.10 Study approval

Tumor biopsies and blood drawing from cancer patients who received brentuximab vedotin were performed upon signing a consent form in accordance with the local institutional review board. Animals were maintained and treated in compliance with the guidelines of the Swiss Federal and the Cantonal Veterinary Office Basel-Stadt.

7 Results

7.1 Microtubule-depolymerizing agents (MDAs) promote DC maturation

7.1.1 Screening for DC-promoting anti-cancer-agents

Owing to their highly sophisticated antigen-presenting machinery DCs are central to the initiation and regulation of anti-cancer immunity [217]. Tumors may, however, hamper the maturation and antigen-processing capacity of tumor-residing DCs [218-220]. In contrast to mature DCs that efficiently launch immune responses, immature or dysfunctional DCs are rather immune suppressive [217, 221, 222]. Therapeutic approaches that activate DCs, and thereby promote priming of tumor antigen-specific T cells, may induce durable immunity against cancer. Recent work has identified several cytotoxic agents, including the mitotic spindle inhibitor vinblastine, as potent activators of DC maturation [223-225]. On the other hand, some anti-tumor therapeutics do block DC maturation and therefore antagonize anti-tumor immunity. Hence, it is of great importance to investigate the impact of chemotherapeutic compounds of different classes on the maturational state of DCs.

In order to analyze the effects of cytotoxic agents on DC maturation, a previously established primary murine DC line ($SP37A3$), which resembles immature DCs [140], as well as human monocyte-derived DCs (moDCs) were used to screen a library of 22 chemotherapeutics. These included microtubule-stabilizing (paclitaxel, patupilone A/B, docetaxel), and -destabilizing agents (*vinca*-alkaloids, combretastatin-$A4$-phosphate, ansamitocin $P3$, dolastatin 10), a tubulin polymerization inhibitor (D-64131), cyclooxygenase (COX)-inhibitors (naproxen, celecoxib), the angiokinase inhibitor BIBF1120, the angiotensin-converting-enzyme inhibitor enalapril, the nitric-oxide-synthase inhibitor l-NMMA, the DNA replication blocker gemcitabine, the alkylating agent mafosfamide, the receptor tyrosine kinase inhibitor sunitinib and the histone deacetylase inhibitor SAHA. To delineate which of these compounds could induce DC maturation, murine $SP37A3$ splenic DCs and human moDCs were incubated with these drugs at concentrations ranging from 1 to 0.001 µM. Cell viability and expression of CD86 were assessed by flow cytometry after 24h as shown for a drug concentration of 0.1 µM in Figure 7-1, A-B. Ansamitocin $P3$ (red circle) and dolastatin 10 (red triangle) were by far the most potent inducers of CD86 on murine and human DCs (Figure 7-1, C). Cell viability was only modestly affected at this drug concentration. Of note, all microtubule-destabilizing agents including the *vinca*-alkaloids (blue), dolastatin 10 and ansamitocin $P3$ (red), displayed a pronounced capacity to upregulate CD86 on murine as well as human DCs, in contrast to microtubule-stabilizing agents such as the taxanes (green) and compounds of other classes.

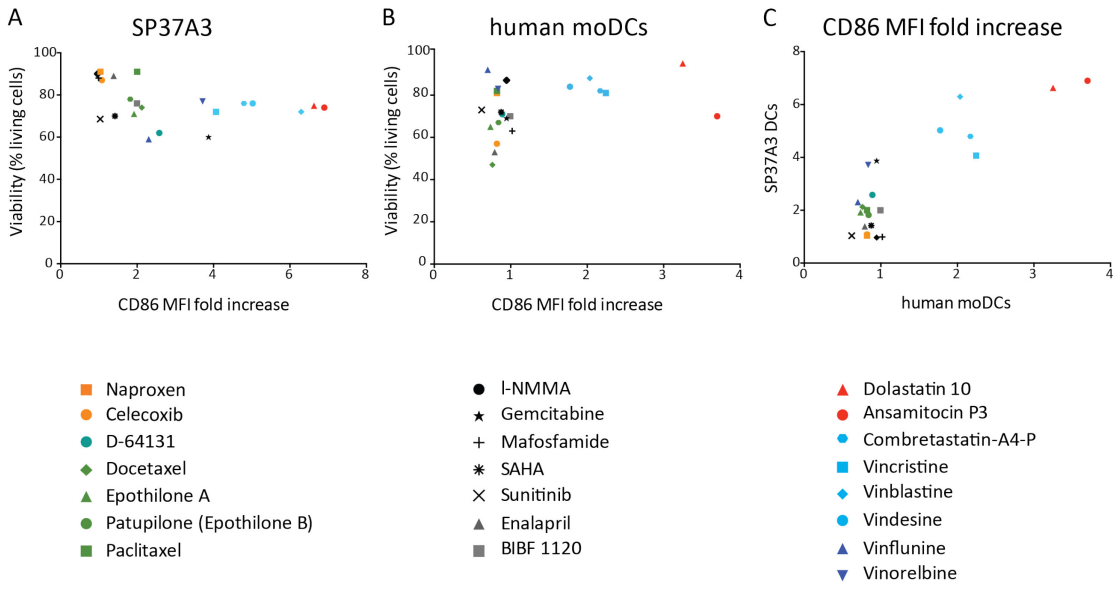

Figure 7-1 ***Identification of ansamitocin P3 and dolastatin 10 as potent inducers of DC maturation in vitro.*** (A-C) SP37A3 murine DCs and human moDCs were incubated with the indicated chemotherapeutic compounds (0.1 µM) for 24h. (A+B) Expression of CD86 on murine SP37A3 DCs and human moDCs after exposure to chemotherapeutic agents was correlated with viability (left and middle panel). (C) Mean fluorescence intensity (MFI) fold change in murine SP37A3 DCs vs. MFI fold change in human moDCs is shown in the right panel. MFI was assessed by flow cytometry; graphs show fold change of MFI compared to untreated cells, which were set as 1. Data are representative of two independent experiments with similar results.

7.1.2 MDA-triggered phenotypic and functional DC maturation

The next aim was to determine whether the observed DC maturation reflected a class-effect. This would imply that different compounds of the class of microtubule-depolymerizing agents (MDAs) demonstrate equal capacities to induce DC maturation, independent of their varying binding sites on microtubules (Table 4-1). Vinblastine (VBL) was included into the experimental set-up as representative member of the *vinca*-alkaloid family based on previously published data showing its capacity to mature murine DCs [224, 225]. Dolastatin 15, dolastatin 10 and its synthetic analogue MMAE represent the family of dolastatins, whereas ansamitocin P3 and its analogue DM1 belong to the family of maytansines. All of these compounds are used as chemotherapeutics due to their capacity to block mitosis as a result of suppression of microtubule dynamics at low (pM) concentrations in tumor cells. At higher concentrations, i.e. 10-100 nM, they induce active depolymerization of MTs [169]. LPS was included in all following experiments as positive control due to its well-known capacity to induce the full spectrum of DC maturation *via* TLR4 triggering.

The capacity of above-mentioned MDAs to induce upregulation of further costimulatory receptors and maturation markers on DCs was assessed by flow cytometry. To this end, SP37A3 DCs were exposed to distinct MDAs for 24 h prior to analysis of CD80, CD86, CD40 and MHCII expression. Dead cells were detected using a commercial live/dead stain (L/D Near-IR, Invitrogen) and were excluded from further analysis. DC viability was slightly decreased after incubation at nanomolar

concentrations, but stayed stable up to a concentration of approximately 10 µM (Figure 7-2, D-F). Compared with untreated controls, all MDAs significantly increased expression of DC maturation markers in a dose-dependent manner (Figure 7-2). Of note, dolastatin 10 and ansamitocin P_3 displayed the highest DC maturing potency, which correlated with their increased tumor cell cytotoxicity when compared to dolastatin 15, VBL, MMAE or DM1 (see Introduction chapter 4.4.1). Also, these results were confirmed using dolastatin 10 and ansamitocin P_3 on mouse bone marrow-derived DCs (BMDCs; Figure 7-4, A).

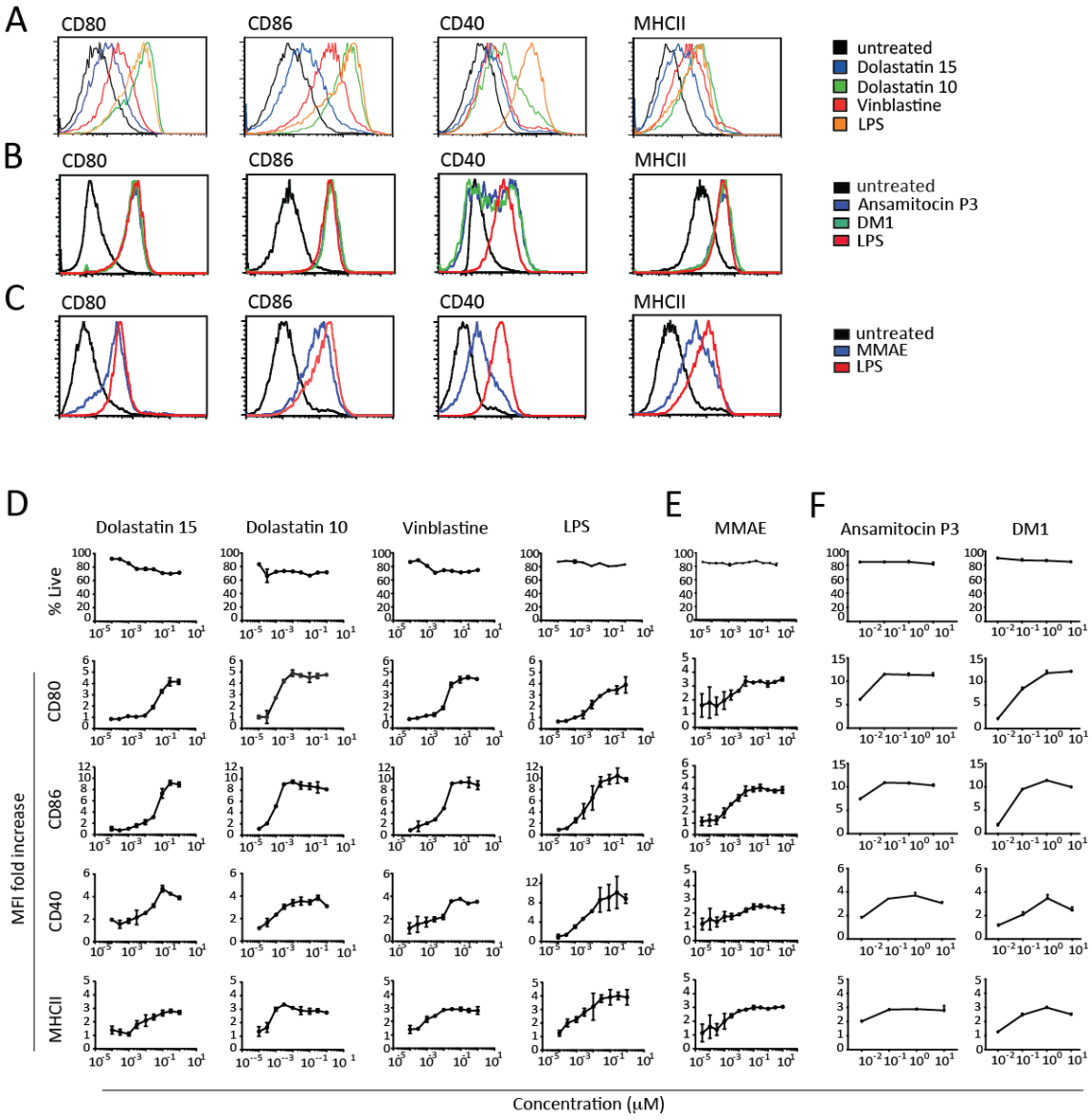

Figure 7-2 ***MDA-induced phenotypic DC maturation in vitro.*** (A-C) Representative histograms (n=3) for the expression of MHCII and costimulatory molecules CD80, CD86, and CD40 by $SP37A_3$ murine DCs exposed to (A) dolastatin 15 (0.1 µM), dolastatin 10 (0.1 µM), vinblastine (0.1 µM), (B) ansamitocin P_3 (0.1 µM), DM1 (0.1 µM) or (C) MMAE (0.1 µM). LPS (500 ng/mL) was used as positive control in all experiments. (D-F) MFI was assessed by flow cytometry; graphs show fold change of MFI compared with untreated cells, which were set as 1. Viability was determined by L/D staining and is depicted as percentage of viable cells (viability of untreated cells was set as 100%). All data are representative of at least three independent experiments with similar results. Mean ± SD of one representative experiment is shown.

In order to assess functional activation of DCs, supernatants from DC cultures described in Figure 7-2, D-F were analyzed for pro-inflammatory cytokines that have been demonstrated to play critical roles in regulating T cell function and anti-tumor immune responses [226]. Dolastatin 10, ansamitocin P_3, MMAE and, to a lesser extent, DM1 and vinblastine triggered production of IL-1β, IL-6, and IL-12p40 (Figure 7-3). Intracellular cytokine staining utilizing $SP_{37}A_3$ DCs (Figure 7-3, A-B) and BMDCs (Figure 7-4, B-C) confirmed the pattern of cytokine expression, whereas cytokine production in BMDCs was generally less pronounced. Importantly, expression of the costimulatory molecules CD80 and CD86 as well as production of all three cytokines was induced to a similar degree by all MDAs and LPS on $SP_{37}A_3$ DCs (Figure 7-3).

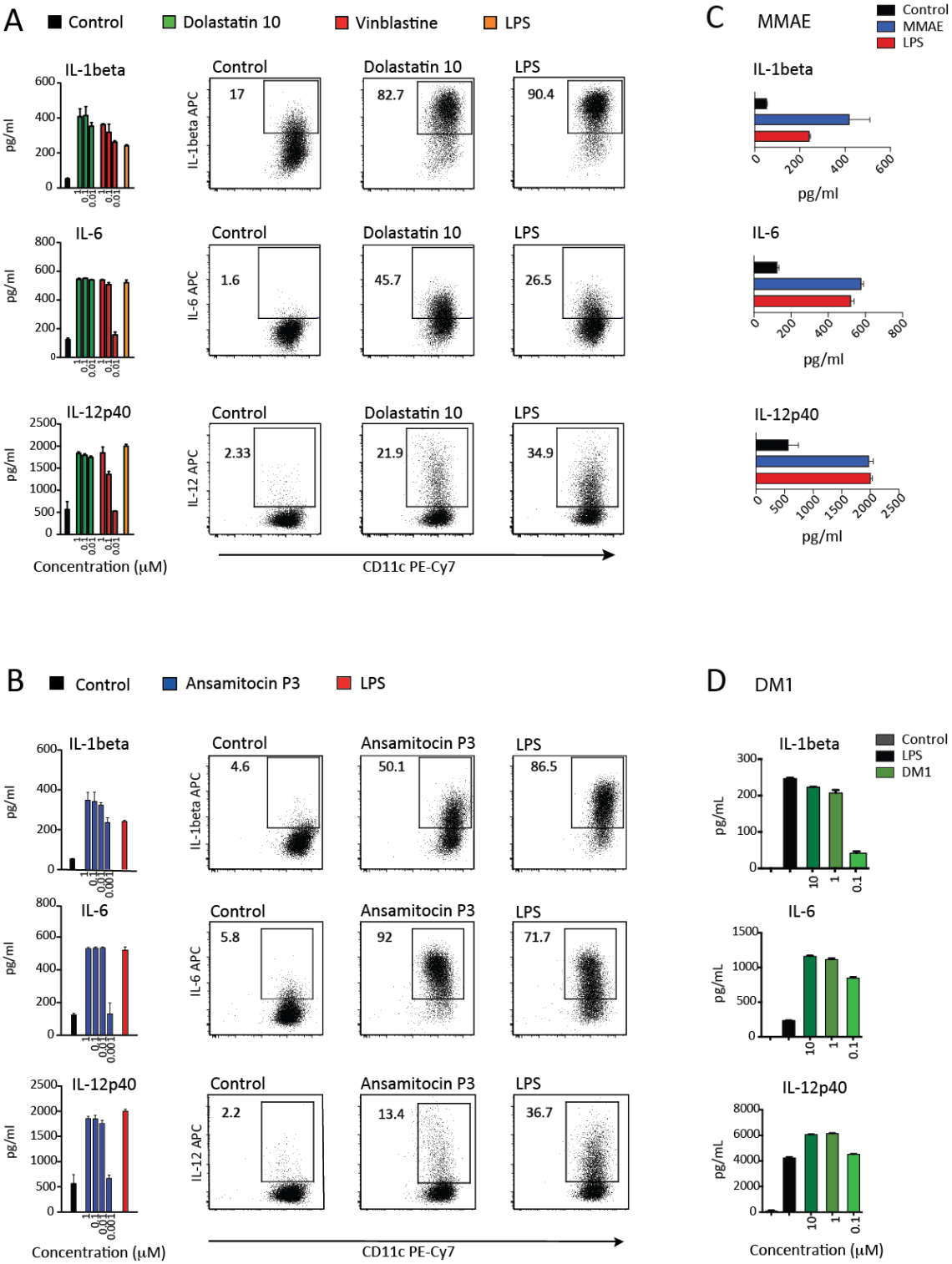

Figure 7-3 ***MDA-induced expression of pro-inflammatory cytokines by SP37A3 DCs.*** (A-D) Bar graphs depict secretion of IL-1β, IL-6, and IL-12p40 assessed in supernatants from cultures described in Figure 7-2, D-F using ELISA. MMAE was used at 0.1μM, LPS at 500 ng/mL. Dot plots illustrate cytokine expression by (A) dolastatin 10 (0.01 μM) or LPS (500 ng/mL) and (B) ansamitocin P3 (0.01 μM) or LPS (500 ng/mL) pretreated DCs, assessed by intracellular staining and flow cytometric analysis. Controls indicate untreated DCs. Three experiments in triplicates were performed with similar results. Bar graphs depict mean ± SD of one representative experiment.

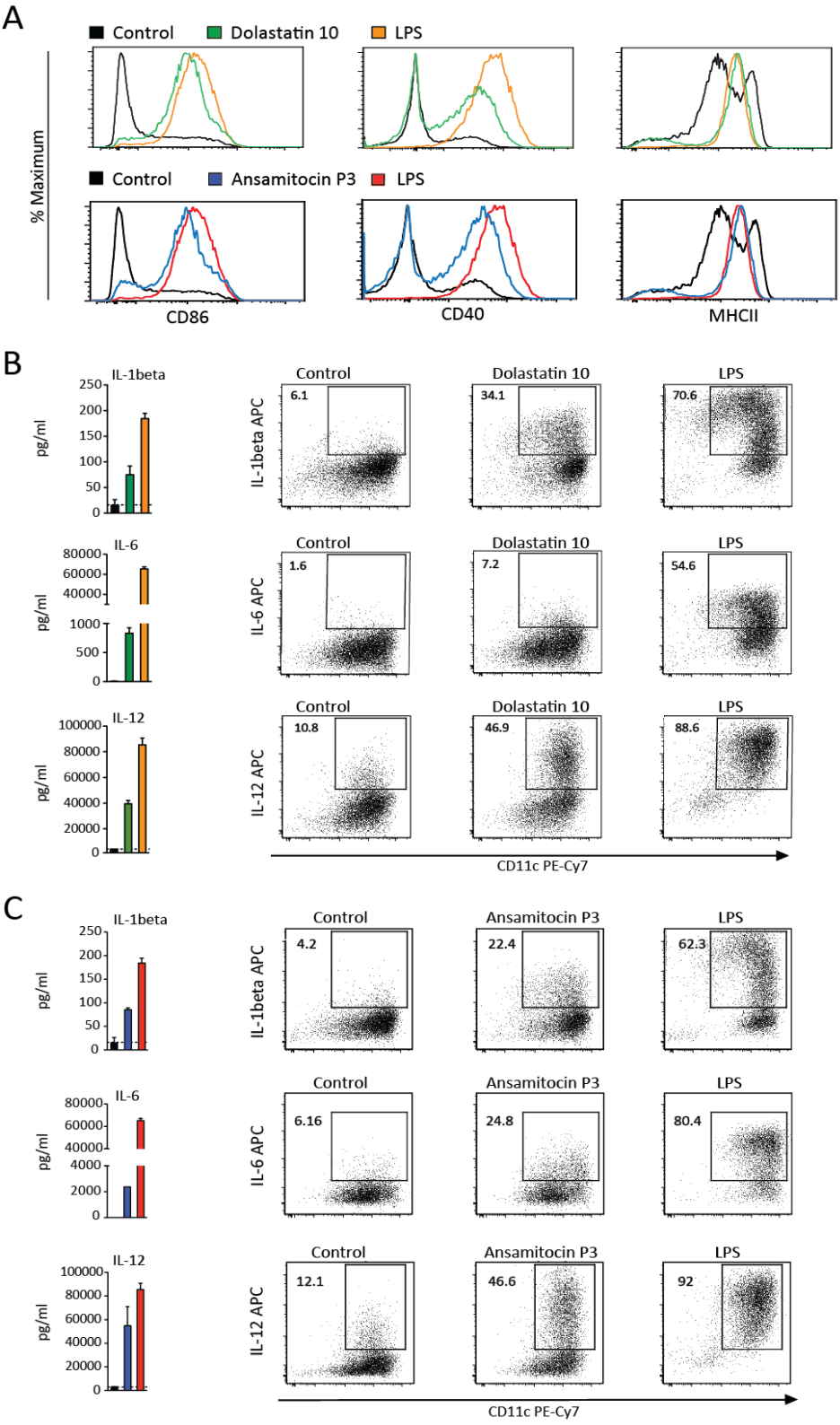

Figure 7-4 ***Phenotypic and functional BMDC maturation by MDAs.*** (A) Representative histograms (n=3) for the expression of MHCII and costimulatory molecules CD80, CD86, and CD40 by C57Bl/6 BMDC cultures exposed to dolastatin 10 (0.01 µM; upper panel) or ansamitocin P3 (0.01 µM; lower panel). LPS (500 ng/mL) was used as positive control. (B+C) Cytokine expression by (B) dolastatin 10 (0.01 µM) or LPS (500 ng/mL) and (C) ansamitocin P3 (0.01 µM) or LPS (500 ng/mL) treated BMDCs was assessed by ELISA (bar graphs) as well as by intracellular staining and flow cytometric analysis. Controls indicate untreated DCs. Three experiments in triplicates were performed with similar results.

Given that all investigated MDAs displayed similar capacities to induce phenotypic as well as functional maturation of murine DCs, it appears that the observed effects on DCs could be attributed to a general class effect of MDAs. During the initial screen of different classes of chemotherapeutics it has become evident that the second class of microtubule-binding compounds, i.e., the class of microtubule-stabilizing agents (MSAs), including the taxanes as its most prominent members, displayed no direct immune-stimulatory effects on DCs in our setting. To further support this hypothesis, induction of maturation markers and pro-inflammatory cytokines has been tested upon incubation of SP37A3 DCs with the microtubule-stabilizing compound paclitaxel. This compound binds to a distinct site on β-tubulin when compared to MDAs, such as the *vinca*-alkaloids, maytansines or colchicine [227]. Paclitaxel was compared to ansamitocin P3 as MDA, and etoposide, which represents a cytotoxic agent of a non-relevant class (topoisomerase inhibitor). As expected, paclitaxel and etoposide failed to induce expression of maturation markers (Figure 7-5, A) or the pro-inflammatory cytokines IL-1β, IL-6, and IL-12p40 in SP37A3 DCs (Figure 7-5, B). Consistent with previous data, a moderate upregulation of MHCII was detected in paclitaxel treated samples [116, 228].

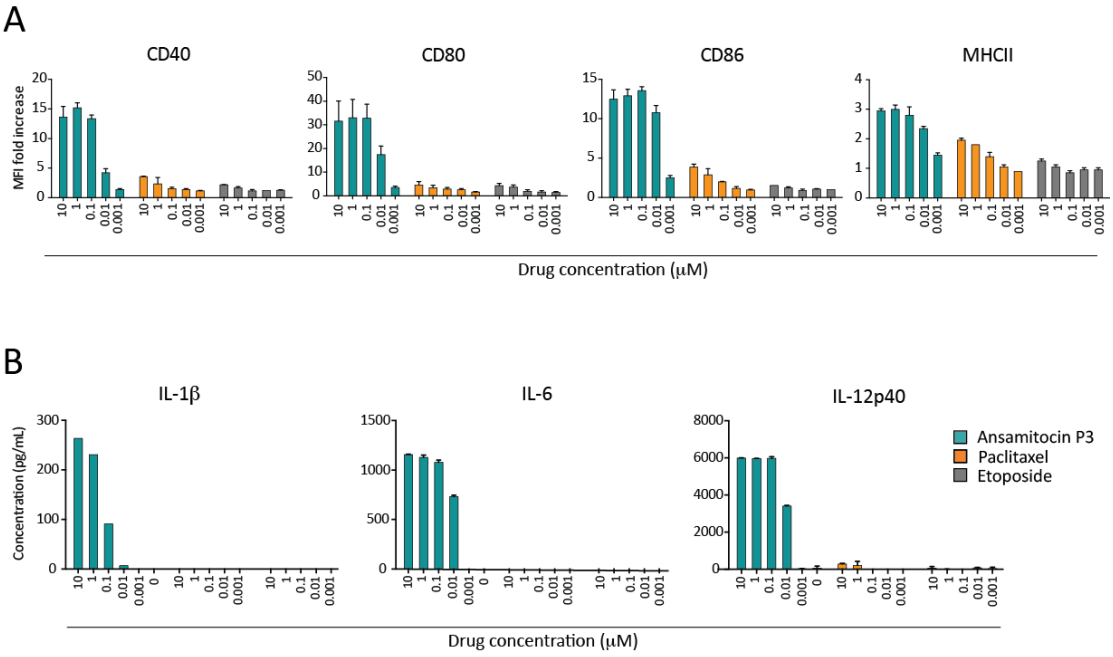

Figure 7-5 ***DC maturation in response to MDAs but not MSAs.*** (A) Upregulation of maturation markers CD40, CD80, CD86 and MHCII on SP37A3 DCs upon culture with ansamitocin P3, paclitaxel or etoposide in the indicated concentrations. MFI was assessed by flow cytometry as described in Figure 7-2. (B) Secretion of IL-1β, IL-6, and IL-12p40 was assessed in supernatants from cultures described in (A) using ELISA. All data are representative of at least three independent experiments with similar results. Mean ± SD of one representative experiment is shown.

Consequently, it seems that microtubule-destabilization in contrast to -stabilization, is a prerequisite for the observed immune-stimulatory capacity of MDAs. This issue will be addressed in the third chapter of the results section (see chapter 7.3 Molecular mechanism of MDA-induced DC maturation). Importantly, as all tested MDAs displayed similar DC-maturing capacity and due to the

limited frame of this work, only dolastatin 10 and ansamitocin P_3 will be used for further investigations. Both compounds demonstrated to be representative of their drug class and are most potent in inducing DC maturation.

The following experiments were divided in two further chapters. Chapter 7.2 illustrates the in-depth description of MDA-induced anti-tumor immune responses. To this end, 1.) DC maturation and migration, 2.) subsequent T cell priming and expansion and 3.) the therapeutic efficacy of dolastatin 10 alone, or in combination with immunotherapy, was assessed in murine *in vitro* and *in vivo* models. Importantly, these results could be translated into the human setting and were extended by the analysis of immune cell activation after exposure to therapeutic antibody-drug conjugates that use the dolastatin analogue MMAE as cytotoxic payload. Hence, dolastatin 10 and MMAE were used as representative MDAs during chapter 7.2. Experiments described in chapter 7.3 focus on the molecular events in DCs that ultimately translate into potent activation of host innate immune responses and therefore possibly trigger the effects observed in chapters 7.1 and 7.2. Ansamitocin P_3 as MDA, as well as paclitaxel as MSA were chosen to compare DC signaling cascades induced in response to microtubule-disruption and -stabilization, respectively.

7.2 MDAs potentiate anti-tumor immunity

7.2.1 *In vivo* maturation of skin Langerhans cells and tumor-resident DCs

Infiltration of DCs into primary tumor lesions has been associated with significantly prolonged patient survival and a reduced incident of metastatic disease in patients with distinct cancers such as head and neck tumors, lung, bladder or gastric carcinomas [229]. Furthermore, Langerhans cell (LC) infiltration has been associated with regression of primary cutaneous melanomas [230, 231]. In contrast to other DC subsets, skin-resident LCs promote peripheral tolerance by constantly migrating to skin-draining LNs to present dermal and epidermal antigens to $CD4^+$ T cells, which induces anergy due to their immature phenotype [129]. In order to elucidate whether dolastatins are capable of reverting their immature state, dolastatin 10 or 15 were injected into the ears of C57Bl/6 mice. Consistent with previous *in vitro* observations, dolastatin 10 and, to a lesser extent, dolastatin 15 induced the expression of CD86 and MHCII on LCs (Figure 7-6, A-B). Compatible with *in situ* maturation of LCs, immunofluorescence staining revealed an enlarged cell size, profound morphological changes, such as dendrite hyper-elongation, a strong upregulation of the costimulatory molecule CD86, and a marked decrease in LC density, which may reflect migration of LCs to the draining lymph nodes (LN) (Figure 7-6, C). Hence, the migratory behavior of dolastatin 10 activated DCs was investigated using FITC-dextran (FITC-Dx), a carbohydrate with a high molecular mass, which is readily taken up by DCs during early activation [232]. FITC-Dx was injected intratumorally either together with dolastatin 10 or with PBS into C57Bl/6 mice bearing subcutaneous E.G7 tumors. In mice treated with vehicle alone, DCs from tumor-draining LNs showed almost no increased FITC signal. In stark contrast, FITC-Dx-bearing DCs could be robustly detected and correlated with high CD86 expression in tumor-draining LNs of mice treated with dolastatin 10 (Figure 7-6, D-E). FITC-dextran bearing DCs could not be detected in non-tumor-draining LN in both cases, providing evidence for local, tumor-selective DC-stimulatory effects of dolastatin 10 treatment.

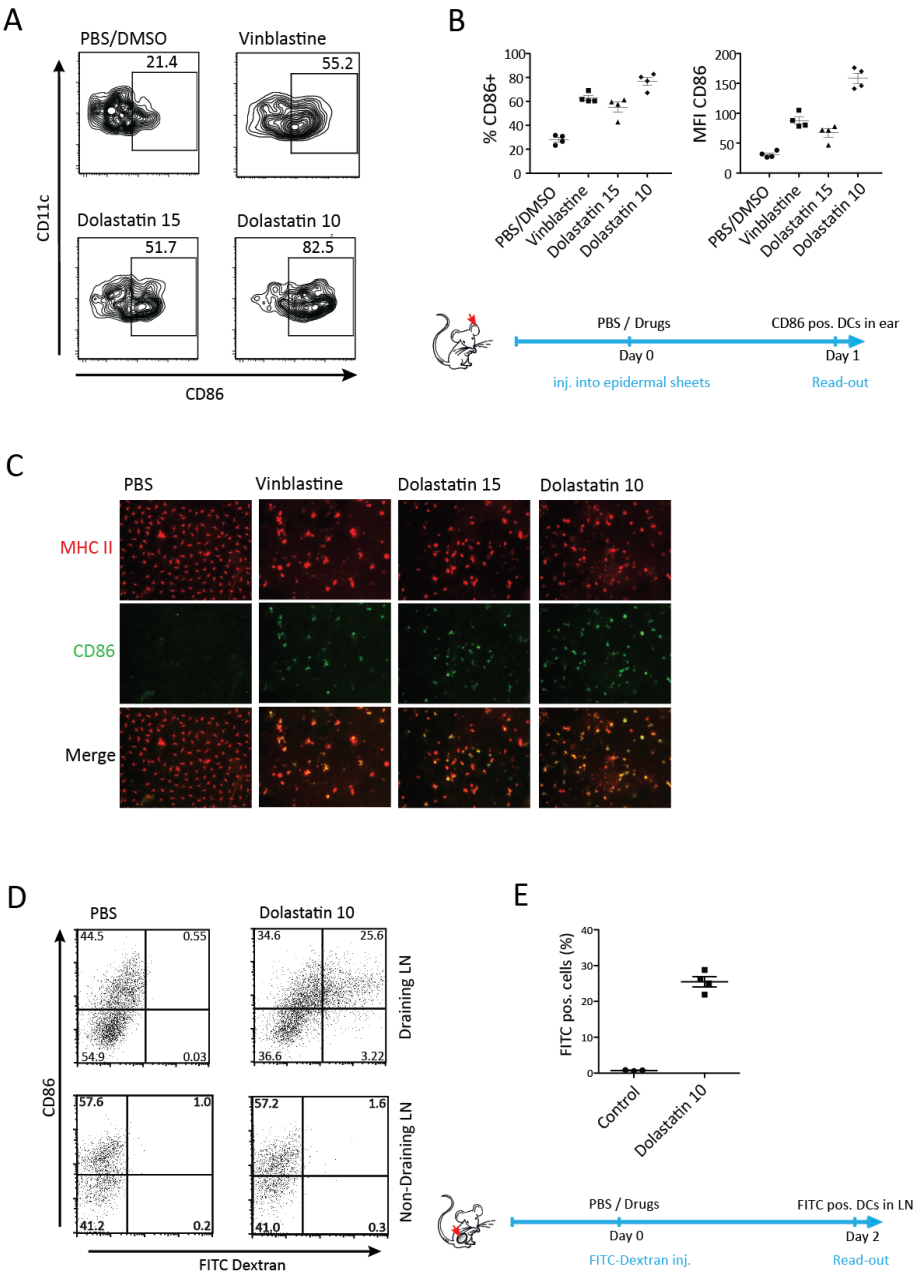

Figure 7-6 ***In situ maturation of skin LCs and DC homing to tumor-draining LNs triggered by dolastatin 10.*** (A-C) Dolastatin 10 (10 µg/animal), dolastatin 15 (10 µg/animal), vinblastine (17.6 µg/animal) or vehicle alone was injected intradermally into the ears of C57Bl/6 mice (four mice per group, two ears per point; mock treated = ears of PBS/carrier injected mice). Ear skin specimens were collected 24h later and epidermal sheets were digested. Cells were stained for CD45, CD11c, MHCII, and CD86 and subsequently analyzed by flow cytometry. Data show the mean (n=2) of % $CD86^{high}$ cells and MFI of CD86 within the $CD45^{+}MHCII^{+}CD11c^{+}$ population per data point (B). One representative contour plot per group from three independent experiments is shown (A). (C) Mice were treated as in (A+B); epidermal sheets were fixed in acetone, stained for MHCII (red) and CD86 (green) and analyzed by immunofluorescence. (D+E) Mice bearing subcutaneous E.G7 tumors were injected intratumorally with FITC-conjugated dextran suspended in vehicle alone (PBS/DMSO) or in vehicle containing dolastatin 10 (10 µg per mouse). 48 hours later, tumor-draining LNs were examined for the presence of FITC-dextran-bearing DCs ($CD45^{+}MHCII^{+}CD11c^{+}$) by flow cytometry. (D) Representative plots depict $FITC^{+}$ DCs detected in tumor-draining LNs after PBS/DMSO (left) or dolastatin 10 (right) injection. (E) Graphs summarize percent of $FITC^{+}$ DCs from one experiment; representative results from one of three experiments are shown.

7.2.2 Activation of antigen-specific T cells

To assess the capacity of MDA-treated DCs to activate naïve, antigen-specific T cells *in vitro*, OVA-specific, TCR transgenic OT-I and OT-II mice were used. Thus, SP37A3 DCs or BMDCs were exposed to dolastatin 10 or LPS for 16 h prior to loading with $OVA_{257-264}$ or $OVA_{323-339}$ peptide. Meanwhile, T cells were isolated from LNs and spleen of OT-I ($CD8^+$) and OT-II ($CD4^+$) mice, labeled with the proliferation dye eFluor670 and co-cultured with DCs for three days. Notably, dolastatin 10-pretreated, peptide-pulsed DCs induced robust expansion of both OT-I and OT-II T cells (Figure 7-7, A). In a next step, DCs were loaded with recombinant OVA full-length protein prior to incubation with dolastatin 10 or LPS and subsequent co-culture with OT-I or OT-II T cells. Both SP37A3 and BMDCs were capable to induce significant proliferation of both OT-I and OT-II antigen-specific T cells (Figure 7-7, B). Thus, dolastatin treatment of DCs allowed efficient antigen uptake and processing for both MHC class II and class I antigen-presentation, the latter pathway being commonly referred to as cross-presentation [233]. Of note, DCs exposed to dolastatin 10 supported T-cell proliferation to levels comparable to that of LPS-stimulated DCs.

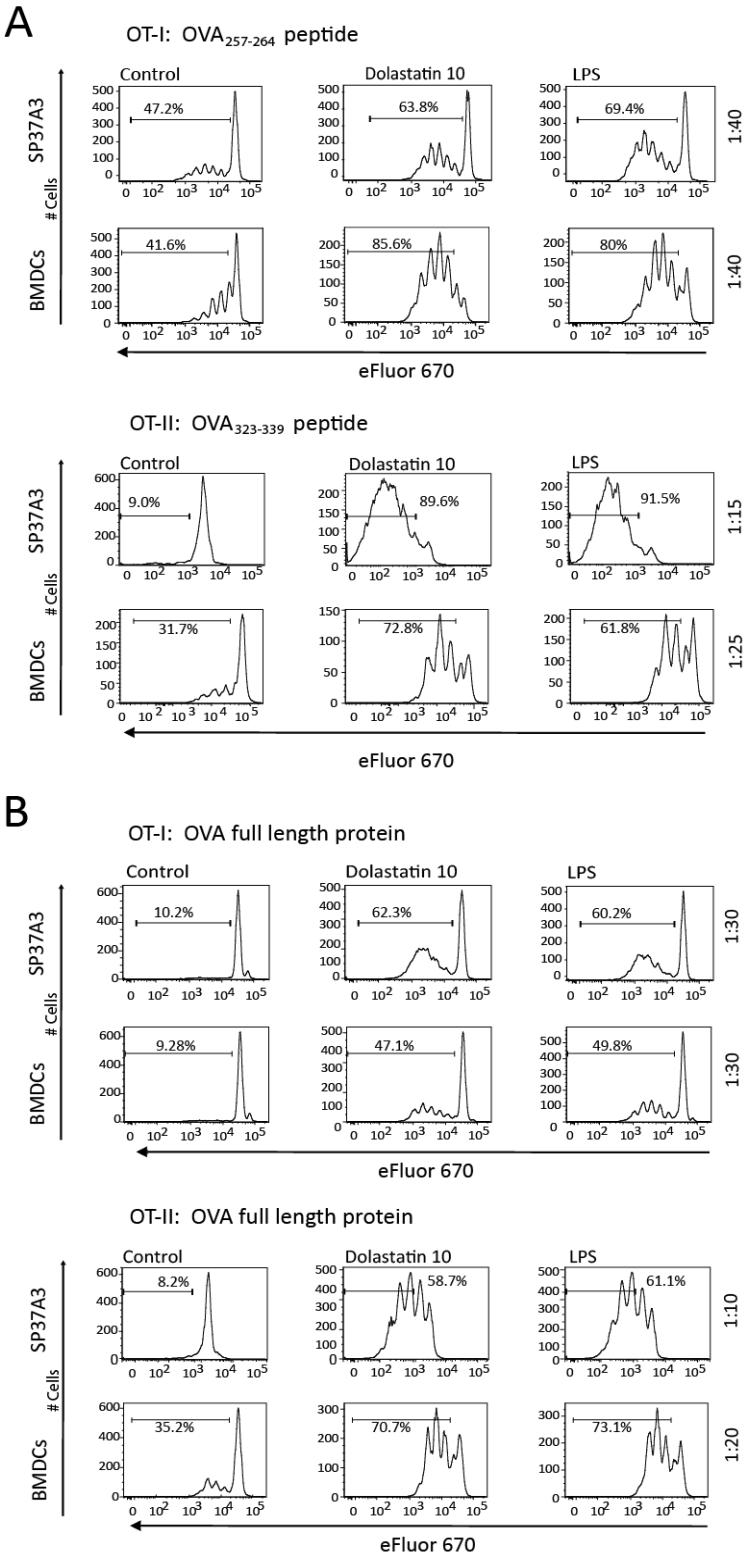

Figure 7-7 ***Activation of antigen-specific T cells in vitro.*** (A+B) $SP37A3$ DCs or BMDCs were treated with dolastatin 10 (0.1 µM) or LPS (500 ng/mL) for 16 h before or after loading with peptide or protein, respectively. Controls indicate untreated, antigen-pulsed DCs. DCs were pulsed with $OVA_{257-264}$ or $OVA_{323-339}$ peptide (A) or loaded with OVA protein (B) and added to micro-cultures of transgenic $CD8^+$ OT-I (upper panels) or $CD4^+$ OT-II T cells (lower panels). DC:T cell ratios are indicated. Proliferation of OT-I/OT-II T cells was assessed by flow cytometry. Data show representative histograms from one of at least three independent studies.

We furthermore assessed whether dolastatins promoted expansion of antigen-specific T cells *in vivo*. Naïve $CD8^+$ and $CD4^+$ T cells from OT-I and OT-II transgenic mice (Ly5.2) were adoptively transferred into congenic C57Bl/6 (Ly5.1) recipient mice bearing established subcutaneous MC38 tumors. T-cell responses were measured following tail-base immunization with a weak agonist peptide derived from the original $OVA_{257-264}$ peptide SIINFEKL (T4= SIITFEKL) [234] and the $OVA_{323-339}$ peptide, respectively. A much stronger proliferation of both OT-I and OT-II T cells was observed in mice receiving peptide plus dolastatin 10 compared with dolastatin 10 or peptide alone (Figure 7-8). Therefore, under *in vivo* conditions, dolastatin 10 is capable of inducing efficient antigen presentation, thereby augmenting antigen-specific T-cell responses. Most importantly, T cell proliferation was observed to the same degree in tumor draining as well as non-draining lymph nodes.

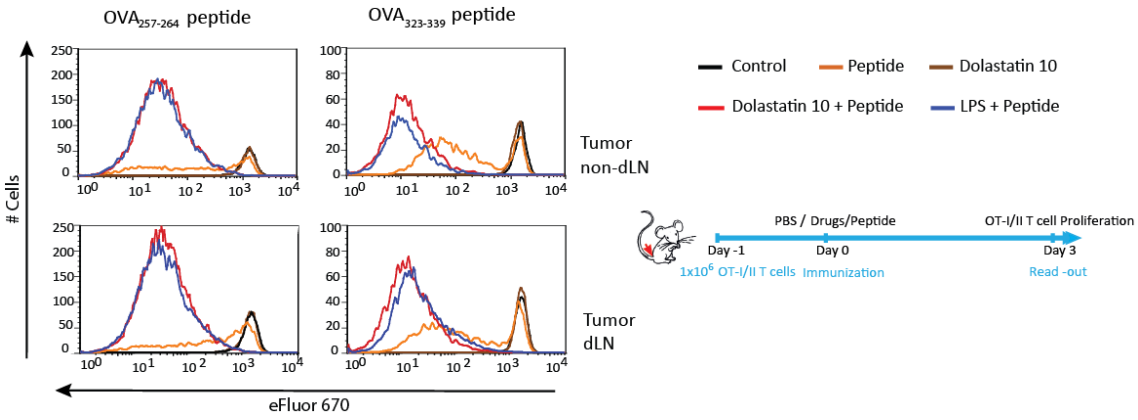

Figure 7-8 ***Activation of antigen-specific T cells in vivo***. T cells from spleen and LNs of naïve OT-I or OT-II transgenic mice (Ly5.2) were adoptively transferred into congenic C57Bl/6-Ly5.1 recipient mice bearing subcutaneous MC38 tumors. After 24h, mice were immunized using 25 µg $OVA_{257-264}$ T4 (SIITFEKL) and 5 µg $OVA_{323-339}$ peptide in the absence (PBS/DMSO) or presence of dolastatin 10 (1 µg per mouse) or LPS (25 µg per mouse). Proliferation of donor-derived transgenic $CD8^+$ OT-I T cells or $CD4^+$ OT-II T cells was assessed 4 days after adoptive transfer by flow cytometry. Histograms show data from one representative experiment. The experiment was performed independently three times.

7.2.3 Contribution of host immunity to the therapeutic efficacy of dolastatins

Next, the requirement of T cells and/or IFN-γ for the efficacy of dolastatin 10-based treatments was assessed using E.G7 T cell lymphoma, Lewis Lung carcinoma (3LL-OVA) or MC38 adenocarcinoma subcutaneous tumors (Figure 7-9). In immunocompetent syngeneic wild type (WT) mice, systemic treatment with dolastatin 10 was sufficient to suppress growth of all three tumors. Depletion of $CD8^+$ cells or neutralization of IFN-γ with monoclonal antibodies (mAbs) administered prior to dolastatin 10 treatment severely abrogated the antitumor effect of the drug in an established tumor setting, as evidenced by significant loss of tumor growth suppression (Figure 7-9, A). Abrogation of dolastatin 10 efficacy was not observed in mice depleted of $CD4^+$ cells. To investigate the specific role of $CD11c^+$ DCs in dolastatin 10 mediated tumor rejection, CD11c-DTR transgenic mice were used [235]. Injection of diphtheria toxin (DT) led to transient systemic depletion of $CD11c^+$ cells in these mice (data not shown). Consequently, CD11c-DTR mice with established MC38 tumors were treated with diphtheria toxin before treatment with dolastatin 10 or vehicle. Interestingly, depletion of $CD11c^+$ cells was sufficient to abrogate the antitumor effect of dolastatin 10 (Figure 7-9, B). In addition, $RAG2^{-/-}$ and IFN-$\gamma R1^{-/-}$ mice have been used to investigate tumor growth kinetics in E.G7 and 3LL-OVA tumors upon treatment with dolastatin 10. In immunocompetent syngeneic WT mice, treatment with dolastatin 10 was sufficient to induce persistent regression of transplanted tumors. In both $RAG2^{-/-}$ and IFN-$\gamma R1^{-/-}$ mice, the therapeutic effect of dolastatin 10 treatment was significantly reduced (Figure 7-9, C-D). These data underline the importance of $CD11c^+$ DCs and, subsequently, T cells and IFN-γ as critical determinants of the anti-tumor effects of dolastatins, irrespective of the tumor model.

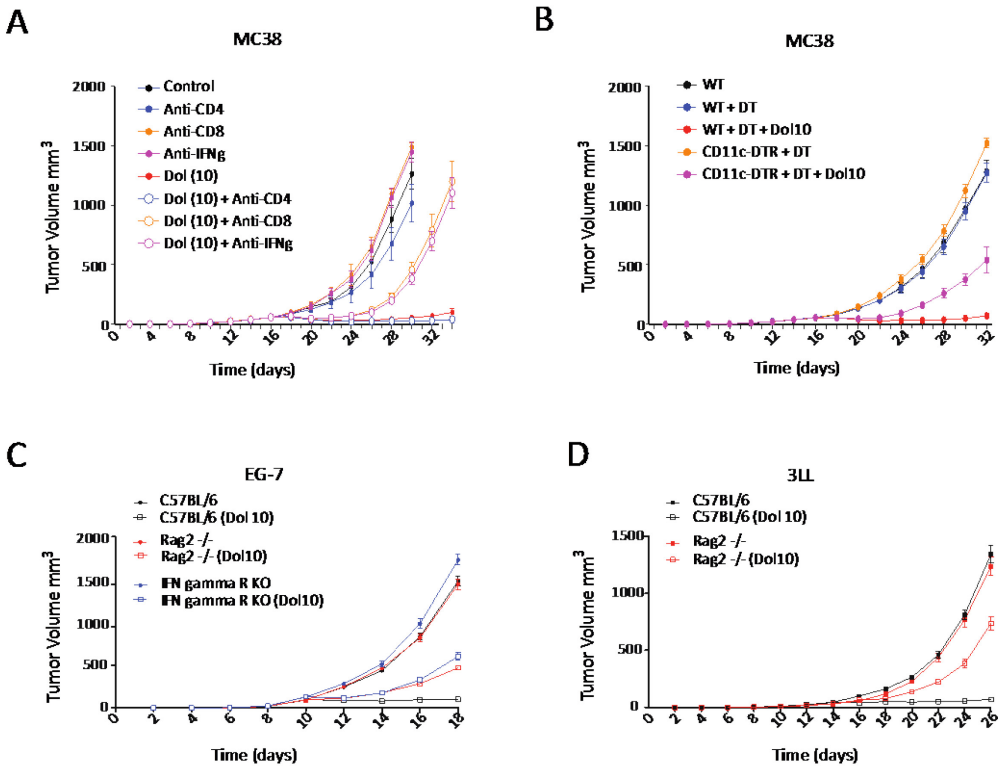

Figure 7-9 ***Requirement of intact host immunity for full therapeutic efficacy of dolastatins.*** (A+B) Growth of MC38 tumors during treatment with dolastatin 10 (0.4 mg/kg) in tumor bearing (A) C57Bl/6 WT control mice and upon depletion of CD_4 or CD8 T cells or neutralization of IFN-γ with monoclonal antibodies and (B) CD11c-DTR mice (depleted of CD11c DCs) bearing 16-day established subcutaneous MC38 tumors. (C+D) Tumor growth during treatment with dolastatin 10 (0.4 mg/kg) in C57Bl/6 WT, $Rag2^{-/-}$ or $INF\gamma R1^{-/-}$ mice bearing 10-day established subcutaneous (C) E.G7 tumors or 15-day established subcutaneous D) 3LL-OVA tumors. Control, tumor-bearing, mock-treated mice. All data are expressed as mean ± SEM (n=11-12). Two independent experiments were performed; pooled data are shown.

7.2.4 Therapeutic synergy of dolastatins and immune-based therapies

Given its capacity to augment anti-tumor immunity, dolastatin was thought to synergize with and enhance the efficacy of immunomodulatory agents. In order to test this hypothesis, mice with established ovalbumin-expressing 3LL tumors (3LL-OVA) were treated by systemic administration of dolastatin 10 and subsequent vaccination using a recombinant adenovirus expressing ovalbumin (Adeno-OVA). Indeed, the overall survival of mice treated with $5x10^7$ pfu Adeno-OVA plus dolastatin 10 was significantly longer than that of mice given dolastatin 10 or vaccination alone (Figure 7-10). Thus, dolastatin 10 improved the efficacy of antigen-specific vaccination in a setting with established tumors.

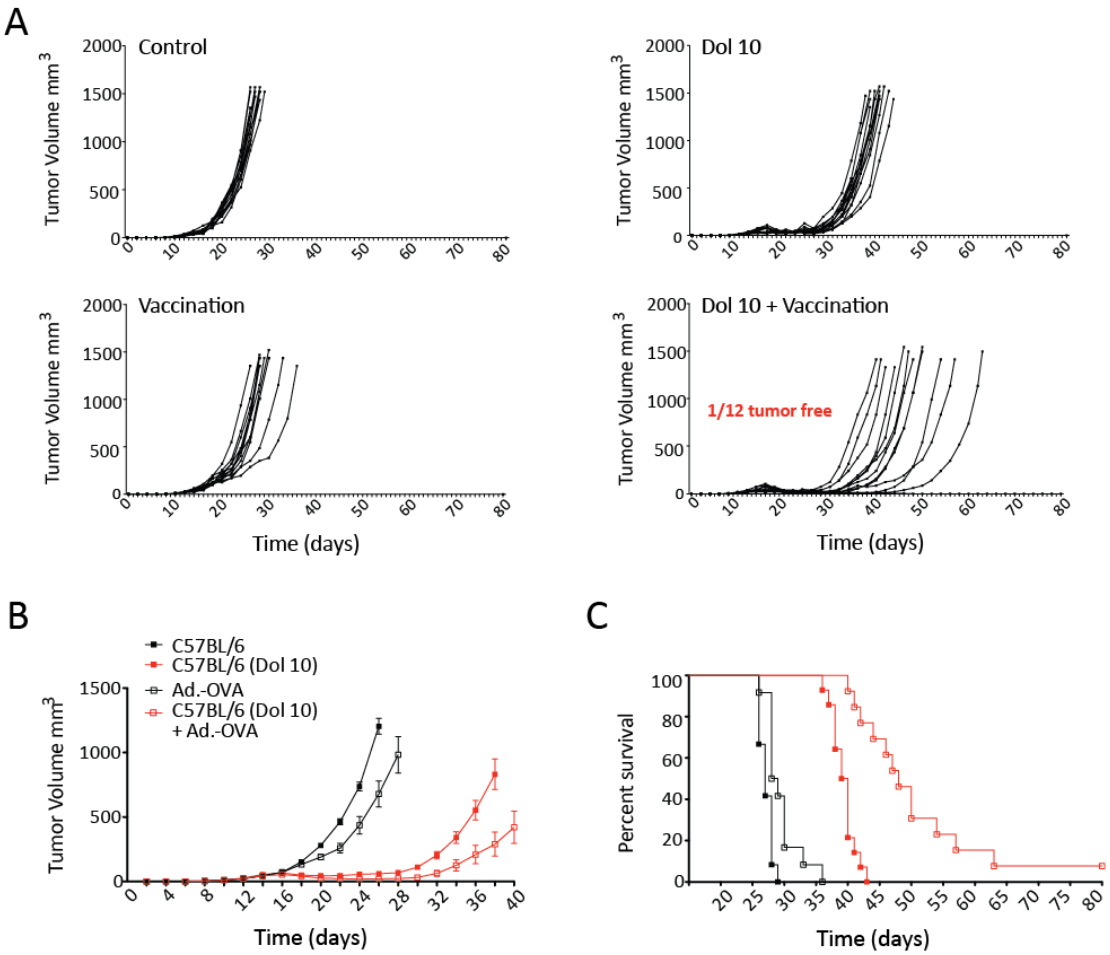

Figure 7-10 *Synergy of dolastatin 10 treatment and tumor-antigen-specific vaccination.* (A) WT mice bearing 15-day established subcutaneous 3LL-OVA tumors were treated with vaccination alone, comprising $5x10^7$ pfu of Ad-OVA (intra muscular), dolastatin 10 alone (0.4 mg/kg) or the combination of both. All data are expressed as mean ± SEM (n=12-14). Two independent experiments were performed and pooled results are shown as individual tumor-growth curves or cumulative tumor volume over time (B) and in a Kaplan-Meier survival plot; Log-rank (Mantel-Cox) Test, P value <0.0001 (C).

Impressive clinical success has been achieved by novel cancer immunotherapies that target immune-regulatory checkpoints on T cells [76, 236, 237]. Only recently and in accordance with preclinical data from a murine B16 melanoma model [238], unprecedented clinical benefits with rapid and deep responses have been reported with concurrent CTLA-4/PD-1 blockade [239]. Hence, therapeutic synergies between dolastatin 10 treatment and immune checkpoint inhibition were delineated. Mice with established MC38 tumors were treated using a combination of anti-CTLA-4/PD-1 antibodies and systemically administered dolastatin 10. Slower tumor outgrowth was observed with monotherapy using either dolastatin 10 or anti-CTLA-4/PD-1 compared with the control group. In the dolastatin 10 group, 1 out of 12 mice experienced complete tumor regression compared with 3 out of 12 mice in the anti-CTLA-4/PD-1 group. In contrast, concomitant treatment with dolastatin 10 and anti-CTLA-4/PD-1 achieved complete tumor rejection in 7 out of 12 mice and significantly delayed outgrowth in

the rest of the mice (Figure 7-11). These results demonstrate therapeutic synergy between dolastatin 10 and immunotherapy treatment approaches, leading to potent induction of anti-tumor immunity and finally tumor rejection.

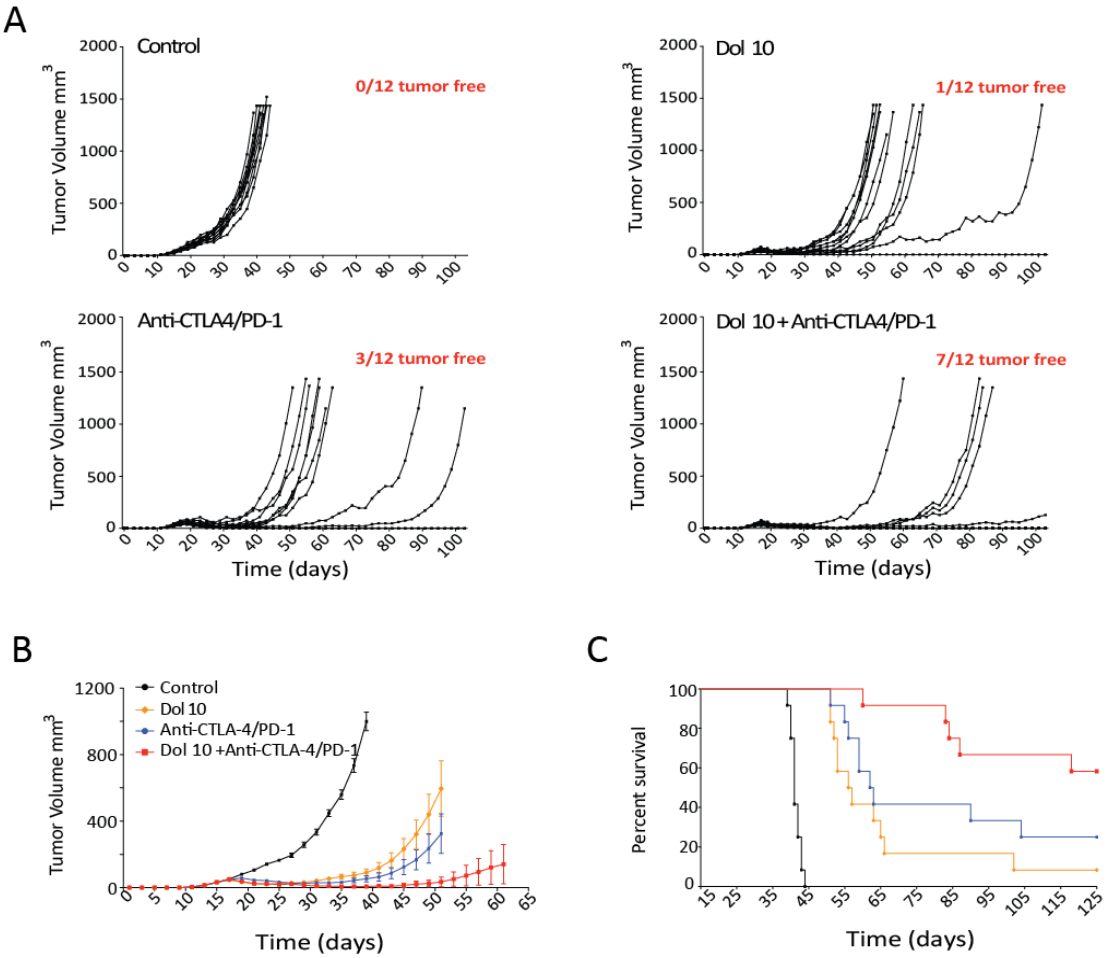

Figure 7-11 ***Treatment synergy of dolastatin 10 combined with antibody-mediated blockade of T-cell inhibitory receptors PD-1 and CTLA-4.*** (A+B) Tumor growth during treatment with dolastatin 10 (0.4 mg/kg), anti-PD-1/CTLA-4 (each 250 µg/mouse) or the combination in C57Bl/6 WT mice bearing 16-day established subcutaneous MC38 tumors. Control, tumor-bearing mice received matched isotype control Abs. All data are expressed as mean ± SEM (n=11-12). Two independent experiments were performed, and the pooled data are shown. Results are depicted as individual tumor-growth curves (A), cumulative tumor volume over time (B), and as a Kaplan-Meier survival plot (C); the x-axis depicts post-tumor implantation (days).

7.2.5 Increased intratumoral effector T cell to Treg ratio upon combination therapy

To define the immunological mechanism of action of a treatment approach combining dolastatins and anti-CTLA-4/PD-1 antibodies, tumor-infiltrating lymphocytes were analyzed 10 days after treatment onset. To this end, the impact of the indicated treatments on the frequency of Tregs and IFN-γ-producing intratumoral $CD8^+$ effector T cells (Teff) was determined. A significantly lower frequency of intratumoral Tregs was observed in dolastatin and anti-CTLA-4/PD-1 treated tumors, which was even more pronounced in tumors exposed to the combination treatment (Figure 7-12, A+C). Similarly, the number of IFN-γ producing $CD8^+$ T cells in dolastatin treated tumors was found to be increased, in particular in combination with anti-CTLA-4/PD-1 blocking antibodies (Figure 7-12, B+C). Previous work has demonstrated a correlation between the therapeutic efficacy of immunotherapies and a shift in the intratumoral Teff to Treg ratio [240]. Accordingly, a significant increase in the $CD3^+IFN\text{-}\gamma^+$ and $CD8^+IFN\text{-}\gamma^+$ Teff to Treg ratio could be documented in the combination group compared with non-treated, dolastatin only or anti-CTLA-4/PD-1 only treated tumors (Figure 7-12, C). Absolute cell numbers of the respective cell populations are provided in Figure 7-12, D. Overall, the therapeutic efficacy of the combined treatment with dolastatin and CTLA-4/PD-1 blockade correlated with a shift in the intratumoral balance between Teff cells and Tregs towards a more anti-tumorigenic profile.

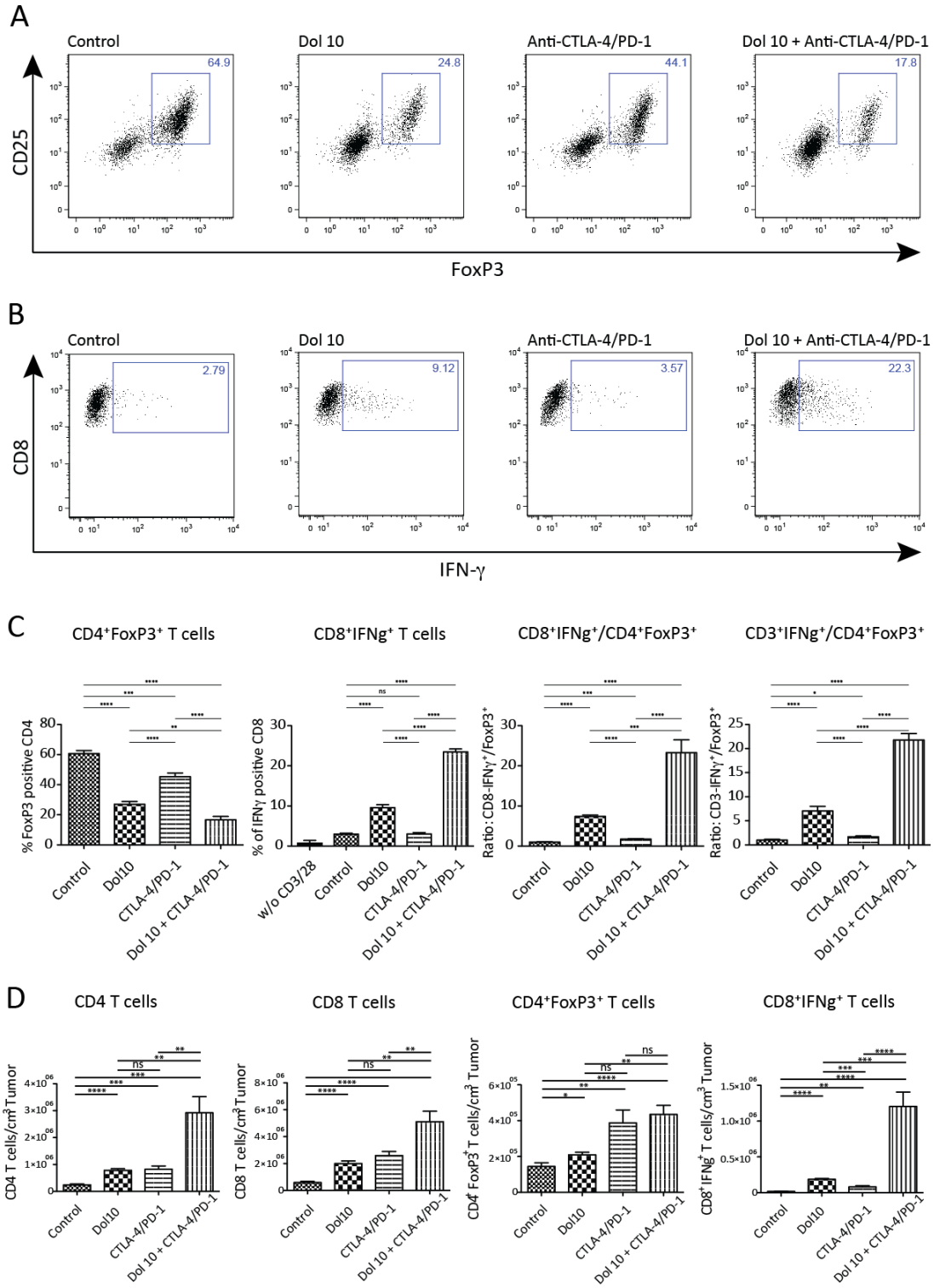

Figure 7-12 ***Combined effects of dolastatin 10 and anti-CTLA-4/PD-1 treatment on tumor infiltrating lymphocyte subsets.*** Established MC38 tumors were treated as indicated in Materials and Methods and analyzed for (A) Tregs or (B) IFN-γ producing $CD8^+$ effector cells. For IFN-γ analysis whole tumor digests were incubated for 16 hours with soluble anti-CD_3/28 (2/4 µg/ml) and monensin. $CD8^+$IFN-γ^+/$FoxP_3^+$ and CD_3^+IFNγ^+/$FoxP_3^+$ ratios are depicted in (C). In addition total CD_4 and CD8 as well as $CD_4^+FoxP_3^+$ and $CD8^+$IFN-γ^+ cell counts are shown in (D). Results represent pooled data from two independent experiments (Mean ± SEM); $p < 0.05$ *, $p < 0.01$ **, $p < 0.001$ ***, $p < 0.0001$ ****.

7.2.6 Enhanced T cell-stimulatory capacity of MDA-treated human DCs

To determine whether human DCs respond comparably to their murine counterparts, the maturation stage of monocyte-derived DCs (moDCs) from healthy blood donors was analyzed during exposure to dolastatin 10 and MMAE. The dolastatin analogue MMAE is currently successfully used in clinics as cytotoxic component of the antibody-drug conjugate (ADC) brentuximab vedotin for treatment of relapsed or refractory Hodgkin lymphoma (HL) and systemic anaplastic large cell lymphomas (ALCL). MMAE was therefore included in all tests performed on human cells. In line with data from the murine $SP37A3$ dendritic cell line, a dose-dependent upregulation of the surface expression of CD86, CD83, CD40, and MHCII (HLA-DR) by human moDCs was observed after over night exposure to dolastatin 10 (Figure 7-13, A). Additionally, the potential of the dolastatin analogue MMAE to induce upregulation of important costimulatory molecules on human moDCs was confirmed (Figure 7-13, B). DC viability did not significantly change as determined by SytoxGreen® staining using dolastatin 10 or MMAE at the indicated concentrations (data not shown).

To further address the functional activation of human DCs during treatment with dolastatin 10 or MMAE, the capability of pretreated monocyte-derived DCs to induce proliferation of allogeneic CD8 T cells was analyzed in mixed-lymphocyte cultures. A consistent >2-fold increase was observed in T-cell proliferation following pretreatment of DCs with dolastatin 10 ($p<0.0001$) or MMAE ($p=0.0002$). Similar results were obtained when human DCs were stimulated using LPS ($p<0.0001$; Figure 7-13, C).

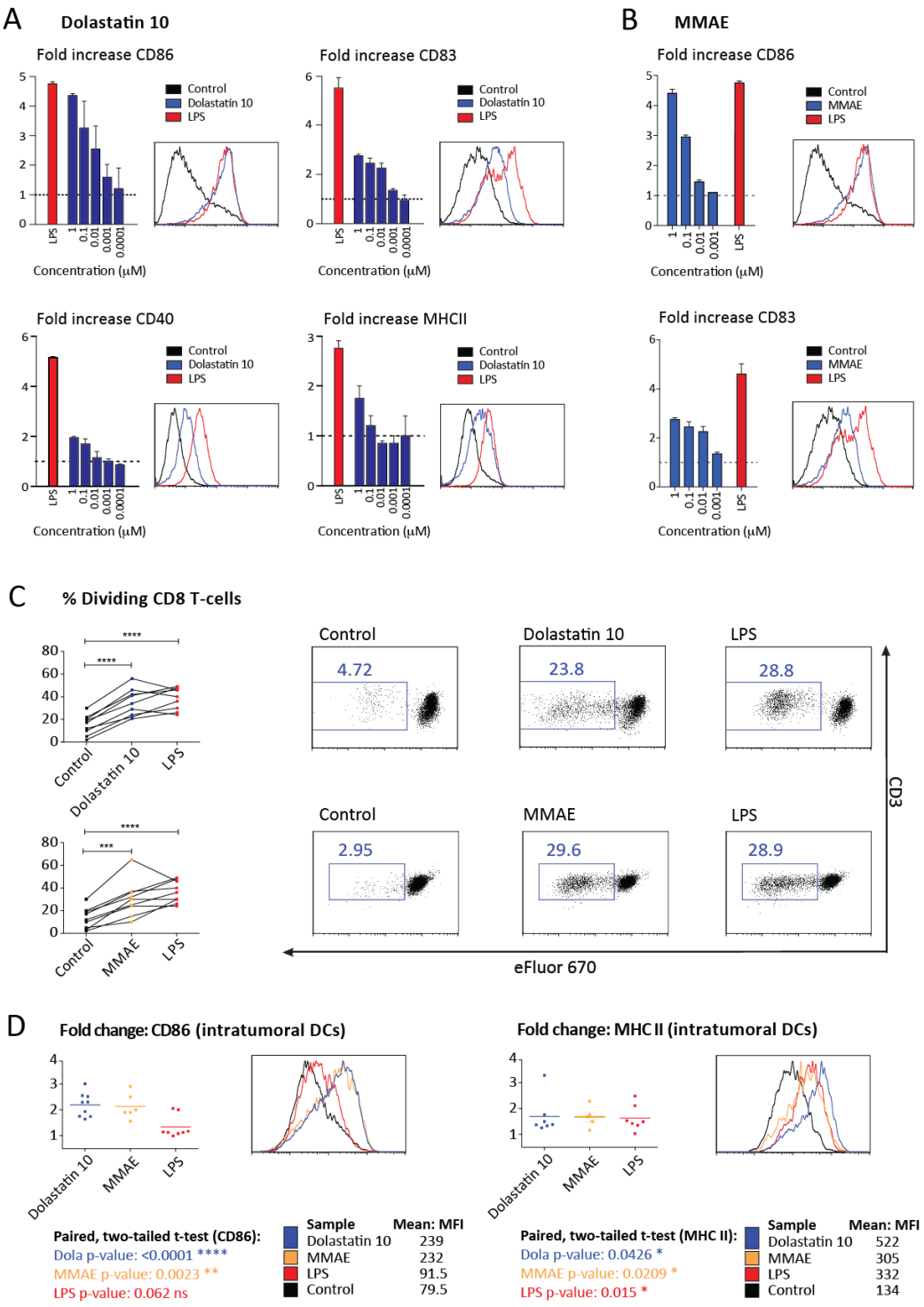

Figure 7-13 Maturation and T cell-stimulatory capacity of *human DCs exposed to dolastatin 10 or MMAE*. (A+B) Expression of CD86, CD83, CD40, and MHCII by (A) dolastatin-treated or (B) MMAE-treated human moDC;. graphs show MFI fold change normalized to untreated cells. All data are representative of at least three independent experiments. Data are depicted as mean ± SD. (C) moDCs were exposed to dolastatin 10 or MMAE, and subsequently used in a MLR with allogeneic $CD8^+$ T cells. T-cell proliferation was measured after 4 days. (D) Human tumor biopsies were incubated with dolastatin 10, MMAE, LPS or left untreated for 24-36h. Expression of CD86 and MHCII by tumor-resident DCs was assessed by flow cytometry. Graphs summarize all performed experiments and show fold change of MFI compared with untreated specimens, which were set as 1. Histograms depict analysis of one representative tumor explant; p< 0.001 ***, p< 0.0001 ****.

7.2.7 Increased costimulatory capacity of human tumor-resident DCs

To directly demonstrate maturation of tumor-resident DCs, matched pieces of human tumor resections were incubated with dolastatin 10, MMAE, or LPS and, after 24 h, analyzed for the expression of CD86 and HLA-DR as indicators of DC maturation. The origin of tumor biopsies is depicted in Table 7-1. Single-cell suspensions of treated and control tumor pieces were analyzed by flow cytometry. A >2-fold upregulation of CD86 by tumor-infiltrating DCs ($CD45^+CD11c^+CD11b^-$) treated with dolastatin 10 ($p<0.0001$) or MMAE ($p<0.003$) was observed (Figure 7-13, D). Interestingly, LPS treatment was not able to reverse the immature state of tumor-resident DCs in terms of CD86 expression ($p=0.062$, ns) to the same degree as dolastatins. In contrast, expression of HLA-DR was induced to the same extent by all three agents, namely dolastatin 10 ($p<0.05$), MMAE ($p<0.03$) and LPS ($p<0.02$). Overall, these data demonstrate that dolastatin 10 and its analogue MMAE are able to phenotypically and functionally mature human moDCs. Most important, both agents are capable of reversing the immature state of tumor-resident DCs in human tumor explants.

Table 7-1 *Human tumor biopsy origin and fold increase expression of CD86 and HLA-DR upon MDA or LPS treatment (n/a= not assessed).*

	Dolastatin 10		MMAE		LPS	
Tumor	**CD86**	**HLA-DR**	**CD86**	**HLA-DR**	**CD86**	**HLA-DR**
Non-small cell lung cancer (NSCLC)	1.9	1.4	1.6	1.7	1.1	1.4
NSCLC	2.3	1.3	2.9	1.2	1.1	1.5
NSCLC	3.0	3.3	2.5	n/a	1.1	2.1
NSCLC	1.7	n/a	n/a	n/a	1	n/a
NSCLC	2.3	n/a	n/a	n/a	n/a	n/a
Colon cancer	2.6	1.8	1.9	1.5	2	1.5
Colon cancer	1.8	1.4	1.9	2.3	2.1	2.5
Colon cancer	2.6	1.3	2	1.8	2	1.4
Renal cell carcinoma	1.6	1.5	n/a	n/a	0.9	1

7.2.8 Promotion of DC maturation by MMAE-coupled ADCs

In order to determine whether systemically administered, tumor targeted MMAE-coupled ADCs allow sufficient release of free MMAE in the tumor vicinity to induce maturation of tumor-resident DCs, an ADC was used, which specifically binds to a mouse tumor in fully immune-competent C57Bl/6 mice. To this end MMAE was conjugated to an antibody against the model antigen Thy1.1 (anti-Thy1.1-MMAE ADC) and the resulting ADC has been tested in tumor-bearing animals using Thy1.1-transfected RMA lymphoma cells. To directly show DC activation, which is reflected by early

antigen uptake and migration of tumor-resident DCs to the tumor-draining lymph nodes, fully immune-competent mice bearing subcutaneous RMA-Thy1.1 tumors were injected intratumorally with FITC-conjugated dextran 24 h prior to systemic administration of the anti-Thy1.1-MMAE ADC or PBS/carrier. Single cell suspensions from tumor-draining and non-draining LNs were prepared 48 h after injection and analyzed by flow cytometry. In mice treated with vehicle alone, DCs from tumor-draining LNs showed almost no increased FITC signal. In stark contrast, FITC-dextran-bearing DCs could be robustly detected and correlated with high CD86 expression in the tumor-draining LNs of mice systemically treated with anti-Thy1.1-MMAE ADC (Figure 7-14, A-B). Consistent with previous observations on free dolastatins, treatment with the anti-Thy1.1-MMAE ADC induced DC activation restricted to the tumor site, since FITC-Dx-bearing DCs could not be detected in non-tumor-draining LNs.

To further substantiate these findings with a clinically relevant ADC, it was explored whether brentuximab vedotin (BV) elicits maturation of human moDCs in co-culture with human lymphoma cell lines. Brentuximab vedotin was highly potent and selective against the $CD30^+$ tumor cell lines L-540 (HL) and Karpas-299 (ALCL) with an IC_{50} of 10 ng/mL and 30 ng/mL, respectively, but more than 1000-fold less active on the $CD30^-$ tumor cell lines Raji and Ramos (both Burkitt NHL) (data not shown; [241]). In contrast to co-culture of human moDCs with brentuximab vedotin-treated $CD30^-$ lymphoma cells (Ramos) or brentuximab vedotin only, a substantial upregulation of the surface expression of CD86 by human moDCs was observed after co-culture with brentuximab vedotin-treated $CD30^+$ L-540 and Karpas-299 lymphoma cells (Figure 7-14, C-D). Notably, DC maturation in response to BV-treated $CD30^+$ lymphoma cells was comparable to that induced by free MMAE.

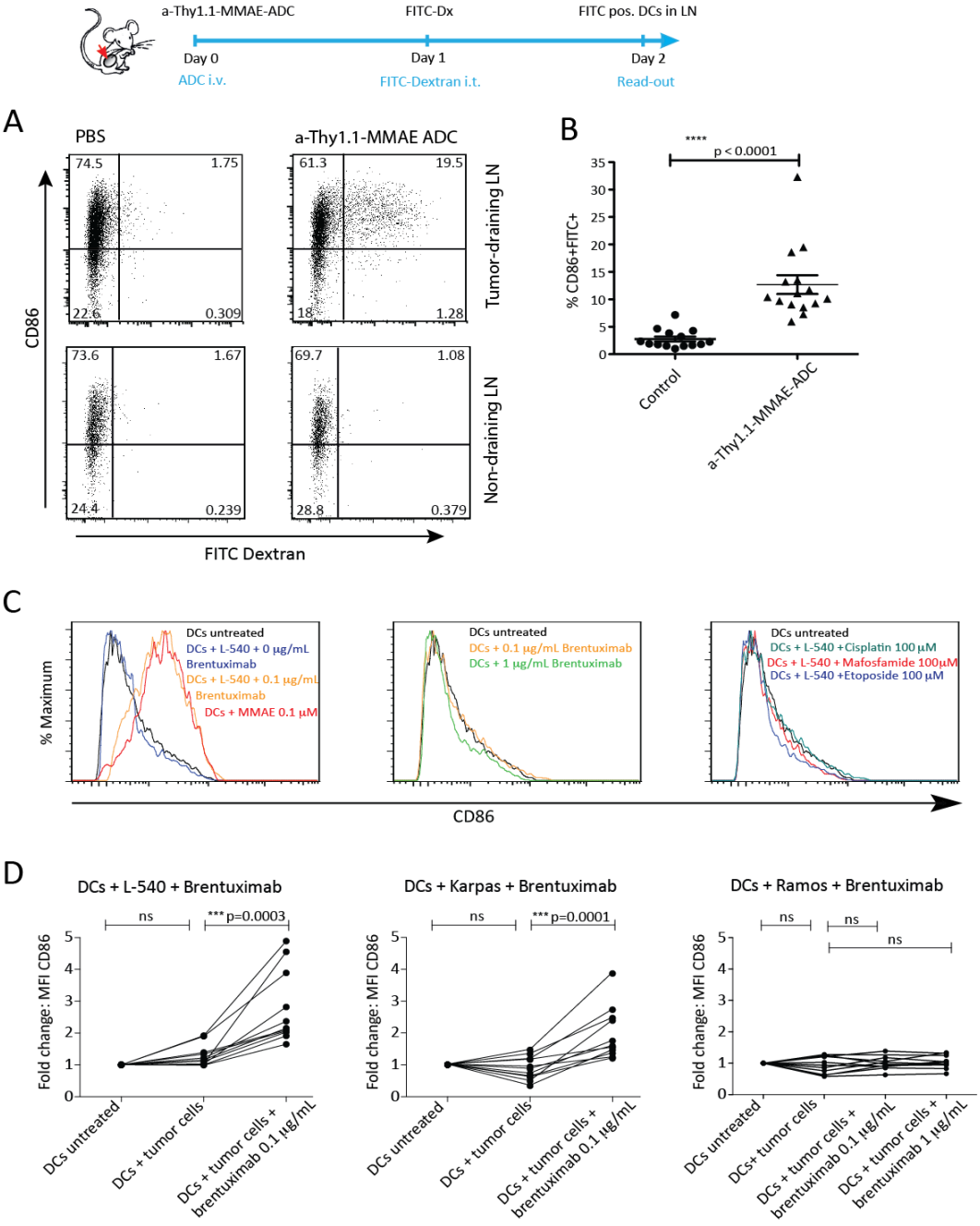

Figure 7-14 ***In vivo DC homing and in vitro maturation of human moDCs by MMAE-coupled ADCs.*** (A+B) C57Bl/6 mice bearing subcutaneous RMA-Thy1.1 tumors of approx. 100 mm^3 size were treated as outlined. Briefly, anti-Thy1.1-MMAE ADC was administered systemically 24h before intratumoral injection of FITC-Dextran. On day 2 after ADC treatment, tumor-draining LNs were examined for the presence of $FITC^+CD86^+$ DCs by flow cytometry. (A) Representative plots depict $FITC^+$ DCs detected in tumor-draining LNs after PBS/DMSO or ADC injection. (B) Graph depicts pooled data from two independent experiments. (C+D) $CD30^+$ Karpas-299 and L-540 as well as $CD30^-$ Ramos cells were incubated with brentuximab vedotin for 3 days. On day 3 immature moDCs were added and co-cultured for 24 h. (C) CD86 expression by DCs after co-culture with brentuximab vedotin-treated L-540 cells (orange). Control DCs were left untreated (black), incubated with L-540 cells alone (blue) or incubated with free MMAE at 0.1 µM for 24h (red; left panel). DCs were cultured in presence of brentuximab vedotin without tumor cells at the indicated concentrations (middle panel) and with L-540 cells treated with 3 distinct chemotherapeutics at 100 µM (right panel) to exclude DC maturation induced by tumor cell death. (D) CD86 MFI fold change as compared to untreated moDCs; graphs show data from 11 independent experiments.

7.2.9 Activation of adaptive immunity in brentuximab-treated lymphoma patients

In collaboration with Dr. Theurich and Prof. von Bergwelt-Baildon from the German Hodgkin Group (University Hospital Cologne), initiation of anti-tumor immune responses upon systemic treatment with brentuximab vedotin was assessed. To this end, PBMCs from six patients with relapsed Hodgkin and $CD30^+$ T-cell lymphoma have been collected before and after brentuximab vedotin administration. All patients exhibited marked clinical and metabolic responses using PET-CT scans (data not shown). Surprisingly, a significant decrease in the number of $CD4^+CD25^+FoxP3^+$ Tregs was observed when comparing PBMCs before and after brentuximab vedotin administration (Figure 7-15, A). While the relative numbers of CD4 and CD8 T cells remained unchanged (data not shown), a significant increase of both CD4 and CD8 T cell activation as determined by the expression of CD25, could further be documented (Figure 7-15, B). To determine the activation of peripheral DCs and B cells, the latter being increasingly recognized as potent antigen-presenting cells and key players in anti-tumor immunity, the expression of CD86 on $lin^-CD11c^+CD11b^{low}$ DCs and $CD20^+$ B cells before and after brentuximab treatment was assessed using flow cytometry. As shown in Figure 7-15, C, expression of this marker substantially increased after brentuximab vedotin administration. Taken together, these results demonstrate that brentuximab vedotin leads to lower frequency of Tregs and increases activation of T and B cells in patients with relapsed Hodgkin lymphoma, thereby reflecting induction of cellular immunity.

To analyze changes in the degree and type of tumor-infiltrating lymphocytes in response to treatment with brentuximab vedotin, skin biopsies were performed on a patient with relapsed $CD30^+$ cutaneous T cell Lymphoma before (pre) and after (post) brentuximab vedotin treatment. In addition to H&E staining, immunohistochemical reactions were carried out using specific antibodies for $CD30^+$ lymphoma cells and $CD4^+$ T_H cells as well as $CD8^+$ CTLs. Compatible with the clinical response upon treatment with brentuximab vedotin, a decrease in the number and density of $CD30^+$ lymphoma cells could be observed. Notably, a substantial increase in total lymphocytes from pre to post tumor specimens was detected. Immunohistochemistry revealed a pronounced increase in both CD4 and CD8 lymphocytic infiltrates in the post skin biopsy (Figure 7-15, D). When performing similar analyses in a patient with relapsed $CD30^+$ Hodgkin lymphoma, a comparable increase in total lymphocyte numbers with a preferential accumulation of T cells could be observed (data not shown).

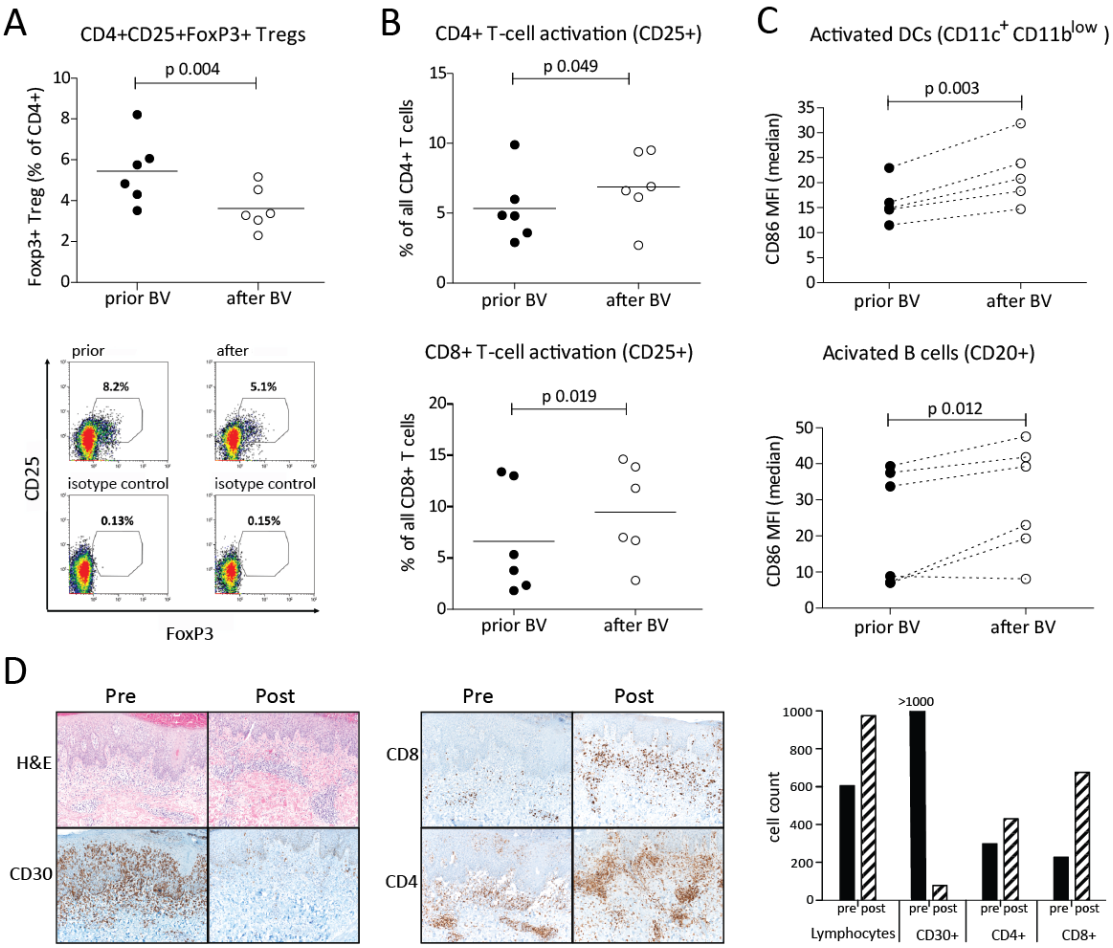

Figure 7-15 ***Cellular immune responses in Brentuximab vedotin-treated lymphoma patients***. (A-C) PBMCs from six patients with relapsed $CD30^+$ malignancies (HL n= 5; $CD30^+$ ALCL n=1) were collected before and after brentuximab vedotin treatment and analyzed by flow cytometry. (A) Data show the percentage of $FoxP3^+$ Tregs (upper panel) and representative dotplots before and after treatment (lower panel). (B) Graphs depict percentages of activated $CD4^+$ (upper panel) and $CD8^+$ T cells (lower panel). (C) Flow cytometric analysis of CD86 expression is shown in $lineage^-$, $CD11c^+$ $CD11b^{low}$ DCs (upper panel) and $CD20^+$ B cells (lower panel) prior and post brentuximab treatment. (D) H&E (upper left) and immunohistochemistry for $CD30^+$ lymphoma cells (lower left), $CD8^+$ (upper right) and $CD4^+$ (lower right) reactive lymphocytes in tumor specimens from one patient with a $CD30^+$ cutaneous T cell lymphoma obtained before and after brentuximab treatment (10x magnification). Tumor immune infiltrates and $CD30^+$ tumor cells were quantified in an area of 10 high power fields (400x) and counts are depicted in the right panel.

7.3 Molecular mechanism of MDA-induced DC maturation

7.3.1 Role of pattern recognition receptor signaling in MDA-induced DC maturation

Previous studies have demonstrated a critical role for pattern recognition receptor (PRR) signaling in DC activation [146]. In order to elucidate the role of these receptors in MDA-induced DC maturation, BMDCs were generated from mice lacking the genes for Toll-like receptor (TLR) or NOD-like receptor (NLR) cytosolic adaptor proteins. Amongst TLR adapter proteins, MyD88 is central because it is shared by most TLRs, with the exception of TLR3, while TLR4 may use either MyD88 or TRIF in two alternative pathways [242]. To determine whether activation of DCs requires MyD88 during exposure to the MDA dolastatin 10, we analyzed its effect on the maturation of BMDCs derived from WT and MyD88$^{-/-}$ mice *in vitro* (Figure 7-16, A) and injected dolastatin 10 into the ears of WT and MyD88$^{-/-}$ mice as previously described in Figure 7-6, A (Figure 7-16, B). The TLR9 ligand CpG1668 was used as positive control. Unlike CpG, which was not able to up-regulate CD86, CD40, and MHCII in MyD88$^{-/-}$ mice, activation of DCs during exposure to dolastatin 10 occurred independently of MyD88 signaling, both *in vitro* and *in vivo*.

To determine the role of TLR3 and TLR4 in MDA-triggered activation of DCs, BMDCs deficient of the TLR3 adaptor protein TRIF, and, as TLR4 uses either TRIF or MyD88 as adaptor protein, receptor-deficient TLR4$^{-/-}$ BMDCs were used. Further PRRs include the NOD-like receptors NOD1 and NOD2, which use receptor-interacting protein 2 (RIP2) as adaptor, as well as the NALP3 (NLRP3) containing protein complex termed the inflammasome. Consequently, both RIP2$^{-/-}$ and NALP3$^{-/-}$ BMDCs were obtained. However, neither IPS-1$^{-/-}$ mice, intended to study the role of the cytosolic RIG-I-like helicases (RLRs), nor mice lacking genes for C-type lectin receptor signaling could be obtained from external collaborators.

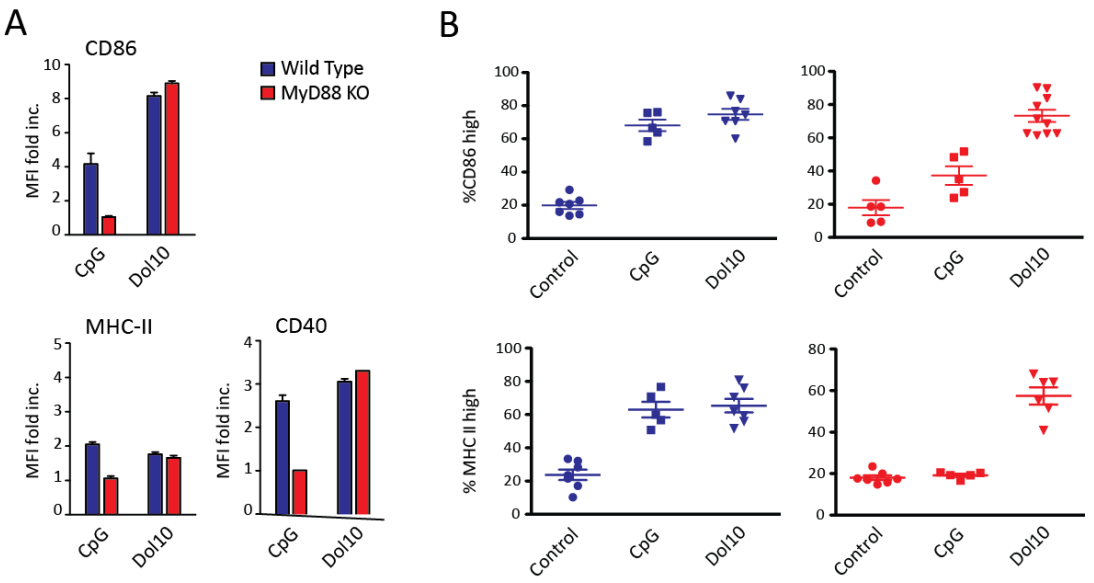

Figure 7-16 ***MyD88-independent immune-stimulatory effect of dolastatin 10***. (A) Expression of CD86, MHCII and CD40 by BMDCs from WT and MyD88$^{-/-}$ mice exposed to dolastatin 10 (0.1 µM) or CpG1668 (1 µg/mL) for 24 h compared with untreated BMDCs. Data are expressed as fold change of MFI compared with untreated cells, which were set as 1. Each bar represents mean ± SD of duplicate cultures from one representative experiment out of three independent experiments. (B) WT or MyD88$^{-/-}$ mice were treated as described in Figure 7-6, A-B. Expression of CD86 by skin Langerhans cells was detected by flow cytometry. Data depict mean (two ears per data point; data were pooled from three independent experiments) % CD86^{high} cells within the CD45^{+}CD11c^{+}MHCII^{+} population (upper panel) and % MHCII^{high} cells (lower panel) in WT mice (blue) or MyD88$^{-/-}$ mice (red).

DC maturation in response to MDA exposure was tested in above mentioned TRIF$^{-/-}$, TLR4$^{-/-}$, RIP2$^{-/-}$ and NALP3$^{-/-}$ BMDCs and known stimulators of each pathway were included as positive controls: LPS (TLRpure®, Invivogen) as a trigger of TLR4; Poly I:C (high molecular weight, Invivogen) as activator of TLR3; muramyl dipeptide (MDP) as activator of NOD2 and nigericin (Nig), an antibiotic, which has been shown to serve as trigger for activation of the NALP3 inflammasome [243]. CpG1668 was included as potent stimulator of DC maturation independent of any of the pathways tested here. Knockout- as well as WT BMDCs were exposed to controls or MDAs (i.e., dolastatin 10 and ansamitocin P3) at indicated concentrations for 20 h prior to flow cytometric assessment of DC maturation marker expression (Figure 7-17, A-B). As expected, the response to LPS, Poly I:C or MDP was abrogated in TLR4$^{-/-}$, TRIF$^{-/-}$ or RIP2$^{-/-}$ BMDCs, respectively. In contrast, upregulation of CD80, CD86, CD40 and MHCII in knockout BMDCs in response to MDA treatment was comparable to that induced in WT BMDCs. Thus, phenotypic maturation of BMDCs in response to the MDAs ansamitocin P3 and dolastatin 10 was independent of TRIF, TLR4, or RIP2 signaling.

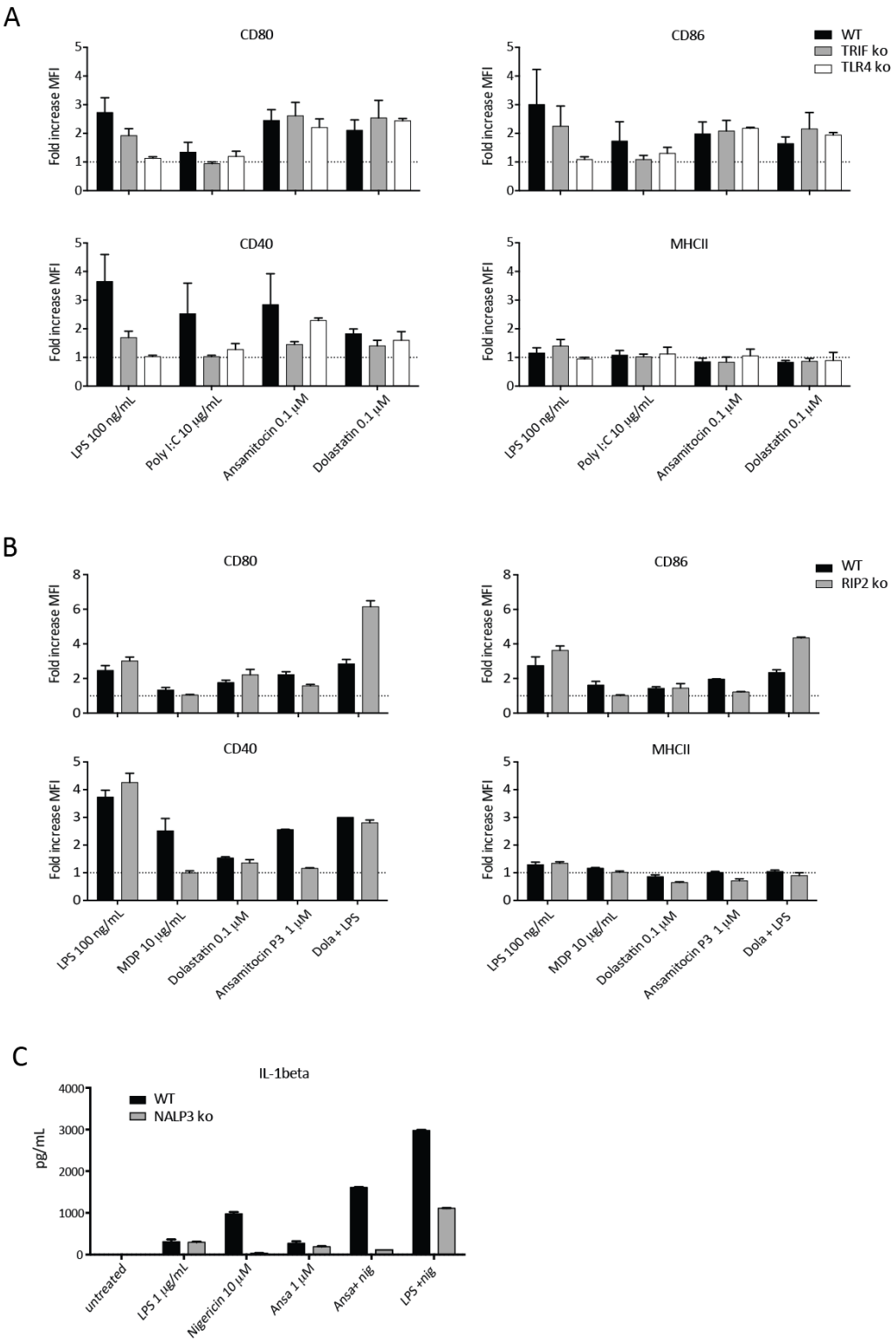

Figure 7-17 ***Upregulation of DC maturation markers and IL-1β expression upon MDA exposure is independent of TLR, NLR or NALP3 inflammasome signaling.*** (A+B) WT, $TLR4^{-/-}$, $TRIF^{-/-}$ (A), as well as WT and $RIP2^{-/-}$ (B) BMDCs were incubated with the indicated chemotherapeutic compounds (0.1 µM) or controls for 24h. Expression of CD80, CD86, CD40 and MHCII was assessed by flow cytometry; graphs show fold change of MFI compared to mock-treated cells, which were set as 1. Pooled data from two independent experiments are shown. (C) Expression of IL-1β in supernatants of WT and $NALP3^{-/-}$ BMDCs upon 24h exposure to ansamitocin P_3 (1 µM), LPS (1 µg/mL), nigericin (10 µM) or combinations thereof as detected by ELISA. Bars represent mean ± SD of duplicate cultures from one out of two independent experiments.

NALP3-inflammasome activation triggers secretion of large amounts of mature IL-1β [158]. Therefore, release of IL-1β was tested in NALP3$^{-/-}$ and WT BMDC cultures. As observed before, ansamitocin P3 triggered IL-1β expression in WT BMDCs to similar extent as LPS (Figure 7-17, C). Importantly, while the nigericin-triggered increase in IL-1β observed in WT BMDCs was markedly reduced in NALP3$^{-/-}$ BMDCs, equal levels of IL-1β were detected in WT and knockout BMDCs in response to LPS and ansamitocin P3. Therefore, functional DC activation in terms of IL-1β expression is independent of NALP3-inflammasome activation. Taken together, these data indicate that MDA-induced DC maturation is independent of TLRs, the major NLRs NOD1 and NOD2, and the NALP3-inflammasome. Due to the structures of the tested MDAs (see Introduction chapter 4.4.1), it seems unlikely that the nucleic acid sensing RLRs, or C-type-lectin receptors recognizing sugar-associated structures are involved in the observed DC maturation. Rather, it appears that the process of active depolymerization of microtubules may be the triggering event to induce signaling pathways that ultimately lead to innate immune responses. These may be a result of profound cellular and biological changes within a dendritic cell.

7.3.2 Characterization of the MDA-induced cytokine pattern

Chemotherapeutics with similar impact on immune activation and known underlying signaling events were compared to MDAs in order to find out whether similar signaling pathways might be triggered by MDAs. In this context, various studies reported activation of tumor-resident DCs and murine macrophages by the chemotherapeutic agent 5,6-Dimethylxanthenone-4-acetic acid (DMXAA), a vascular-disrupting agent (VDA) [244-246]. Unlike other VDAs, DMXAA does not bind microtubules, and although its mechanism of tumor-cell cytotoxicity is largely unknown, it has been proposed that DMXAA inhibits various kinases as well as vascular endothelial growth factor receptor (VEGFR)-2 [247]. Upon stimulation with DMXAA, macrophages produced large amounts of type I IFNs (mainly IFN-β) mediated *via* the TANK-binding kinase 1 (TBK1)/interferon-regulating factors IRF3/IRF7 signaling axis, as well as TNF-α and IL-6. To test whether microtubule-depolymerizing agents may display a comparable activation profile, transcriptional induction of IFN-α/-β, TNF-α, and further pro-inflammatory cytokines by SP37A3 DCs was determined by real-time quantitative PCR (Figure 7-18). Upon MDA-stimulation, mRNA of both type I IFNs or TNF-α was induced only to low levels compared to DMXAA. Also, when using microtubule-destabilizing drugs, no induction of IRF7 or IRF1 mRNA was detected, while mRNA of the IRF3 target gene IP-10 (CXCL-10) was induced only weakly (data not shown). In contrast, strong induction of IL-1β and IL-6 mRNA was detected at early time points (before 4 h). Interestingly, IL-12p40 as well as IL-23p19, which both belong to the IL-12 family, displayed slightly delayed kinetics (see also Figure 7-23). Hence, these data indicate that the MDA-induced cytokine pattern differs from that observed upon DMXAA, and thus suggest that distinct molecular mechanisms may be responsible for stimulation of DCs. In essence, DMXAA induced anti-viral type I IFN responses *via* induction of TBK1 and IRFs, whereas MDAs triggered pro-

inflammatory responses including early and pronounced induction of IL-1β and IL-6, which are generally associated with the activation of NF-κB and AP-1 transcription factor families rather than IRFs.

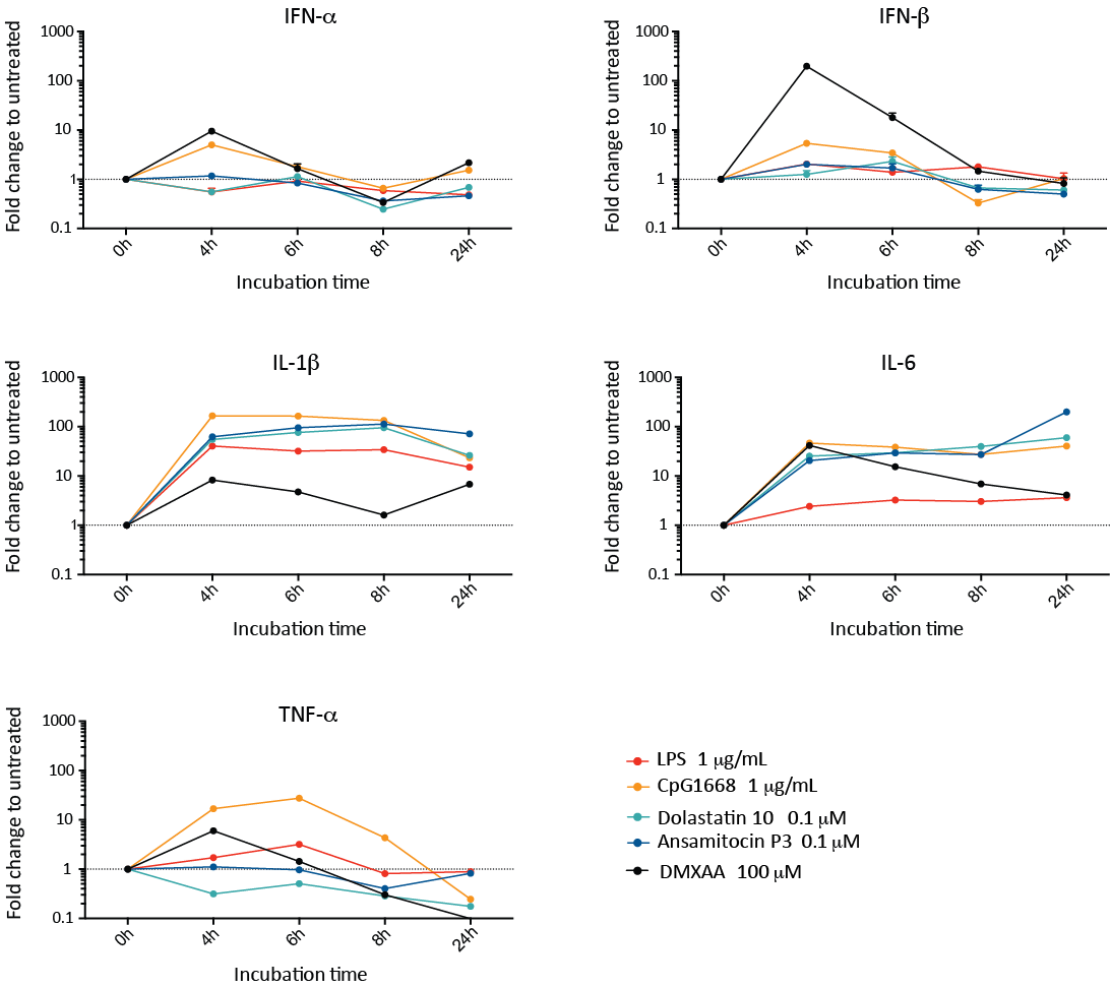

Figure 7-18 ***MDAs promote pro-inflammatory cytokine responses rather than type I IFNs.*** Expression of type I IFN and pro-inflammatory cytokine mRNA by SP37A3 DCs upon 4-24 h exposure to microtubule-destabilizers dolastatin 10 and ansamitocin P3, the vascular-disrupting agent DMXAA, or LPS and CpG1668 as control substances. Expression values were normalized to expression of S18RNA as reference gene, as well as to the expression levels in untreated cells using the ΔΔCT formula as indicated in Methods. One representative experiment of two independent experiments is shown.

7.3.3 Differential activation of c-Jun by MT-binding compounds

Next, investigations were directed towards signaling pathways that are known to be activated in tumor cells upon exposure to microtubule (MT)-binding compounds. In spite of the fact that these compounds generally lead to apoptosis in tumor cells and therefore, provoke distinct outcomes to those observed in DCs, it is known that disruption of MTs in tumor cells induces signaling effectors such as MAPKs, which are equally involved in innate responses [248]. These early signals could then diverge at later time points or with additional signaling events. As shown in Figure 7-5, only microtubule-*destabilizing* compounds had the capacity to induce DC maturation. In contrast, *stabilizing* compounds, such as paclitaxel induced only low levels of MHCII, but no expression of

cytokines. Accordingly, elucidation of signaling events that are differentially induced by MDAs and MSAs will likely give a hint on the pathway(s) responsible for triggering the DC phenotype observed upon exposure to MDAs. In this line, paclitaxel was used as control in selected subsequent experiments. Particularly, Kolomeychuck et *al*. demonstrated that in tumor cells both vinblastine (VBL; destabilizer) and taxol (stabilizer) induced mRNA as well as protein expression of the transcription factor c-Jun and activated the c-Jun N-terminal kinases (JNK), as evidenced by nuclear translocation of JNK1 and JNK2 [249]. However, only VBL induced phosphorylation of c-Jun and activation of the AP-1 site in the c-Jun promoter region. Therefore, it was investigated whether MDA-induced activation of c-Jun occurred in SP37A3 DCs in the same manner as observed for tumor cells. As shown by western blotting, ansamitocin P_3 induced c-Jun phosphorylation at serine 73 (Ser73) as well as enhanced expression of total c-Jun protein in SP37A3 DCs. In stark contrast, no significant increase of phosphorylated or total c-Jun was observed in paclitaxel treated DCs (Figure 7-19).

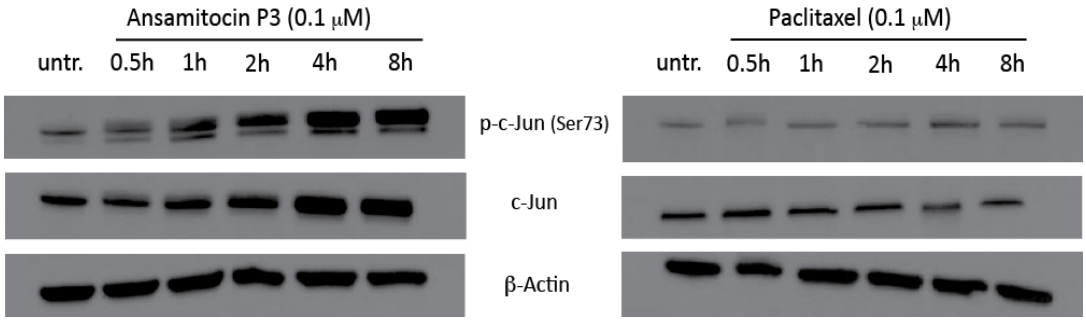

Figure 7-19 ***Differential induction of c-Jun expression and phosphorylation by ansamitocin P3 and paclitaxel***. SP37A3 DCs were incubated with ansamitocin P_3 (0.1 μM) or paclitaxel (0.1 μM) for the indicated time periods before collection of whole cell lysates in RIPA buffer. 10 μg total protein was separated by SDS-PAGE and the total amount of specific proteins and their phosphorylated forms were detected using anti-c-Jun, anti-phospho-c-Jun (Ser73) and anti-β-Actin as loading control. One representative experiment of three independent experiments is shown.

7.3.4 Role of RhoA activation in ansamitocin P3-triggered DC maturation

Consequently, possible upstream regulators of c-Jun were investigated in the context of cytoskeletal rearrangement. Indeed, the small GTPase RhoA has been shown to stimulate c-Jun expression through Rho-associated protein kinase (ROCK) by activating JNK, which led to the phosphorylation and activation of c-Jun and activating transcription factor (ATF)-2 that are bound to the AP-1 site in the c-Jun promoter [202]. Interestingly RhoA activation by the MDA vinblastine has previously been

shown for tumor cells as well as for DCs [199, 200]. Thus, GTP-bound, i.e., active RhoA from DC whole cell lysates was detected using a commercially available kit in ELISA format (G-LISA, Cytoskeleton Inc.). Indeed, RhoA activation could be confirmed upon exposure to ansamitocin P_3 in $SP_{37}A_3$ dendritic cells, with maximum RhoA activation after 30-60 minutes of stimulation (Figure 7-20, A). Furthermore, pre-treatment of $SP_{37}A_3$ DCs with the pharmacological RhoA inhibitor CCG-1423 (Selleckchem) resulted in a dose-dependent reduction of phenotypic maturation as reflected by expression of the costimulatory receptors CD80, CD86 and CD40, as well as MHCII (Figure 7-20, B). Of note, cells were serum starved for 16 h during the assay, which possibly explains the low viability of treated and untreated cells. Together, these data indicate that MDAs induce activation of RhoA, which is required for complete phenotypic DC maturation.

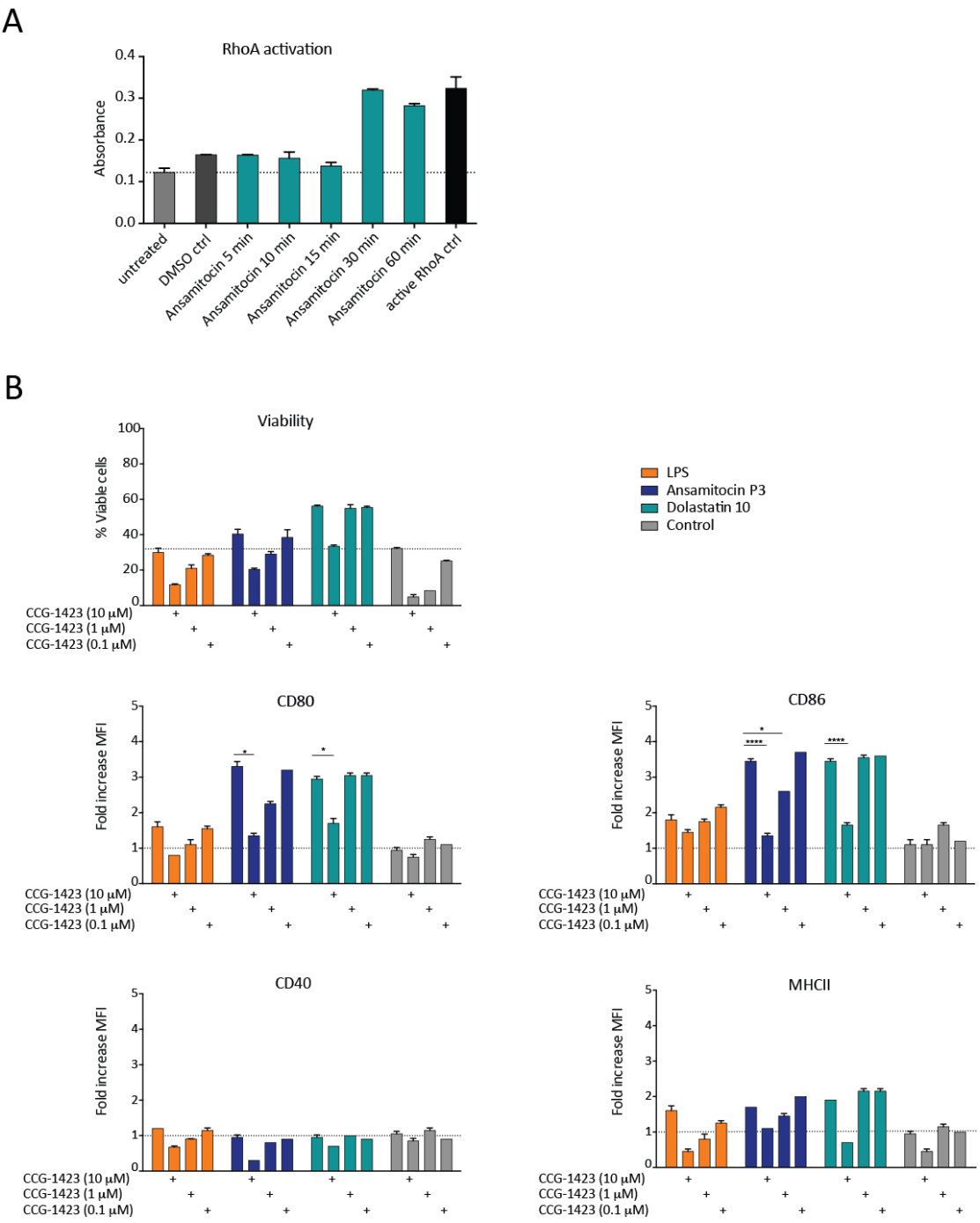

Figure 7-20 ***Activation of RhoA upon exposure to ansamitocin P3***. (A) $SP37A3$ DCs were incubated with ansamitocin $P3$ (0.1 µM) for the indicated time periods before collection of whole cell lysates. Equal amounts of total protein were added to the G-LISA plate in duplicates and processed as outlined in Methods. (B) $SP37A3$ DCs were pretreated with the RhoA-inhibitor CCG-1423 for two hours before addition of ansamitocin $P3$ (0.1 µM), dolastatin 10 (0.1 µM), or LPS (500 ng/mL) for another 14 h. The assay was conducted in serum-free medium; concentrations are indicated. Viability is depicted as percentage of viable cells (viability of untreated cells cultured in presence of serum was set to 100%). MFI was assessed by flow cytometry; graphs show fold change of MFI compared with untreated cells, which were set as 1. Data are representative of three independent experiments with similar results. Mean ± SD of one representative experiment is shown; $p < 0.05$ *; $p < 0.0001$ ****.

7.3.5 Release of the MT–associated GEF-H1 upon ansamitocin P3 treatment

Small Rho GTPases have been described as major regulators of cytoskeleton function and are themselves carefully regulated by a large amount of activators, such as guanine nucleotide exchange factors (GEF), and inhibitors, such as GTPase-activating proteins (GAP) [190]. Amongst the activating guanine nucleotide exchange factors, GEF-H1 (also: Arhgef, murine: lfc) is uniquely associated with microtubules [193, 194]. Furthermore, Krendel and colleagues provided experimental evidence that GEF-H1 is responsible for regulating Rho activity in response to microtubule depolymerization, and that microtubule disassembly resulted in the activation of Rho. In addition, nocodazole-induced depolymerization of microtubules disrupted the inhibited (i.e., phosphorylated) GEF-H1 complex, resulting in potent activation of GEF-H1 [195, 198]. Therefore, immunofluorescence was used to determine whether GEF-H1 was expressed in SP37A3 DCs and, whether GEF-H1 co-localized with MTs in DCs. As demonstrated in Figure 7-21, A, GEF-H1 (green) was found to co-localize with microtubules (α-tubulin, red) in most untreated control DCs. Since microtubule structures are highly temperature-sensitive, some residual cytoplasmic GEF-H1 might be a result of MT-instability due to the handling of the cells during the collection and staining procedure. Importantly, these data demonstrate that ansamitocin P3 treatment induced rapid disruption of the MT network in dendritic cells after only 5 to 15 minutes of incubation. MT-disruption furthermore led to release of GEF-H1 and cytoplasmic accumulation of both GEF-H1 and α-tubulin subunits (Figure 7-21, B). Importantly, GEF-H1 release from MTs has been confirmed using live cell imaging of APRE epithelial cells (data not shown, time lapse video file). Since dendritic cells are generally difficult to transfect, we used these epithelial cells in order to monitor GEF-H1 localization and behavior upon ansamitocin P3 stimulation in real-time (total duration: one hour).

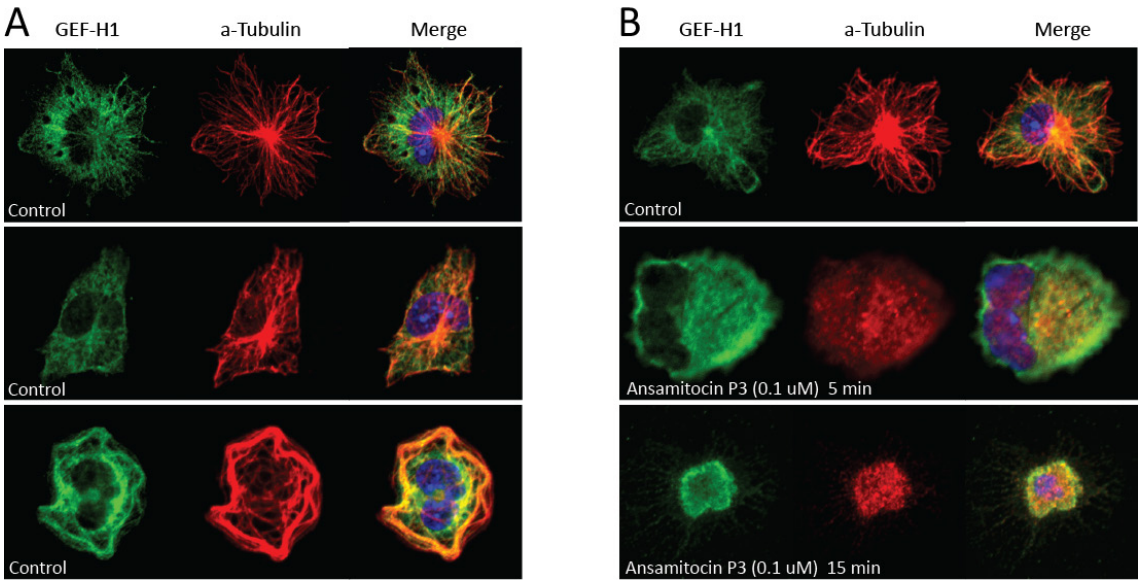

Figure 7-21 GEF-H1 co-localized with microtubules and was released upon MT disruption by ansamitocin P3. (A+B) SP37A3 DCs were seeded onto polylysine-coated coverslips in serum-free medium and treated with ansamitocin P_3 (1 µM) for the indicated time periods or left untreated (control). Cells were fixed and stained with anti-α-tubulin and anti-lfc (GEF-H1) mAbs followed by anti-rabbit Alexa647 and anti-sheep Alexa488 secondary antibodies, respectively. Slides were then mounted with antifade reagent containing DAPI as nuclear stain (blue) and were analyzed by confocal microscopy (LSM 710 Rocky, Zeiss).

7.3.6 Role of GEF-H1 in ansamitocin P3-induced MAPK/AP-1 activation

In light of these data, a collaboration with the laboratory of Prof. Hans-Christian Reinecker at the Massachusetts General Hospital, Boston was initiated due to the lab`s long-standing expertise in GEF-H1-dependent innate signaling [250-252]. Furthermore, GEF-H1 deficient mice were established and maintained in the Reinecker Lab. Consequently, DC maturation upon ansamitocin P_3 treatment was tested in GEF-H1 deficient ($Arhgef^{-/-}$) BMDCs. These experiments were intended to elucidate whether GEF-H1 was indeed the MT-associated trigger of downstream signaling events leading to c-Jun phosphorylation and ultimately inducing expression of maturation markers as well as pro-inflammatory cytokines in response to MDAs. To this end, day 7 $Arhgef^{-/-}$ and WT (both C57Bl/6) BMDCs were incubated with ansamitocin P_3 for 20 h prior to analysis of maturation marker expression by flow cytometry (Figure 7-22, A). Expression of CD80 and CD86 was significantly reduced in $Arhgef^{-/-}$ BMDCs upon treatment with ansamitocin P_3, dolastatin 10 and also LPS when compared to WT BMDCs. Interestingly, Guo *et al.* have demonstrated that LPS-induced NF-κB activation and IL-8 synthesis in endothelial cells is regulated by both a MyD88-dependent as well as by a GEF-H1-RhoA-dependent pathway [253]. Thus, these data provide a possible explanation for the reduced expression of CD80 and CD86 in LPS-stimulated $Arhgef^{-/-}$ BMDCs. As upregulation of CD40 by either MDA was only modest, a slight, but non-significant reduction of CD40 expression was observed in $Arhgef^{-/-}$ BMDCs. Of note, no upregulation of MHCII was detected because all CD11c-positive cells expressed high levels of MHCII before treatment and DCs were gated based on a $CD11c^{high}$, hence $MHCII^{high}$ phenotype.

As a next step, it was assessed whether GEF-H1 was required for the previously observed induction of c-Jun. Since JNKs (also: stress-activated protein kinases; SAPK/JNK) are the major MAPKs responsible for phosphorylation of c-Jun at both the serine residues 63 and 73 [254], activation of SAPK/JNK (i.e. their two splicing forms p46 and p54) was determined in Arhgef$^{-/-}$ and WT BMDCs. Furthermore, paclitaxel-treated BMDCs were analyzed in order to assess whether the observed difference in c-Jun activation by ansamitocin P_3 and paclitaxel in SP37A3 DCs (Figure 7-19) could be confirmed. As demonstrated in Figure 7-22, B ansamitocin P_3 treatment strongly induced phosphorylation of c-Jun at Ser73 as well as at Ser63 in WT BMDCs. In addition, total c-Jun protein expression was enhanced by ansamitocin P_3 in WT BMDCs. Both phosphorylation of c-Jun as well as induction of total protein in response to ansamitocin P_3 was significantly reduced in Arhgef$^{-/-}$ BMDCs, although not completely abrogated (Figure 7-22, B, left panel). Accordingly, activation of SAPK/JNK as determined by phosphorylation at threonine 183 and tyrosine 185 residues, was significantly enhanced by ansamitocin in WT BMDCs and reduced in Arhgef$^{-/-}$ BMDCs. Importantly, activation of c-Jun as well as SAPK/JNK was detected as early as after one hour of ansamitocin P_3 treatment and was evident for up to 12 hours, with a peak expression after eight hours. These data are consistent with the kinetics observed for induction of pro-inflammatory cytokine mRNA, that was detected after four hours of ansamitocin P_3 treatment and stayed high for at least 24 hours (Figure 7-18). Supporting the hypothesis that only MT-destabilizing agents are able to trigger profound DC maturation, neither c-Jun phosphorylation, nor total c-Jun induction or activation of SAPK/JNK was detected in paclitaxel-treated WT or Arhgef$^{-/-}$ BMDCs (Figure 7-22, B, right panel).

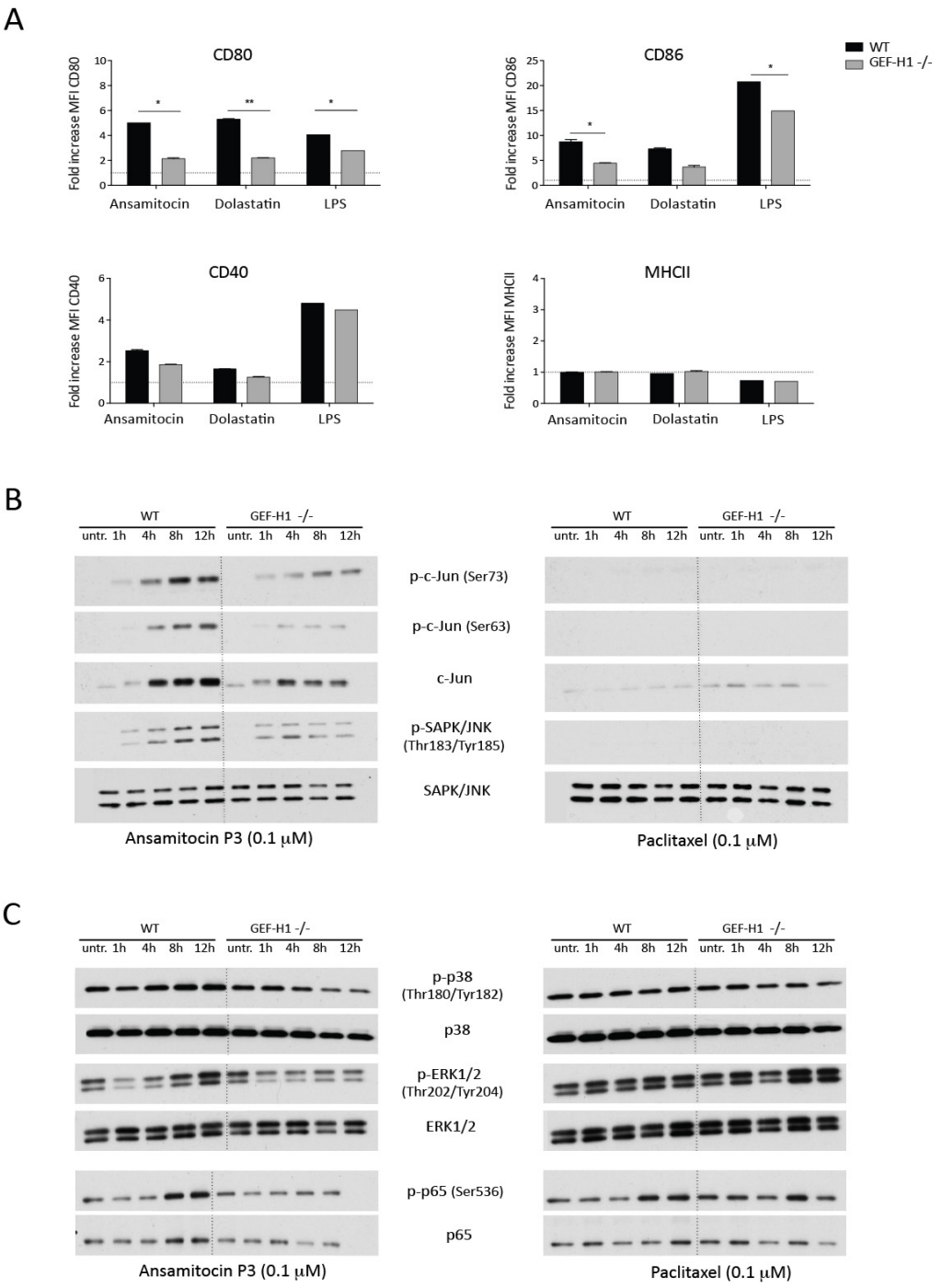

Figure 7-22 Requirement of *GEF-H1 for MDA-induced expression of costimulatory molecules and activation of JNK/c-Jun*. (A) Expression of CD80, CD86, MHCII and CD40 by BMDCs from WT and Arhgef$^{-/-}$ mice exposed to ansamitocin P3 (0.1 μM), dolastatin 10 (0.1 μM) or LPS (500 ng/mL) for 20 h. Data are expressed as fold change of MFI compared with untreated cells, which were set as 1. Each bar represents mean ± SD of duplicate cultures from one representative experiment out of two independent experiments; p< 0.05*; p< 0.01**. (B+C) WT and Arhgef$^{-/-}$ BMDCs were incubated with ansamitocin P3 (0.1 μM) or paclitaxel (0.1 μM) for the indicated time before collection of whole cell lysates in RIPA buffer. Total proteins were separated by SDS-PAGE and transferred to PVDF membranes. The total amount of specific proteins and their phosphorylated forms were detected using anti-phospho-c-Jun (Ser73), anti-phospho-c-Jun (Ser63), anti-c-Jun, anti-phospho-SAPK/JNK, anti-SAPK/JNK (B) and anti-phospho-p38, anti-p38, anti-phospho-ERK1/2, anti-ERK1/2, anti-phospho-p65 or anti-p65 (C). One representative experiment of two independent experiments is shown.

Activation of innate immunity, as for example in response to PRR triggering, mostly results in induction of multiple pathways involving further MAPKs and subsequent induction of not only AP-1 but also NF-κB or IRF transcription factor family members (Figure 4-7, Introduction) [146, 148, 149]. However, rather low induction of type I IFNs in response to MDAs indicated no or only minor activation of IRF dependent pathways. Therefore, it appears that mainly MAPK and AP-1 or NF-κB-dependent pathways may be responsible for expression of pro-inflammatory cytokines in response to MDAs. Thus, phosphorylation of the MAPKs p38 (Thr180/Tyr182) and ERK1/2 (p42/44; Thr202/Tyr204), as well as of the NF-κB family member p65 (Ser536) was tested upon ansamitocin P_3 or paclitaxel treatment in WT and Arhgef$^{-/-}$ BMDCs (Figure 7-22, C). Interestingly, no change in p38 activation was observed in either sample, while ERK1/2 phosphorylation was detected upon ansamitocin P_3 as well as paclitaxel treatment after eight to 12 hours of incubation, although only at moderate levels. Of note, GEF-H1 deficiency led to reduced p-ERK1/2 in response to ansamitocin P_3 treatment, while paclitaxel induced ERK1/2 phosphorylation was unaffected. Phosphorylation of p65 was generally moderate and, similar to the ERK activation pattern, appeared to be GEF-H1 independent in case of paclitaxel (Figure 7-22, C). These data thus indicate a more prominent role for AP-1 rather than NF-κB in mediating DC maturation responses upon MDA treatment.

7.3.7 Requirement of GEF-H1 for transcriptional regulation of DC maturation markers and pro-inflammatory cytokines

Induction of CD80 and CD86 mRNA was tested in WT and Arhgef$^{-/-}$ BMDCs in order to determine whether increased surface expression of these costimulatory molecules was regulated on the transcriptional level as part of a primary response to GEF-H1 and subsequent c-Jun activation. Enhanced mRNA levels of both CD80 and CD86 in WT BMDCs in response to ansamitocin P_3 indeed suggest induction of a transcriptional DC maturation program rather than, or possibly in addition to, receptor recycling or relocation (Figure 7-23, A). Interestingly, both CD80 and CD86 mRNA was induced early and reached a plateau already after four hours, while expression was sustained beyond 12 hours of MDA treatment in WT BMDCs. In contrast, Arhgef$^{-/-}$ BMDCs almost completely failed to induce CD80 and CD86 mRNA in response to ansamitocin P_3. Compatible with previous findings on induction of costimulatory molecules by MSAs, paclitaxel was not able to induce upregulation of CD80 or CD86 mRNA in either WT or Arhgef$^{-/-}$ BMDCs. In order to understand whether induction of pro-inflammatory cytokines was an equally direct result of GEF-H1 activation upon MT disruption, mRNA expression patterns were assessed in WT and knockout BMDCs. Indeed, IL-1β, IL-6, IL-12p35, IL-12p40 and IL-23p19 expression in Arhgef$^{-/-}$ BMDCs exposed to ansamitocin P_3 was found to be decreased to almost baseline levels, as observed in untreated WT BMDCs (Figure 7-23, B-C). Furthermore, these data confirmed the previously noted distinct kinetics of early induced IL-1β, IL-6 and IL-12p35 as compared to late responding, but equally high IL-12p40 and IL-23p19 mRNA production.

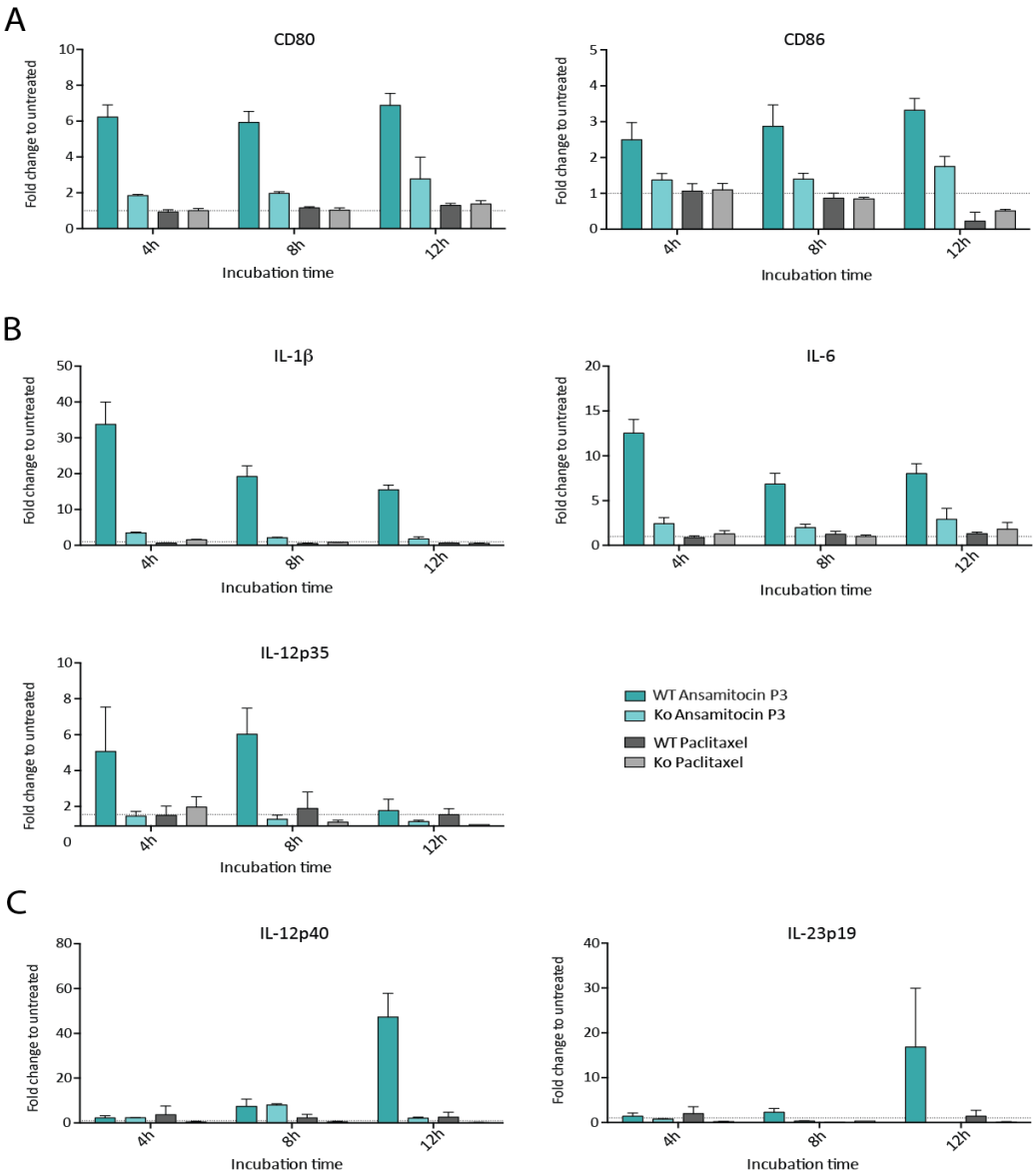

Figure 7-23 ***GEF-H1 is required for transcriptional regulation of maturation markers and pro-inflammatory cytokines in DCs***. Expression of CD80, CD86 and pro-inflammatory cytokine mRNA by WT and Arhgef$^{-/-}$ BMDCs upon 4-12 h exposure to the MDA ansamitocin P_3 (0.1 µM) or the MSA paclitaxel (0.1 µM). Expression values were normalized to expression of S18RNA as reference gene, as well as to expression in untreated cells using the ΔΔCT formula. One representative experiment of two independent experiments is shown.

8 Discussion

8.1 Microtubule-depolymerizing agents promote dendritic cell maturation

With the aim to characterize immunostimulatory anti-cancer compounds for the use in chemo-immunotherapy approaches, we screened classical chemotherapeutic agents with proven tumor cell cytotoxicity for their DC-stimulatory potential. As a result, we identified microtubule-depolymerizing agents as unique and potent inducers of dendritic cell maturation [255, 256]. Compounds of this class investigated in the present study include: a) the maytansinoids ansamitocin P_3 and its synthetic analogue DM1, b) the dolastatins dolastatin 15, dolastatin 10 and the synthetic analogue MMAE, and c) the *vinca* alkaloid vinblastine (VBL). Importantly, all MDAs tested displayed a pronounced capacity to phenotypically and functionally mature murine as well as human DCs in a dose-dependent manner and to similar extent as LPS. These data indicate that MDA-induced DC maturation possibly reflects a class effect common to all microtubule-depolymerizing compounds despite their different molecular structures (see Introduction, chapter 4.4.1) [173]. In our settings, neither microtubule-*stabilizing* agents (MSAs), nor compounds of other classes, such as for example topoisomerase II inhibitors, alkylating agents, HDAC inhibitors or tyrosine kinase inhibitors, displayed significant DC-promoting features (Figures 7-1 and 7-5). On account of this, our data is partially consistent with a functional screen of 54 chemotherapeutic agents that identified not only the microtubule-depolymerizing agent vinblastine, but also the microtubule-stabilizing taxanes, as well as compounds of other classes such as topoisomerase I inhibitors as inducers of DC maturation [118]. This discrepancy might originate from a) different DC cell lines used in both studies, b) the nature of the reporter construct used by Takashima and colleagues, which detected DC activation based on the induction of the IL-1β promoter with high sensitivity, and c) the threshold set by the investigators for determination of DC maturation. Furthermore, the authors observed that induction of the IL-1β promoter did not correlate with a complete DC maturation (defined as simultaneous expression of maturation markers and pro-inflammatory cytokines as well as induction of T cell stimulation), since various compounds that had been identified as DC-stimulatory by the reporter failed to induce expression of more than one costimulatory molecule or pro-inflammatory cytokines, for instance [118, 223]. Consequently, the most prominent compounds were additionally tested in BMDCs. Interestingly, only vinblastine was shown to induce the full spectrum of DC maturation *in vitro* as well as *in vivo* [119]. Furthermore, various studies have reported modulation of DC phenotype upon exposure to low, non-cytotoxic concentrations of the MSA paclitaxel and other chemotherapeutics [114-117]. Yet, these studies mostly evaluated DC function and phenotypic maturation in the context of drug-pretreated tumor cells, or in combination with LPS treatment. Direct effects of paclitaxel and other chemotherapeutics on DCs were generally very moderate and thus, are largely consistent with our data.

Both MDAs and MSAs are used as chemotherapeutics due to their capacity to block mitosis as a result of suppression of microtubule dynamics at low (pM) concentrations in tumor cells *in vitro*. At higher concentrations, i.e. 10-100 nM, they actively induce depolymerization or stabilization of MTs, respectively [169]. Intriguingly, the latter is the concentration range able to induce potent phenotypic DC maturation in case of MDAs. As a logical consequence, it seems that the process of active depolymerization of MT structures, in contrast to stabilization, is a prerequisite for activation of innate immune responses in dendritic cells. In support of this hypothesis, we observed that drug potency in terms of tumor cell cytotoxicity correlated well with potency in terms of DC stimulation (i.e., minimal drug-concentration needed to induce expression of cytokines). Yet, the molecular basis for the differential induction of cell death in tumor cells as compared to DCs remains to be determined. While MT depolymerization induces apoptosis in fast-dividing tumor cells, DC viability was only modestly affected and stayed stable up to a concentration of 10 µM. A reason for this might be reduced sensitivity to apoptosis induction towards microtubule-targeting agents in non- or less-dividing cells such as endothelial cells or DCs [257, 258].

8.2 MDAs potentiate anti-tumor immunity and synergize with immunotherapy

Based on the DC-stimulatory capacity of MDAs and the unique role of DCs in initiating adaptive immunity, we set out to characterize the extent and nature of MDA-promoted anti-tumor immune responses. Since the expansion of effector T cells upon activation is especially sensitive to the toxicity mediated by most chemotherapeutics, we intended to carefully monitor not only DC activation, but also initiation of subsequent T cell responses upon exposure to MDAs using tumor-bearing animals as well as in human *in vitro* assays. For this purpose, we used dolastatin 10 as representative and, besides ansamitocin P_3, most potent member of its class. In summary, the studies presented in this thesis demonstrate that, *first*, dolastatins trigger a program of phenotypic and functional activation of tumor-resident DCs. *Second*, these DCs migrate to the tumor-draining LNs upon antigen-uptake and maturation, where they encounter and activate tumor-antigen-specific T cells. *Third*, $CD11c^+$ DCs and the adaptive immune system are essential for the full therapeutic activity of dolastatins. *Fourth*, when combined with tumor-antigen-specific vaccination or checkpoint inhibitor blocking antibodies, dolastatins show synergistic anti-tumor activity and promote tumor destruction. And *fifth*, ADCs coupled to the dolastatin analogue MMAE, such as brentuximab vedotin, induce DC homing in murine mouse models, maturation of human DCs in lymphoma cell-DC co-cultures, and activation of T as well as B cells in patients, thereby reflecting augmentation of tumor-specific immunity (illustrated as Graphical Abstract, chapter 2).

In extension of the data obtained by the initial screen, we demonstrate that dolastatin 10 is capable to induce maturation and migration of intratumoral DCs *in vivo*. Hence, rather "pro-tumorigenic" tumor-resident DCs [259, 260] may thereby be reprogrammed into "anti-tumor" DCs capable of

promoting functional tumor antigen-specific T cells as a result of increased costimulation and production of T cell-licensing cytokines such as IL-12. Activated T cells in turn, may contribute to tumor rejection. As depicted by enhanced FITC-Dextran uptake that was restricted to tumor-draining LNs, activation of tumor-resident DCs seems to be a local phenomenon, while expansion of antigen-specific T cells in response to dolastatin injection resulted in a broad systemic response. These data led to the hypothesis that dolastatin treatment might function as adjuvant when used in combination with tumor antigen-specific vaccination. Indeed, we observed significant treatment synergies when combining dolastatin 10 with antigen-specific, adenovirus-based anti-tumor vaccination. Thus, these data add to accumulating evidence promoting further clinical evaluation of immunostimulatory chemotherapy that acts on both the immune system and the tumor to create a microenvironment that allows for better implementation of vaccination approaches [56]. Yet, our conclusions are based on improved overall anti-tumor efficacy of the MDA/vaccination combination, while the exact characterization of tumor-antigen-specific T cell responses such as the induction of memory T cells, has not been addressed in the present study. In this line, previous studies by our lab have observed that induction of antigen-specific effector T cells and memory T cells crucially depends on the correct dosing, as well as timing of chemotherapeutics with respect to vaccination (Fink, Y., unpublished observations). Thus, determination of an optimal schedule for chemo-immunotherapy regimens is an important issue that should be addressed in follow-up studies.

We furthermore observed that both adaptive and innate immunity are critically required for the therapeutic anti-tumor efficacy of dolastatin 10. In particular, utilizing depletion experiments, we showed that the anti-tumor effect *in vivo* was largely dependent on $CD11c^+$ DCs, IFN-γ and CD8 T cells. The first studies to report a functional interplay between chemotherapy and the immune system have described the dependency of anthracyclines on adaptive immunity for their full therapeutic efficacy [261]. These agents are meanwhile known to activate APCs *via* stimulation of an immunogenic tumor cell death (ICD) [94, 99, 262-264]. Thus, ICD triggered by anthracyclines could lead to the release of cellular cues, which may elicit an anti-tumor immune response. We cannot formally rule out that dying tumor cells upon MDA treatment emit a series of danger signals that may elicit the recruitment and activation of antigen-presenting cells such as in ICD. However, in our experiments, DC activation by various MDAs has been observed in the absence of tumor cell death. Besides, tumor cell death induced by cytotoxic agents such as cisplatin, mafosfamide, and etoposide, which presumably is non-immunogenic, was not sufficient to activate DCs (Figure 7-14, C).

Similar to conditions in chronic infections, T cells in the tumor microenvironment frequently display restrained effector T cell functions as reflected by incapability to produce cytokines such as IL-2, IFN-γ and TNF-α, or cytotoxic mediators such as granzyme B and perforin [265, 266]. Besides, tumor-associated T cells often express an array of inhibitory receptors [267]. Consequently, blockade of inhibitory T cell checkpoint receptors aims at overcoming tumor-induced T cell exhaustion, and

indeed, therapeutic blockade of CTLA-4 and PD-1/ PD-L1 has demonstrated impressive clinical benefits by at least partially reverting T cell dysfunction [268-270]. Based on enhanced specific T cell responses upon dolastatin treatment, we explored a functional interplay between MDA treatment (i.e., dolastatin 10) and CTLA-4/PD-1 antibodies. The combination was significantly more potent against established tumors than dolastatin 10 or antibodies alone. Interestingly, as a result of the combination therapy, the frequency and number of intratumoral IFN-γ producing effector CD8 T cells increased, while Treg frequency decreased. This led to a substantial increase in the intratumoral ratio of Teffs (defined as IFN-γ^+ T cells) to Tregs, which is considered to be an indicator of a favorable anti-tumor immune response [240, 271]. From a mechanistic standpoint, we envision that the anti-tumor immune response, which is activated upon dolastatin administration, is subsequently dampened by the engagement of inhibitory receptors, such as CTLA-4 and PD-1 on tumor-infiltrating T cells. The concomitant application of antagonistic antibodies blocking these inhibitory receptors efficiently unleashes as well as sustains the T cell response against the tumor.

Nevertheless, clear limitations of our *in vivo* studies are the nature of the tumor models used. We employed syngeneic tumor models in order to describe the host´s immune system in response to tumors. Subcutaneous tumors, however, are generated by injecting tumor cell lines that may have originated from a distinct organ, into the flanks of the mice. These tumors lack the heterogeneity of tumor cells normally characterizing human tumors. In addition, these tumors grow unnaturally fast, which possibly leads to a distinct architecture of the tumor microenvironment as compared to human tumors. Tumor formation in humans involves the co-evolution of tumor cells together with vascular endothelial, stromal and immune cells, as well as extracellular matrix components [272]. By introducing artificial antigens such as OVA into these tumors, we furthermore modulate tumor cell immunogenicity and might thereby bias our observations. Hence, accurate modeling of tumor complexity and heterogeneity is a difficult task that is best met by the use of genetically engineered mouse models (GEMMs). Tumors in these models usually arise within the native tissue and incorporate many features of the tumor and the tumormicro-environment [272]. Consequently, the lab has meanwhile adopted the K-ras/p53 mutated KP model [273] in order to mimic non-small cell lung cancer, as well as models of breast cancer based on targeted expression of oncogenes and growth factors under the control of the mouse mammary tumor virus (MMTV) in mammary glands [274]. These models will ultimately allow monitoring of anti-tumor immune responses in a more physiological setting.

Next, we intended to translate our findings from murine models into the human setting. Accordingly, we have confirmed that both dolastatin 10 and its synthetic analogue MMAE are capable to mature peripheral, monocyte-derived DCs as well as intra-tumoral DCs obtained from primary resections of cancer patients. The latter experiments confirmed previous observations in murine models and suggest that dolastatins indeed may convert, at least in part, the immature status of tumor-resident

DCs [275, 276], into a rather anti-tumorigenic one. These data are of further clinical relevance, as MMAE and the ansamitocin P3 analogue DM1 are both frequently explored as cytotoxic payloads of ADCs [277]. With the approval of the MMAE-based brentuximab vedotin (BV) and DM1-bound trastuzumab emtansine (T-DM1), the excitement over ADCs is steadily building and this class of drugs is readily integrated into the treatment regimen of cancer patients [278-281]. Brentuximab vedotin has recently been shown to induce sustained clinical responses in heavily pre-treated patients [282]. In addition to direct tumor cytotoxicity, it has been reported that BV interferes with the immunosuppressive environment by decreasing the release of cytokines [283]. Moreover, Theurich and colleagues have reported a significant and lymphoma-specific increase of $CD161^+$ T cells in patients with $CD30^+$ lymphomas previously treated with BV [284, 285]. These data suggest that induction of tumor-specific immunity could play a more substantial role for the therapeutic efficacy of brentuximab than so far appreciated. According to the effects of free dolastatins, BV elicits maturation of human moDCs in co-culture with CD30-expressing lymphoma cells, underlining that MMAE can diffuse from tumor cells into the vicinity, resulting in DC activation. In addition, we were able to demonstrate that systemic brentuximab vedotin treatment activates cellular immune responses in patients with $CD30^+$ lymphomas. In the peripheral blood we observed a consistent upregulation of costimulatory markers in both T and B cells after brentuximab vedotin administration. The frequency of circulating regulatory T cells was substantially decreased, which may further support the induced and/or enhanced anti-lymphoma immune response. Of particular note, we found an increase in $CD8^+$ and $CD4^+$ TILs in response to the treatment with brentuximab vedotin early after commencement. Our data thus suggest that brentuximab vedotin favorably alters the balance between tumor-mediated immune suppression and anti-tumor immunity, which may considerably contribute to its therapeutic efficacy.

In accordance with the data presented in this thesis and based on our findings of the DC-stimulatory properties of DM1, we demonstrate that T-DM1 induces tumor infiltration of effector T-cells, both in patient-derived and murine breast tumors. While primary resistance to immune checkpoint blocking antibodies occurred, combining T-DM1 treatment with blockade of the PD-1/CTLA-4 inhibitory pathway demonstrated striking synergy and greatly enhanced T-cell responses, including complete tumor rejection in a murine breast cancer model derived from a transgenic MMTV-human HER2-driven murine tumor model (Mueller *et al.*, submitted). Yet, additional studies are required to further investigate the specific immune response, in particular the generation of an immunological memory, upon treatment with ADCs in patients and to correlate these findings with clinical outcome. Consequently, the laboratory initiated a SAKK (Schweizerische Arbeitsgemeinschaft für Klinische Krebsforschung) translational research project to elucidate the immunomodulatory capacity of T-DM1 in patients with HER2-positive breast cancers. Importantly, this study aims at providing an accurate immunological definition of the mode of action of antibody-maytansinoid-conjugates.

Ultimately, the final picture of all data should guide others and us to initiate early clinical trials evaluating the combination of ADCs with immunotherapy for the benefit of the patients.

8.3 Molecular mechanism of MDA-induced DC maturation

Activation of innate immune cells such as dendritic cells is mostly associated with triggering of pattern recognition receptors [146, 242]. Consequently, we have elucidated the role of these receptors in MDA-induced DC maturation by using BMDCs from mice lacking the genes for TLR or NLR cytosolic adaptor proteins. Interestingly, dolastatin 10 and ansamitocin P_3 triggered upregulation of CD40, CD80, CD86 and MHCII independently of MyD88, TLR4, TRIF or RIP2. Similar, ansamitocin P_3-induced secretion of mature IL-1β, which is considered the major response of $NALP_3$ inflammasome activation [286], was comparable in WT and $NALP_3^{-/-}$ BMDCs. Thus, we conclude that the tested MDAs exhibit DC-maturing properties by mechanisms other than engagement of TLRs or NLRs such as NOD1, NOD2 or the $NALP_3$ inflammasome. Due to the molecular structures of the tested MDAs (see Introduction chapter 4.4.1), it seems unlikely that other PRRs such as the nucleic acid-sensing RIG-I like receptors (RLRs), or C-type-lectin receptors recognizing sugar-associated structures, are involved in the observed DC maturation. In this line, we were able to determine that MDA-induced DC maturation requires the ability of the MDA to diffuse through the plasma membrane, indicating that no active receptor-mediated uptake of the drug is involved. In particular, we observed that the highly polar and thus poorly membrane-permeable MMAE-analogue MMAF was not able to trigger phenotypic DC maturation when applied as free agent (data not shown). We therefore hypothesize that the tested MDAs mediate their effects by binding to MTs after entering the dendritic cell by diffusion. Nevertheless, whether MDAs may bind distinct, yet unknown cell-surface or intracellular receptors remains unclear. Due to the observed class effect, however, we speculate that the process of active depolymerization of microtubules may be the initial event triggering innate signaling pathways. These might lead to inflammatory responses as a result of profound cellular and biological changes within a dendritic cell; a concept that has previously been reported for inflammation in response to endoplasmatic reticulum stress [287].

In fact, microtubule-binding agents can efficiently activate NF-κB and MAPK signaling pathways in tumor cells [288-292]. Based on the observation that only destabilizing agents induce functional DC maturation, we focused on pathways that were *differentially* engaged in response to MDAs as compared to MSAs. Particularly, Kolomeychuck *et al.* demonstrated differential activation of the AP-1 transcription factor family member c-Jun by vinblastine (VBL; destabilizer) and taxol (i.e., paclitaxel; stabilizer) in tumor cells [249]. Consistent with these data, Berry and colleagues reported a distinct composition of AP-1 heterodimers in response to VBL and taxol, resulting in c-Jun phosphorylation and transcriptional activation of AP-1 only by VBL [293]. In line with these observations, we demonstrate activation of c-Jun in response to the MDA ansamitocin P_3, while the

MSA paclitaxel failed to trigger phosphorylation of c-Jun as well as induction of c-Jun protein in $SP_{37}A_3$ DCs. The AP-1 transcription factor (TF) family, together with NF-κB, cAMP response element-binding protein (CREB), CCAAT-enhancer-binding proteins (c/EBP), and IRF families of TFs, operates downstream of MAPKs and regulates transcription of costimulatory molecules as well as expression of pro-inflammatory cytokines in response to PRR engagement [149]. Considering this functional property of AP-1, it appears that activation of c-Jun is functionally important for MDA-induced DC maturation. Accordingly, it seems that the failure of paclitaxel-treatment to induce complete DC maturation might be related to its incapability to mediate AP-1 activation in DCs. Additionally, the observation that MDAs trigger a rather pro-inflammatory cytokine pattern including expression of IL-1β, IL-6, IL-12 and IL-23 and significantly lower levels of TNF-α and type I IFNs, suggests involvement of NF-κB and AP-1-dependent pathways rather than IRFs (Figure 4-7, Introduction).

Major upstream regulators of c-Jun include the MAPKs JNK (also: SAPK/JNK) and, although to lesser extent, p38 [294]. Besides, small GTPases have been implicated as signaling effectors in the context of cytoskeletal rearrangement [190]. Indeed, RhoA has been shown to stimulate c-Jun expression through ROCK by activating JNK [202]. Interestingly, RhoA activation by vinblastine has previously been shown for tumor cells as well as for DCs [199, 200]. Consequently, we determined that MDAs trigger activation of RhoA in DCs, which is furthermore required for complete phenotypic maturation as demonstrated by decreased expression of DC costimulatory receptors in presence of the pharmacological RhoA inhibitor CCG-1423. It has been reported that paclitaxel inhibits RhoA activity in primary rat neurons [295]. Yet, the effect of paclitaxel on RhoA activation in dendritic cells remains to be determined. This may help to conclude on the specific role of RhoA in mediating the differential effects of MDAs and MSAs on DC maturation. Since small GTPases themselves require activation by specific upstream regulators, we investigated the role guanine nucleotide exchange factors (GEF) in the context of MT disassembly. Of the MT-associated GEFs, to date only GEF-H1 (also: lfc, arhgef) is known to sense MT depolymerization [194]. Importantly, various studies provide experimental evidence that GEF-H1 is responsible for regulating RhoA activity in response to microtubule depolymerization (Figure 4-11, Introduction) [195-198]. Accordingly, we here describe that *first*, GEF-H1 is associated to microtubules in resting DCs, and *second*, after a short exposure to ansamitocin P_3 microtubules start to disassemble, resulting in release and subsequent accumulation of GEF-H1 in the cytoplasmic area. Furthermore, by using GEF-H1 (Arhgef) deficient BMDCs, we have determined a major contribution of GEF-H1 to the induction of MDA-mediated functional DC maturation. Expression of CD80 and CD86, both on the transcriptional and on the protein level, as well as induction of IL-1β, IL-6, IL-12 and IL-23 mRNA in response to ansamitocin P_3 requires presence of GEF-H1. Our data furthermore demonstrate reduced activation of c-Jun, JNK, p38, ERK1/2 and NF-κB (p65) in GEF-H1 deficient BMDCs when compared to WT BMDCs stimulated with ansamitocin P_3. Importantly, while inducing p38, ERK1/2 and NF-κB (p65) to equal amounts as

ansamitocin P3, paclitaxel completely failed to induce phosphorylation of c-Jun and JNK in both WT and GEF-H1$^{-/-}$ BMDCs. These data thus confirm a prominent role for the JNK/c-Jun (AP-1) signaling axis in mediating the differential effects on DC phenotype and function observed upon exposure to MDAs as compared to MSAs. Of note, GEF-H1 deficiency resulted in reduced p-p38, p-ERK1/2 and p-p65 only in response to ansamitocin P3 treatment, while paclitaxel-induced phosphorylation of p38, ERK1/2 and p65 was unaffected in Arhgef$^{-/-}$ BMDCs, suggesting that in contrast to MDAs, MSAs trigger MAPK and NF-κB pathways *via* distinct, GEF-H1-independent mechanisms. Considering that MT destabilization is a prerequisite for GEF-H1 release, and presumably activation, it seems plausible that paclitaxel-induced stabilization of MTs counteracts GEF activation. Experiments assessing the phosphorylation status of GEF-H1 after exposure to ansamitocin P3 and paclitaxel are underway to ultimately prove or disprove this assumption.

In light of these data, we propose the following model (Figure 8-1):

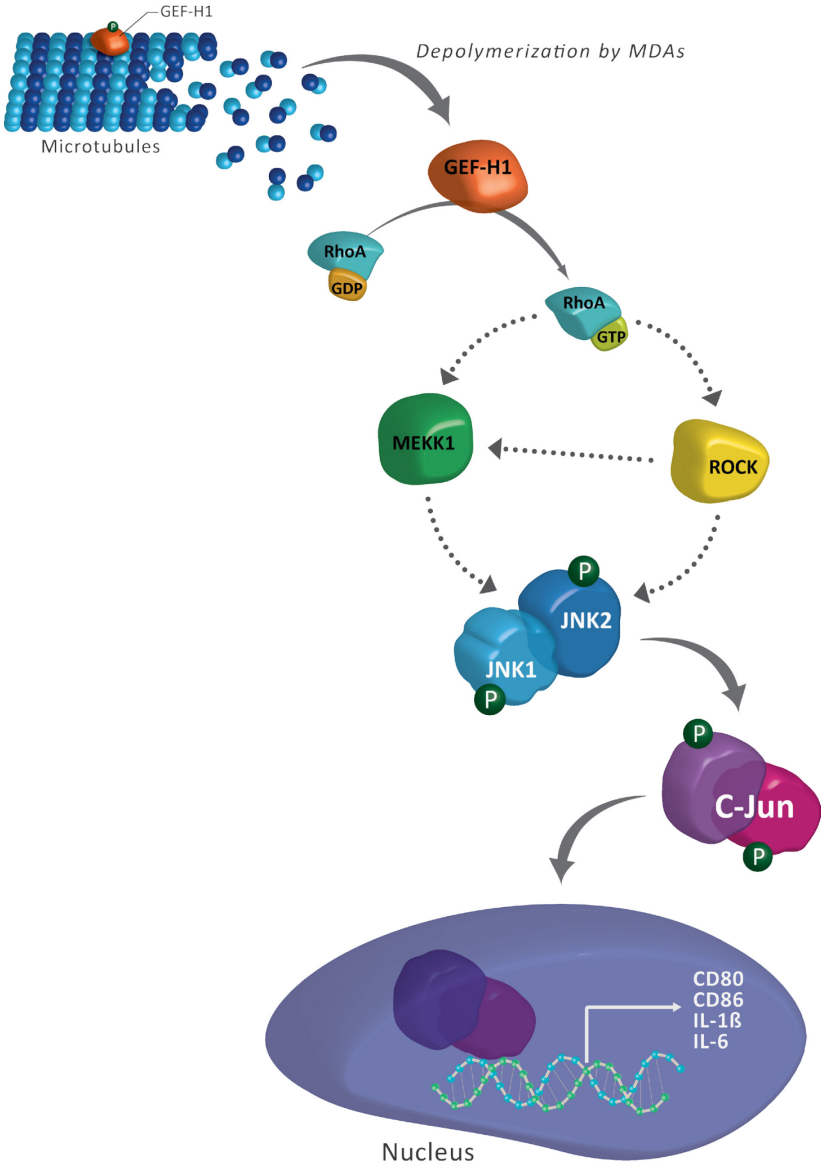

Figure 8-1 ***Molecular mechanism of MDA-induced DC maturation.*** Microtubule-depolymerization leads to release and activation of the guanine nucleotide exchange factor GEF-H1, which in turn induces the small GTPase RhoA. GTP-bound RhoA might induce downstream JNK phosphorylation either directly via ROCK or via the MAPK-family members MEKK1 and MKK4/7. Whether other MAP3Ks, such as TAK1 could possibly be involved instead of MEKK1, or if ROCK induces MEKK1 activation, is part of ongoing research. JNK phosphorylation subsequently triggers c-Jun that translocates into the nucleus to induce AP-1-dependent gene transcription resulting in pro-inflammatory responses in DCs. Dashed lines indicate hypothetical steps that might be involved in the proposed MDA-triggered signaling cascade. (GTP, guanosin triphosphate; RhoA, Ras homolog gene family, member A; ROCK, RhoA-associated kinase; MAPK, mitogen-activated protein kinase; MEKK1, mitogen-activated protein kinase kinase kinase; MKK4/7, mitogen-activated protein kinase kinase 4/7; MAP3K, MAP kinase kinase kinase; TAK1, MAP3K7 (MAP kinase kinase kinase 7); JNK, c-Jun N-terminal kinases; AP-1, Activator Protein-1).

As depicted by dashed lines, our model still lacks the connecting link between induction of RhoA and phosphorylation of JNK. As indicated earlier, RhoA has been shown to activate JNK via ROCK in 3T3

NIH fibroblasts. This study furthermore implicates a role for the MAP2K MKK4, but not for MKK7 [202]. Both MKK4 and MKK7 are known as major MAP2Ks specific for JNKs (MAP2Ks: mitogen-activated protein kinase kinases; see Introduction chapter 4.3.2.1) [296]. Marinissen *et al.* furthermore hypothesize that MKK4 is presumably not directly phosphorylated by ROCK but rather by additional, yet unknown MAP3Ks (mitogen-activated protein kinase kinase kinases, also: JNKKKs). JNK may be regulated by at least 14 MAP3Ks [163, 254], of which we will mainly discuss MEKK1 and TAK1 (also MAP kinase kinase kinase 7; MAP3K7) as these have been previously associated with microtubule destabilization and/or RhoA activation. For instance, RhoA, but not Rac or Cdc42, binds MEKK1 and regulates its kinase activity [191]. Also, microtubule-disrupting drugs, including both MDAs and MSAs, have been shown to activate MEKK1 [297, 298]. Importantly a recent report on a novel colchicine site–targeted tubulin inhibitor (MT189) determined that this MDA causes activation of the MEKK1/TAK1–MKK4–JNK signaling pathway in human cancer cells [296]. Accordingly, MT189 enhanced the phosphorylation levels of JNK, p38, MEKK1, TAK1, and MKK4, but just marginally changed the level of p-MKK7. The authors found that neither intact nor disrupted microtubules were colocalized with p-MEKK1 or p-TAK1, suggesting involvement of unknown upstream regulators that are associated with MTs [296]. Hence, in order to provide the complete signaling cascade triggered by MDAs in dendritic cells, phosphorylation of MEKK1, TAK1, MKK4 and MKK7 remains to be elucidated. Since ROCK kinase activity is triggered upon binding of GTP-bound RhoA, its role in MDA-mediated JNK activation is best addressed by using the pharmacological inhibitor Y-27632 [299]. Another study supporting our hypothesis demonstrates that the MDA vincristine, but not paclitaxel, cisplatin or etoposide, enhanced cellular invasive ability in human MKN45 cancer cells *via* GEF-H1/RhoA/ROCK/myosin light chain (MLC) signaling [300]. Similar to our conclusions, the authors state that, although both vincristine and paclitaxel act on microtubules as anti-cancer drugs, their data indicated that these drugs influence cellular motility differently depending on their effect on RhoA activity [300].

On the other hand, the microtubule-destabilizing agent combretastatin (CA)-4 and its novel analogue CA-432 have been shown to impair T cell migration through the Rho/ROCK signaling pathway [301]. Combretastatin binds on the colchicine-binding site on β-tubulin (Table 4-1, Introduction) [173] and as microtubule-destabilizing agent has demonstrated DC-maturing capacity during our initial screen (Figure 7-1). However, we have previously discovered that this agent fails to induce IL-1 expression in DCs and thereby induces semi-mature DCs in contrast to the *vinca*-domain-binding MDAs (i.e., dolastatins, maytansines, *vinca*-alkaloids). These results highlight possibly distinct outcomes on DC phenotype and function depending not only on MT-stabilization or destabilization, but also depending on the specific binding sites on β-tubulin. In addition, crucial cell type-specific differences in the outcome of similar signaling pathways are revealed by above-mentioned studies. Therefore, it remains to be elucidated in more detail, which are the specific

effects of *vinca*-domain-binding MDAs on the migratory potential of T cells to conclude on the best possible treatment options in order not to disturb T cell migration into the tumor sites.

Overall, the MT-associated GEF-H1 appears to be crucially required for transduction of major signaling events that profoundly affect DC differentiation and ultimately translate into anti-tumor immunity. Nevertheless, it has to be considered that most responses were found to be reduced, albeit not completely abrogated in Arhgef$^{-/-}$ BMDCs. Thus, GEF-H1 activation seems to be the major mechanism, although other factors might be contributing to the observed DC-modulatory effects. To address the question of additional direct or indirect mechanisms that may amplify the overall immune response induced by MDAs, we will examine samples from ansamitocin P_3 treated WT and GEF-H1 deficient BMDCs by RNA sequencing. With this approach we expect to receive a broader picture on the major pathways modulated by MDAs, as well as on the DC-specific outcomes of the profound cellular changes triggered by MDAs. These insights could reveal DC-modulatory effects that we might have overlooked so far. On a long run, this analysis will possibly also increase our understanding on the pharmacological mechanism of these drugs in innate cells, which might support the development of similar compounds as immunostimulants suitable not only in for cancer therapy.

9 References

1. Chen YT, Scanlan MJ, Sahin U, Tureci O, Gure AO, Tsang S, *et al.* A testicular antigen aberrantly expressed in human cancers detected by autologous antibody screening. *Proc Natl Acad Sci U S A* 1997,**94**:1914-1918.
2. Linnemann C, van Buuren MM, Bies L, Verdegaal EM, Schotte R, Calis JJ, *et al.* High-throughput epitope discovery reveals frequent recognition of neo-antigens by CD4+ T cells in human melanoma. *Nat Med* 2015,**21**:81-85.
3. Kono K. Current status of cancer immunotherapy. *J Stem Cells Regen Med* 2014,**10**:8-13.
4. Dunn GP, Old LJ, Schreiber RD. The immunobiology of cancer immunosurveillance and immunoediting. *Immunity* 2004,**21**:137-148.
5. Ehrlich P. Ueber den jetzigen Stand der Karzinomforschung. *Ned. Tijdschr. Geneeskd* 1909:273–290
6. Burnet M. Cancer; a biological approach. I. The processes of control. *Br Med J* 1957,**1**:779-786.
7. Burnet FM. The concept of immunological surveillance. *Prog Exp Tumor Res* 1970,**13**:1-27.
8. Burnet M. Immunological Factors in the Process of Carcinogenesis. *Br Med Bull* 1964,**20**:154-158.
9. van der Bruggen P, Traversari C, Chomez P, Lurquin C, De Plaen E, Van den Eynde B, *et al.* A gene encoding an antigen recognized by cytolytic T lymphocytes on a human melanoma. *Science* 1991,**254**:1643-1647.
10. Shankaran V, Ikeda H, Bruce AT, White JM, Swanson PE, Old LJ, *et al.* IFNgamma and lymphocytes prevent primary tumour development and shape tumour immunogenicity. *Nature* 2001,**410**:1107-1111.
11. Shinkai Y, Rathbun G, Lam KP, Oltz EM, Stewart V, Mendelsohn M, *et al.* RAG-2-deficient mice lack mature lymphocytes owing to inability to initiate V(D)J rearrangement. *Cell* 1992,**68**:855-867.
12. Dunn GP, Koebel CM, Schreiber RD. Interferons, immunity and cancer immunoediting. *Nat Rev Immunol* 2006,**6**:836-848.
13. Vesely MD, Kershaw MH, Schreiber RD, Smyth MJ. Natural innate and adaptive immunity to cancer. *Annu Rev Immunol* 2011,**29**:235-271.
14. Smyth MJ, Thia KY, Street SE, Cretney E, Trapani JA, Taniguchi M, *et al.* Differential tumor surveillance by natural killer (NK) and NKT cells. *J Exp Med* 2000,**191**:661-668.
15. Vesely MD, Kershaw MH, Schreiber RD, Smyth MJ. Natural innate and adaptive immunity to cancer. *Annual review of immunology* 2011,**29**:235-271.
16. Kaplan DH, Shankaran V, Dighe AS, Stockert E, Aguet M, Old LJ, *et al.* Demonstration of an interferon gamma-dependent tumor surveillance system in immunocompetent mice. *Proc Natl Acad Sci U S A* 1998,**95**:7556-7561.
17. Schiavoni G, Mattei F, Gabriele L. Type I Interferons as Stimulators of DC-Mediated Cross-Priming: Impact on Anti-Tumor Response. *Front Immunol* 2013,**4**:483.
18. Matzinger P. Tolerance, danger, and the extended family. *Annu Rev Immunol* 1994,**12**:991-1045.
19. Matzinger P. The danger model: a renewed sense of self. *Science* 2002,**296**:301-305.
20. Senovilla L, Vitale I, Martins I, Tailler M, Pailleret C, Michaud M, *et al.* An immunosurveillance mechanism controls cancer cell ploidy. *Science* 2012,**337**:1678-1684.
21. Schreiber RD, Old LJ, Smyth MJ. Cancer immunoediting: integrating immunity's roles in cancer suppression and promotion. *Science* 2011,**331**:1565-1570.
22. Dunn GP, Bruce AT, Ikeda H, Old LJ, Schreiber RD. Cancer immunoediting: from immunosurveillance to tumor escape. *Nature immunology* 2002,**3**:991-998.
23. Koebel CM, Vermi W, Swann JB, Zerafa N, Rodig SJ, Old LJ, *et al.* Adaptive immunity maintains occult cancer in an equilibrium state. *Nature* 2007,**450**:903-907.
24. Ascierto PA, Capone M, Urba WJ, Bifulco CB, Botti G, Lugli A, *et al.* The additional facet of immunoscore: immunoprofiling as a possible predictive tool for cancer treatment. *J Transl Med* 2013,**11**:54.
25. Wu X, Peng M, Huang B, Zhang H, Wang H, Huang B, *et al.* Immune microenvironment profiles of tumor immune equilibrium and immune escape states of mouse sarcoma. *Cancer Lett* 2013,**340**:124-133.
26. Teng MW, Vesely MD, Duret H, McLaughlin N, Towne JE, Schreiber RD, *et al.* Opposing roles for IL-23 and IL-12 in maintaining occult cancer in an equilibrium state. *Cancer Res* 2012,**72**:3987-3996.
27. Ochsenbein AF. Immunological ignorance of solid tumors. *Springer Semin Immunopathol* 2005,**27**:19-35.
28. Khong HT, Restifo NP. Natural selection of tumor variants in the generation of "tumor escape" phenotypes. *Nat Immunol* 2002,**3**:999-1005.
29. Shin MS, Kim HS, Lee SH, Park WS, Kim SY, Park JY, *et al.* Mutations of tumor necrosis factor-related apoptosis-inducing ligand receptor 1 (TRAIL-R1) and receptor 2 (TRAIL-R2) genes in metastatic breast cancers. *Cancer Res* 2001,**61**:4942-4946.
30. Dong H, Strome SE, Salomao DR, Tamura H, Hirano F, Flies DB, *et al.* Tumor-associated B7-H1 promotes T-cell apoptosis: a potential mechanism of immune evasion. *Nat Med* 2002,**8**:793-800.

31. Gajewski TF, Meng Y, Blank C, Brown I, Kacha A, Kline J, *et al.* Immune resistance orchestrated by the tumor microenvironment. *Immunol Rev* 2006,**213**:131-145.
32. Hargadon KM. Tumor-altered dendritic cell function: implications for anti-tumor immunity. *Front Immunol* 2013,**4**:192.
33. Gabrilovich DI, Ishida T, Nadaf S, Ohm JE, Carbone DP. Antibodies to vascular endothelial growth factor enhance the efficacy of cancer immunotherapy by improving endogenous dendritic cell function. *Clinical cancer research : an official journal of the American Association for Cancer Research* 1999,**5**:2963-2970.
34. Wrzesinski SH, Wan YY, Flavell RA. Transforming growth factor-beta and the immune response: implications for anticancer therapy. *Clin Cancer Res* 2007,**13**:5262-5270.
35. Bekeredjian-Ding I, Schafer M, Hartmann E, Pries R, Parcina M, Schneider P, *et al.* Tumour-derived prostaglandin E and transforming growth factor-beta synergize to inhibit plasmacytoid dendritic cell-derived interferon-alpha. *Immunology* 2009,**128**:439-450.
36. Lohr J, Ratliff T, Huppertz A, Ge Y, Dictus C, Ahmadi R, *et al.* Effector T-cell infiltration positively impacts survival of glioblastoma patients and is impaired by tumor-derived TGF-beta. *Clin Cancer Res* 2011,**17**:4296-4308.
37. Mocellin S, Marincola FM, Young HA. Interleukin-10 and the immune response against cancer: a counterpoint. *J Leukoc Biol* 2005,**78**:1043-1051.
38. Gabrilovich D. Mechanisms and functional significance of tumour-induced dendritic-cell defects. *Nat Rev Immunol* 2004,**4**:941-952.
39. Shevach EM. Mechanisms of foxp3+ T regulatory cell-mediated suppression. *Immunity* 2009,**30**:636-645.
40. Vignali DA, Collison LW, Workman CJ. How regulatory T cells work. *Nat Rev Immunol* 2008,**8**:523-532.
41. Gabrilovich DI, Nagaraj S. Myeloid-derived suppressor cells as regulators of the immune system. *Nat Rev Immunol* 2009,**9**:162-174.
42. Dilek N, Vuillefroy de Silly R, Blancho G, Vanhove B. Myeloid-derived suppressor cells: mechanisms of action and recent advances in their role in transplant tolerance. *Front Immunol* 2012,**3**:208.
43. Hao NB, Lu MH, Fan YH, Cao YL, Zhang ZR, Yang SM. Macrophages in tumor microenvironments and the progression of tumors. *Clin Dev Immunol* 2012,**2012**:948098.
44. Corthay A. Does the immune system naturally protect against cancer? *Front Immunol* 2014,**5**:197.
45. Clifford GM, Polesel J, Rickenbach M, Dal Maso L, Keiser O, Kofler A, *et al.* Cancer risk in the Swiss HIV Cohort Study: associations with immunodeficiency, smoking, and highly active antiretroviral therapy. *J Natl Cancer Inst* 2005,**97**:425-432.
46. Shiels MS, Cole SR, Kirk GD, Poole C. A meta-analysis of the incidence of non-AIDS cancers in HIV-infected individuals. *J Acquir Immune Defic Syndr* 2009,**52**:611-622.
47. Hoover R, Fraumeni JF, Jr. Risk of cancer in renal-transplant recipients. *Lancet* 1973,**2**:55-57.
48. Engels EA, Pfeiffer RM, Fraumeni JF, Jr., Kasiske BL, Israni AK, Snyder JJ, *et al.* Spectrum of cancer risk among US solid organ transplant recipients. *JAMA* 2011,**306**:1891-1901.
49. Mesa C, Fernandez LE. Challenges facing adjuvants for cancer immunotherapy. *Immunol Cell Biol* 2004,**82**:644-650.
50. Bonifaz LC, Bonnyay DP, Charalambous A, Darguste DI, Fujii S, Soares H, *et al.* In vivo targeting of antigens to maturing dendritic cells via the DEC-205 receptor improves T cell vaccination. *J Exp Med* 2004,**199**:815-824.
51. Caminschi I, Maraskovsky E, Heath WR. Targeting Dendritic Cells in vivo for Cancer Therapy. *Front Immunol* 2012,**3**:13.
52. Rotte A, Bhandaru M, Zhou Y, McElwee KJ. Immunotherapy of melanoma: Present options and future promises. *Cancer Metastasis Rev* 2015,**34**:115-128.
53. Van Nuffel AM, Benteyn D, Wilgenhof S, Pierret L, Corthals J, Heirman C, *et al.* Dendritic cells loaded with mRNA encoding full-length tumor antigens prime CD4+ and CD8+ T cells in melanoma patients. *Mol Ther* 2012,**20**:1063-1074.
54. Palucka K, Banchereau J. Dendritic-cell-based therapeutic cancer vaccines. *Immunity* 2013,**39**:38-48.
55. Radford KJ, Tullett KM, Lahoud MH. Dendritic cells and cancer immunotherapy. *Curr Opin Immunol* 2014,**27**:26-32.
56. Weir GM, Liwski RS, Mansour M. Immune modulation by chemotherapy or immunotherapy to enhance cancer vaccines. *Cancers (Basel)* 2011,**3**:3114-3142.
57. Mitchell DA, Batich KA, Gunn MD, Huang MN, Sanchez-Perez L, Nair SK, *et al.* Tetanus toxoid and CCL3 improve dendritic cell vaccines in mice and glioblastoma patients. *Nature* 2015,**519**:366-369.
58. Bartlett DL, Liu Z, Sathaiah M, Ravindranathan R, Guo Z, He Y, *et al.* Oncolytic viruses as therapeutic cancer vaccines. *Mol Cancer* 2013,**12**:103.
59. Rosenberg SA, Yang JC, Sherry RM, Kammula US, Hughes MS, Phan GQ, *et al.* Durable complete responses in heavily pretreated patients with metastatic melanoma using T-cell transfer immunotherapy. *Clin Cancer Res* 2011,**17**:4550-4557.

60. Chacon JA, Sarnaik AA, Chen JQ, Creasy C, Kale C, Robinson J, *et al.* Manipulating the tumor microenvironment ex vivo for enhanced expansion of tumor-infiltrating lymphocytes for adoptive cell therapy. *Clin Cancer Res* 2015,**21**:611-621.
61. Chmielewski M, Hombach AA, Abken H. Of CARs and TRUCKs: chimeric antigen receptor (CAR) T cells engineered with an inducible cytokine to modulate the tumor stroma. *Immunol Rev* 2014,**257**:83-90.
62. Heslop HE. Safer CARS. *Mol Ther* 2010,**18**:661-662.
63. Porter DL, Levine BL, Kalos M, Bagg A, June CH. Chimeric antigen receptor-modified T cells in chronic lymphoid leukemia. *N Engl J Med* 2011,**365**:725-733.
64. Kalos M, Levine BL, Porter DL, Katz S, Grupp SA, Bagg A, *et al.* T cells with chimeric antigen receptors have potent antitumor effects and can establish memory in patients with advanced leukemia. *Sci Transl Med* 2011,**3**:95ra73.
65. Maude SL, Frey N, Shaw PA, Aplenc R, Barrett DM, Bunin NJ, *et al.* Chimeric antigen receptor T cells for sustained remissions in leukemia. *N Engl J Med* 2014,**371**:1507-1517.
66. Robbins PF, Morgan RA, Feldman SA, Yang JC, Sherry RM, Dudley ME, *et al.* Tumor regression in patients with metastatic synovial cell sarcoma and melanoma using genetically engineered lymphocytes reactive with NY-ESO-1. *J Clin Oncol* 2011,**29**:917-924.
67. Tran E, Turcotte S, Gros A, Robbins PF, Lu YC, Dudley ME, *et al.* Cancer immunotherapy based on mutation-specific CD4+ T cells in a patient with epithelial cancer. *Science* 2014,**344**:641-645.
68. Gargett T, Brown MP. The inducible caspase-9 suicide gene system as a "safety switch" to limit on-target, off-tumor toxicities of chimeric antigen receptor T cells. *Front Pharmacol* 2014,**5**:235.
69. Scott AM, Wolchok JD, Old LJ. Antibody therapy of cancer. *Nat Rev Cancer* 2012,**12**:278-287.
70. Chames P, Baty D. Bispecific antibodies for cancer therapy: the light at the end of the tunnel? *MAbs* 2009,**1**:539-547.
71. Seimetz D, Lindhofer H, Bokemeyer C. Development and approval of the trifunctional antibody catumaxomab (anti-EpCAM x anti-CD3) as a targeted cancer immunotherapy. *Cancer Treat Rev* 2010,**36**:458-467.
72. Zugmaier G, Klinger M, Schmidt M, Subklewe M. Clinical overview of anti-CD19 BiTE and ex vivo data from anti-CD33 BiTE as examples for retargeting T cells in hematologic malignancies. *Mol Immunol* 2015.
73. Friedrich M, Henn A, Raum T, Bajtus M, Matthes K, Hendrich L, *et al.* Preclinical characterization of AMG 330, a CD3/CD33-bispecific T-cell-engaging antibody with potential for treatment of acute myelogenous leukemia. *Mol Cancer Ther* 2014,**13**:1549-1557.
74. Weiner LM, Murray JC, Shuptrine CW. Antibody-based immunotherapy of cancer. *Cell* 2012,**148**:1081-1084.
75. Melero I, Grimaldi AM, Perez-Gracia JL, Ascierto PA. Clinical development of immunostimulatory monoclonal antibodies and opportunities for combination. *Clin Cancer Res* 2013,**19**:997-1008.
76. Robert C, Thomas L, Bondarenko I, O'Day S, Weber J, Garbe C, *et al.* Ipilimumab plus dacarbazine for previously untreated metastatic melanoma. *N Engl J Med* 2011,**364**:2517-2526.
77. Perez-Gracia JL, Labiano S, Rodriguez-Ruiz ME, Sanmamed MF, Melero I. Orchestrating immune check-point blockade for cancer immunotherapy in combinations. *Curr Opin Immunol* 2014,**27**:89-97.
78. Blank C, Gajewski TF, Mackensen A. Interaction of PD-L1 on tumor cells with PD-1 on tumor-specific T cells as a mechanism of immune evasion: implications for tumor immunotherapy. *Cancer Immunol Immunother* 2005,**54**:307-314.
79. Hamid O, Robert C, Daud A, Hodi FS, Hwu WJ, Kefford R, *et al.* Safety and tumor responses with lambrolizumab (anti-PD-1) in melanoma. *N Engl J Med* 2013,**369**:134-144.
80. Robert C, Long GV, Brady B, Dutriaux C, Maio M, Mortier L, *et al.* Nivolumab in previously untreated melanoma without BRAF mutation. *N Engl J Med* 2015,**372**:320-330.
81. Herbst RS, Soria JC, Kowanetz M, Fine GD, Hamid O, Gordon MS, *et al.* Predictive correlates of response to the anti-PD-L1 antibody MPDL3280A in cancer patients. *Nature* 2014,**515**:563-567.
82. Powles T, Eder JP, Fine GD, Braiteh FS, Loriot Y, Cruz C, *et al.* MPDL3280A (anti-PD-L1) treatment leads to clinical activity in metastatic bladder cancer. *Nature* 2014,**515**:558-562.
83. Tumeh PC, Harview CL, Yearley JH, Shintaku IP, Taylor EJ, Robert L, *et al.* PD-1 blockade induces responses by inhibiting adaptive immune resistance. *Nature* 2014,**515**:568-571.
84. Yadav M, Jhunjhunwala S, Phung QT, Lupardus P, Tanguay J, Bumbaca S, *et al.* Predicting immunogenic tumour mutations by combining mass spectrometry and exome sequencing. *Nature* 2014,**515**:572-576.
85. Gubin MM, Zhang X, Schuster H, Caron E, Ward JP, Noguchi T, *et al.* Checkpoint blockade cancer immunotherapy targets tumour-specific mutant antigens. *Nature* 2014,**515**:577-581.
86. Snyder A, Makarov V, Merghoub T, Yuan J, Zaretsky JM, Desrichard A, *et al.* Genetic basis for clinical response to CTLA-4 blockade in melanoma. *N Engl J Med* 2014,**371**:2189-2199.
87. Twyman-Saint Victor C, Rech AJ, Maity A, Rengan R, Pauken KE, Stelekati E, *et al.* Radiation and dual checkpoint blockade activate non-redundant immune mechanisms in cancer. *Nature* 2015,**520**:373-377.

88. Lake RA, Robinson BW. Immunotherapy and chemotherapy--a practical partnership. *Nature reviews. Cancer* 2005,**5**:397-405.
89. Menard C, Martin F, Apetoh L, Bouyer F, Ghiringhelli F. Cancer chemotherapy: not only a direct cytotoxic effect, but also an adjuvant for antitumor immunity. *Cancer Immunol Immunother* 2008,**57**:1579-1587.
90. Zitvogel L, Apetoh L, Ghiringhelli F, Kroemer G. Immunological aspects of cancer chemotherapy. *Nat Rev Immunol* 2008,**8**:59-73.
91. Bracci L, Schiavoni G, Sistigu A, Belardelli F. Immune-based mechanisms of cytotoxic chemotherapy: implications for the design of novel and rationale-based combined treatments against cancer. *Cell Death Differ* 2014,**21**:15-25.
92. Emens LA, Middleton G. The Interplay of Immunotherapy and Chemotherapy: Harnessing Potential Synergies. *Cancer Immunol Res* 2015,**3**:436-443.
93. Chen G, Emens LA. Chemoimmunotherapy: reengineering tumor immunity. *Cancer Immunol Immunother* 2013,**62**:203-216.
94. Obeid M, Tesniere A, Ghiringhelli F, Fimia GM, Apetoh L, Perfettini JL, *et al.* Calreticulin exposure dictates the immunogenicity of cancer cell death. *Nat Med* 2007,**13**:54-61.
95. Tesniere A, Schlemmer F, Boige V, Kepp O, Martins I, Ghiringhelli F, *et al.* Immunogenic death of colon cancer cells treated with oxaliplatin. *Oncogene* 2010,**29**:482-491.
96. Schiavoni G, Sistigu A, Valentini M, Mattei F, Sestili P, Spadaro F, *et al.* Cyclophosphamide synergizes with type I interferons through systemic dendritic cell reactivation and induction of immunogenic tumor apoptosis. *Cancer Res* 2011,**71**:768-778.
97. Michaud M, Martins I, Sukkurwala AQ, Adjemian S, Ma Y, Pellegatti P, *et al.* Autophagy-dependent anticancer immune responses induced by chemotherapeutic agents in mice. *Science* 2011,**334**:1573-1577.
98. Panaretakis T, Kepp O, Brockmeier U, Tesniere A, Bjorklund AC, Chapman DC, *et al.* Mechanisms of pre-apoptotic calreticulin exposure in immunogenic cell death. *EMBO J* 2009,**28**:578-590.
99. Apetoh L, Ghiringhelli F, Tesniere A, Obeid M, Ortiz C, Criollo A, *et al.* Toll-like receptor 4-dependent contribution of the immune system to anticancer chemotherapy and radiotherapy. *Nat Med* 2007,**13**:1050-1059.
100. Ghiringhelli F, Menard C, Terme M, Flament C, Taieb J, Chaput N, *et al.* CD4+CD25+ regulatory T cells inhibit natural killer cell functions in a transforming growth factor-beta-dependent manner. *J Exp Med* 2005,**202**:1075-1085.
101. Lutsiak ME, Semnani RT, De Pascalis R, Kashmiri SV, Schlom J, Sabzevari H. Inhibition of CD4(+)25+ T regulatory cell function implicated in enhanced immune response by low-dose cyclophosphamide. *Blood* 2005,**105**:2862-2868.
102. Ghiringhelli F, Menard C, Puig PE, Ladoire S, Roux S, Martin F, *et al.* Metronomic cyclophosphamide regimen selectively depletes CD4+CD25+ regulatory T cells and restores T and NK effector functions in end stage cancer patients. *Cancer Immunol Immunother* 2007,**56**:641-648.
103. Ge Y, Domschke C, Stoiber N, Schott S, Heil J, Rom J, *et al.* Metronomic cyclophosphamide treatment in metastasized breast cancer patients: immunological effects and clinical outcome. *Cancer Immunol Immunother* 2012,**61**:353-362.
104. Vincent J, Mignot G, Chalmin F, Ladoire S, Bruchard M, Chevriaux A, *et al.* 5-Fluorouracil selectively kills tumor-associated myeloid-derived suppressor cells resulting in enhanced T cell-dependent antitumor immunity. *Cancer Res* 2010,**70**:3052-3061.
105. Suzuki E, Kapoor V, Jassar AS, Kaiser LR, Albelda SM. Gemcitabine selectively eliminates splenic Gr-1+/CD11b+ myeloid suppressor cells in tumor-bearing animals and enhances antitumor immune activity. *Clin Cancer Res* 2005,**11**:6713-6721.
106. Alizadeh D, Trad M, Hanke NT, Larmonier CB, Janikashvili N, Bonnotte B, *et al.* Doxorubicin eliminates myeloid-derived suppressor cells and enhances the efficacy of adoptive T-cell transfer in breast cancer. *Cancer Res* 2014,**74**:104-118.
107. Mikyskova R, Indrova M, Vlkova V, Bieblova J, Simova J, Parackova Z, *et al.* DNA demethylating agent 5-azacytidine inhibits myeloid-derived suppressor cells induced by tumor growth and cyclophosphamide treatment. *J Leukoc Biol* 2014.
108. Michels T, Shurin GV, Naiditch H, Sevko A, Umansky V, Shurin MR. Paclitaxel promotes differentiation of myeloid-derived suppressor cells into dendritic cells in vitro in a TLR4-independent manner. *J Immunotoxicol* 2012,**9**:292-300.
109. Sevko A, Michels T, Vrohlings M, Umansky L, Beckhove P, Kato M, *et al.* Antitumor effect of paclitaxel is mediated by inhibition of myeloid-derived suppressor cells and chronic inflammation in the spontaneous melanoma model. *J Immunol* 2013,**190**:2464-2471.
110. Kodumudi KN, Woan K, Gilvary DL, Sahakian E, Wei S, Djeu JY. A novel chemoimmunomodulating property of docetaxel: suppression of myeloid-derived suppressor cells in tumor bearers. *Clin Cancer Res* 2010,**16**:4583-4594.

111. Trojandt S, Knies D, Pektor S, Ritz S, Mailander V, Grabbe S, *et al.* The chemotherapeutic agent topotecan differentially modulates the phenotype and function of dendritic cells. *Cancer Immunol Immunother* 2013,**62**:1315-1326.
112. Hu J, Kinn J, Zirakzadeh AA, Sherif A, Norstedt G, Wikstrom AC, *et al.* The effects of chemotherapeutic drugs on human monocyte-derived dendritic cell differentiation and antigen presentation. *Clin Exp Immunol* 2013,**172**:490-499.
113. Liu WM, Scott KA, Thompson M, Dalgleish AG. Dendritic cell phenotype can be improved by certain chemotherapies and is associated with alterations to p21(waf1/cip1.). *Cancer Immunol Immunother* 2013,**62**:1553-1561.
114. Shurin GV, Tourkova IL, Kaneno R, Shurin MR. Chemotherapeutic agents in noncytotoxic concentrations increase antigen presentation by dendritic cells via an IL-12-dependent mechanism. *J Immunol* 2009,**183**:137-144.
115. Kaneno R, Shurin GV, Tourkova IL, Shurin MR. Chemomodulation of human dendritic cell function by antineoplastic agents in low noncytotoxic concentrations. *J Transl Med* 2009,**7**:58.
116. Pfannenstiel LW, Lam SS, Emens LA, Jaffee EM, Armstrong TD. Paclitaxel enhances early dendritic cell maturation and function through TLR4 signaling in mice. *Cell Immunol* 2010,**263**:79-87.
117. Marin-Esteban V, Charron D, Gelin C, Mooney N. Chemotherapeutic agents targeting the tubulin cytoskeleton modify LPS-induced cytokine secretion by dendritic cells and increase antigen presentation. *J Immunother* 2010,**33**:364-370.
118. Tanaka H, Matsushima H, Mizumoto N, Takashima A. Classification of chemotherapeutic agents based on their differential in vitro effects on dendritic cells. *Cancer Res* 2009,**69**:6978-6986.
119. Tanaka H, Matsushima H, Nishibu A, Clausen BE, Takashima A. Dual therapeutic efficacy of vinblastine as a unique chemotherapeutic agent capable of inducing dendritic cell maturation. *Cancer Res* 2009,**69**:6987-6994.
120. Mizumoto N, Tanaka H, Matsushima H, Vishwanath M, Takashima A. Colchicine promotes antigen cross-presentation by murine dendritic cells. *J Invest Dermatol* 2007,**127**:1543-1546.
121. Steinman RM, Cohn ZA. Identification of a novel cell type in peripheral lymphoid organs of mice. I. Morphology, quantitation, tissue distribution. *The Journal of experimental medicine* 1973,**137**:1142-1162.
122. Steinman RM, Hemmi H. Dendritic cells: translating innate to adaptive immunity. *Current topics in microbiology and immunology* 2006,**311**:17-58.
123. Banchereau J, Briere F, Caux C, Davoust J, Lebecque S, Liu YJ, *et al.* Immunobiology of dendritic cells. *Annu Rev Immunol* 2000,**18**:767-811.
124. Wan H, Dupasquier M. Dendritic cells in vivo and in vitro. *Cellular & molecular immunology* 2005,**2**:28-35.
125. Satpathy AT, Wu X, Albring JC, Murphy KM. Re(de)fining the dendritic cell lineage. *Nat Immunol* 2012,**13**:1145-1154.
126. Ginhoux F, Liu K, Helft J, Bogunovic M, Greter M, Hashimoto D, *et al.* The origin and development of nonlymphoid tissue CD103+ DCs. *J Exp Med* 2009,**206**:3115-3130.
127. Heath WR, Carbone FR. Dendritic cell subsets in primary and secondary T cell responses at body surfaces. *Nat Immunol* 2009,**10**:1237-1244.
128. Haniffa M, Shin A, Bigley V, McGovern N, Teo P, See P, *et al.* Human tissues contain CD141hi cross-presenting dendritic cells with functional homology to mouse CD103+ nonlymphoid dendritic cells. *Immunity* 2012,**37**:60-73.
129. Schlitzer A, Ginhoux F. Organization of the mouse and human DC network. *Curr Opin Immunol* 2014,**26**:90-99.
130. Lipscomb MF, Masten BJ. Dendritic cells: immune regulators in health and disease. *Physiological reviews* 2002,**82**:97-130.
131. Murphy K, Travers P, Walport M, Janeway C. *Janeway's immunobiology*. 7th ed. New York: Garland Science; 2008.
132. Bracci L, Schumacher R, Provenzano M, Adamina M, Rosenthal R, Groeper C, *et al.* Efficient stimulation of T cell responses by human IFN-alpha-induced dendritic cells does not require Toll-like receptor triggering. *J Immunother* 2008,**31**:466-474.
133. Nakano H, Lin KL, Yanagita M, Charbonneau C, Cook DN, Kakiuchi T, *et al.* Blood-derived inflammatory dendritic cells in lymph nodes stimulate acute T helper type 1 immune responses. *Nat Immunol* 2009,**10**:394-402.
134. Serbina NV, Salazar-Mather TP, Biron CA, Kuziel WA, Pamer EG. TNF/iNOS-producing dendritic cells mediate innate immune defense against bacterial infection. *Immunity* 2003,**19**:59-70.
135. Chung NP, Chen Y, Chan VS, Tam PK, Lin CL. Dendritic cells: sentinels against pathogens. *Histol Histopathol* 2004,**19**:317-324.
136. Sallusto F, Lanzavecchia A. Efficient presentation of soluble antigen by cultured human dendritic cells is maintained by granulocyte/macrophage colony-stimulating factor plus interleukin 4 and downregulated by tumor necrosis factor alpha. *J Exp Med* 1994,**179**:1109-1118.

137. Pickl WF, Majdic O, Kohl P, Stockl J, Riedl E, Scheinecker C, *et al.* Molecular and functional characteristics of dendritic cells generated from highly purified CD14+ peripheral blood monocytes. *J Immunol* 1996,**157**:3850-3859.
138. Inaba K, Inaba M, Romani N, Aya H, Deguchi M, Ikehara S, *et al.* Generation of large numbers of dendritic cells from mouse bone marrow cultures supplemented with granulocyte/macrophage colony-stimulating factor. *J Exp Med* 1992,**176**:1693-1702.
139. Winzler C, Rovere P, Rescigno M, Granucci F, Penna G, Adorini L, *et al.* Maturation stages of mouse dendritic cells in growth factor-dependent long-term cultures. *J Exp Med* 1997,**185**:317-328.
140. Bros M, Jahrling F, Renzing A, Wiechmann N, Dang NA, Sutter A, *et al.* A newly established murine immature dendritic cell line can be differentiated into a mature state, but exerts tolerogenic function upon maturation in the presence of glucocorticoid. *Blood* 2007,**109**:3820-3829.
141. Banchereau J, Steinman RM. Dendritic cells and the control of immunity. *Nature* 1998,**392**:245-252.
142. Smyth MJ, Godfrey DI, Trapani JA. A fresh look at tumor immunosurveillance and immunotherapy. *Nat Immunol* 2001,**2**:293-299.
143. Hubbell JA, Thomas SN, Swartz MA. Materials engineering for immunomodulation. *Nature* 2009,**462**:449-460.
144. Caux C, Ait-Yahia S, Chemin K, de Bouteiller O, Dieu-Nosjean MC, Homey B, *et al.* Dendritic cell biology and regulation of dendritic cell trafficking by chemokines. *Springer Semin Immunopathol* 2000,**22**:345-369.
145. Hackstein H, Thomson AW. Dendritic cells: emerging pharmacological targets of immunosuppressive drugs. *Nat Rev Immunol* 2004,**4**:24-34.
146. Mogensen TH. Pathogen recognition and inflammatory signaling in innate immune defenses. *Clin Microbiol Rev* 2009,**22**:240-273, Table of Contents.
147. Strioga M, Schijns V, Powell DJ, Jr., Pasukoniene V, Dobrovolskiene N, Michalek J. Dendritic cells and their role in tumor immunosurveillance. *Innate Immun* 2013,**19**:98-111.
148. Brubaker SW, Bonham KS, Zanoni I, Kagan JC. Innate immune pattern recognition: a cell biological perspective. *Annu Rev Immunol* 2015,**33**:257-290.
149. Newton K, Dixit VM. Signaling in innate immunity and inflammation. *Cold Spring Harb Perspect Biol* 2012,**4**.
150. Barton GM, Kagan JC. A cell biological view of Toll-like receptor function: regulation through compartmentalization. *Nat Rev Immunol* 2009,**9**:535-542.
151. Jeong E, Lee JY. Intrinsic and extrinsic regulation of innate immune receptors. *Yonsei Med J* 2011,**52**:379-392.
152. Kagan JC, Magupalli VG, Wu H. SMOCs: supramolecular organizing centres that control innate immunity. *Nat Rev Immunol* 2014,**14**:821-826.
153. Chow J, Franz KM, Kagan JC. PRRs are watching you: Localization of innate sensing and signaling regulators. *Virology* 2015.
154. Sun L, Wu J, Du F, Chen X, Chen ZJ. Cyclic GMP-AMP synthase is a cytosolic DNA sensor that activates the type I interferon pathway. *Science* 2013,**339**:786-791.
155. Wu J, Sun L, Chen X, Du F, Shi H, Chen C, *et al.* Cyclic GMP-AMP is an endogenous second messenger in innate immune signaling by cytosolic DNA. *Science* 2013,**339**:826-830.
156. Barbe F, Douglas T, Saleh M. Advances in Nod-like receptors (NLR) biology. *Cytokine Growth Factor Rev* 2014,**25**:681-697.
157. Sabbah A, Chang TH, Harnack R, Frohlich V, Tominaga K, Dube PH, *et al.* Activation of innate immune antiviral responses by Nod2. *Nat Immunol* 2009,**10**:1073-1080.
158. Vanaja SK, Rathinam VA, Fitzgerald KA. Mechanisms of inflammasome activation: recent advances and novel insights. *Trends Cell Biol* 2015.
159. Fontana MF, Vance RE. Two signal models in innate immunity. *Immunol Rev* 2011,**243**:26-39.
160. Shi J, Zhao Y, Wang Y, Gao W, Ding J, Li P, *et al.* Inflammatory caspases are innate immune receptors for intracellular LPS. *Nature* 2014,**514**:187-192.
161. Kyriakis JM, Avruch J. Mammalian MAPK signal transduction pathways activated by stress and inflammation: a 10-year update. *Physiol Rev* 2012,**92**:689-737.
162. Jin HS, Park J-K, Jo E-K. Toll-like Receptors and NOD-like Receptors in Innate Immune Defense during Pathogenic Infection. *Journal of Bacteriology and Virology* 2014,**44**:215.
163. Morrison DK. MAP kinase pathways. *Cold Spring Harb Perspect Biol* 2012,**4**.
164. Kaverina I, Straube A. Regulation of cell migration by dynamic microtubules. *Semin Cell Dev Biol* 2011,**22**:968-974.
165. Dumontet C, Jordan MA. Microtubule-binding agents: a dynamic field of cancer therapeutics. *Nat Rev Drug Discov* 2010,**9**:790-803.
166. Daire V, Pous C. Kinesins and protein kinases: key players in the regulation of microtubule dynamics and organization. *Arch Biochem Biophys* 2011,**510**:83-92.
167. Alberts B. *Essential cell biology*. Fourth edition. ed. New York, NY: Garland Science; 2013.

168. Lopus M, Oroudjev E, Wilson L, Wilhelm S, Widdison W, Chari R, *et al.* Maytansine and cellular metabolites of antibody-maytansinoid conjugates strongly suppress microtubule dynamics by binding to microtubules. *Mol Cancer Ther* 2010,**9**:2689-2699.
169. Jordan MA, Wilson L. Microtubules as a target for anticancer drugs. *Nat Rev Cancer* 2004,**4**:253-265.
170. Akhmanova A, Steinmetz MO. Tracking the ends: a dynamic protein network controls the fate of microtubule tips. *Nat Rev Mol Cell Biol* 2008,**9**:309-322.
171. Kuppens IE. Current state of the art of new tubulin inhibitors in the clinic. *Curr Clin Pharmacol* 2006,**1**:57-70.
172. Carlson RO. New tubulin targeting agents currently in clinical development. *Expert Opin Investig Drugs* 2008,**17**:707-722.
173. Loong HH, Yeo W. Microtubule-targeting agents in oncology and therapeutic potential in hepatocellular carcinoma. *Onco Targets Ther* 2014,**7**:575-585.
174. Pettit GR, Cragg GM, Singh SB. Antineoplastic agents, 122. Constituents of Combretum caffrum. *J Nat Prod* 1987,**50**:386-391.
175. Bai RL, Pettit GR, Hamel E. Binding of dolastatin 10 to tubulin at a distinct site for peptide antimitotic agents near the exchangeable nucleotide and vinca alkaloid sites. *J Biol Chem* 1990,**265**:17141-17149.
176. Islam MN, Iskander MN. Microtubulin binding sites as target for developing anticancer agents. *Mini Rev Med Chem* 2004,**4**:1077-1104.
177. Perez EA, Hillman DW, Fishkin PA, Krook JE, Tan WW, Kuriakose PA, *et al.* Phase II trial of dolastatin-10 in patients with advanced breast cancer. *Invest New Drugs* 2005,**23**:257-261.
178. Maderna A, Leverett CA. Recent Advances in the Development of New Auristatins: Structural Modifications and Application in Antibody Drug Conjugates. *Mol Pharm* 2015.
179. Senter PD, Sievers EL. The discovery and development of brentuximab vedotin for use in relapsed Hodgkin lymphoma and systemic anaplastic large cell lymphoma. *Nat Biotechnol* 2012,**30**:631-637.
180. Liu C, Chari RV. The development of antibody delivery systems to target cancer with highly potent maytansinoids. *Expert Opin Investig Drugs* 1997,**6**:169-172.
181. Cassady JM, Chan KK, Floss HG, Leistner E. Recent developments in the maytansinoid antitumor agents. *Chemical & pharmaceutical bulletin* 2004,**52**:1-26.
182. Issell BF, Crooke ST. Maytansine. *Cancer Treat Rev* 1978,**5**:199-207.
183. Venghateri JB, Gupta TK, Verma PJ, Kunwar A, Panda D. Ansamitocin P3 depolymerizes microtubules and induces apoptosis by binding to tubulin at the vinblastine site. *PLoS One* 2013,**8**:e75182.
184. Alley SC, Okeley NM, Senter PD. Antibody-drug conjugates: targeted drug delivery for cancer. *Curr Opin Chem Biol* 2010,**14**:529-537.
185. Chari RV, Martell BA, Gross JL, Cook SB, Shah SA, Blattler WA, *et al.* Immunoconjugates containing novel maytansinoids: promising anticancer drugs. *Cancer research* 1992,**52**:127-131.
186. Lambert JM, Chari RV. Ado-trastuzumab Emtansine (T-DM1): an antibody-drug conjugate (ADC) for HER2-positive breast cancer. *J Med Chem* 2014,**57**:6949-6964.
187. Sievers EL, Senter PD. Antibody-drug conjugates in cancer therapy. *Annu Rev Med* 2013,**64**:15-29.
188. Janke C. The tubulin code: molecular components, readout mechanisms, and functions. *J Cell Biol* 2014,**206**:461-472.
189. Janke C, Bulinski JC. Post-translational regulation of the microtubule cytoskeleton: mechanisms and functions. *Nat Rev Mol Cell Biol* 2011,**12**:773-786.
190. Etienne-Manneville S, Hall A. Rho GTPases in cell biology. *Nature* 2002,**420**:629-635.
191. Gallagher ED, Gutowski S, Sternweis PC, Cobb MH. RhoA binds to the amino terminus of MEKK1 and regulates its kinase activity. *J Biol Chem* 2004,**279**:1872-1877.
192. Garcia-Mata R, Boulter E, Burridge K. The 'invisible hand': regulation of RHO GTPases by RHOGDIs. *Nat Rev Mol Cell Biol* 2011,**12**:493-504.
193. Ren Y, Li R, Zheng Y, Busch H. Cloning and characterization of GEF-H1, a microtubule-associated guanine nucleotide exchange factor for Rac and Rho GTPases. *J Biol Chem* 1998,**273**:34954-34960.
194. Birkenfeld J, Nalbant P, Yoon SH, Bokoch GM. Cellular functions of GEF-H1, a microtubule-regulated Rho-GEF: is altered GEF-H1 activity a crucial determinant of disease pathogenesis? *Trends Cell Biol* 2008,**18**:210-219.
195. Krendel M, Zenke FT, Bokoch GM. Nucleotide exchange factor GEF-H1 mediates cross-talk between microtubules and the actin cytoskeleton. *Nat Cell Biol* 2002,**4**:294-301.
196. Matsuzawa T, Kuwae A, Yoshida S, Sasakawa C, Abe A. Enteropathogenic Escherichia coli activates the RhoA signaling pathway via the stimulation of GEF-H1. *EMBO J* 2004,**23**:3570-3582.
197. Chang YC, Lee HH, Chen YJ, Bokoch GM, Chang ZF. Contribution of guanine exchange factor H1 in phorbol ester-induced apoptosis. *Cell Death Differ* 2006,**13**:2023-2032.
198. Meiri D, Marshall CB, Mokady D, LaRose J, Mullin M, Gingras AC, *et al.* Mechanistic insight into GPCR-mediated activation of the microtubule-associated RhoA exchange factor GEF-H1. *Nat Commun* 2014,**5**:4857.
199. Shurin GV, Tourkova IL, Shurin MR. Low-dose chemotherapeutic agents regulate small Rho GTPase activity in dendritic cells. *J Immunother* 2008,**31**:491-499.

200. Selimovic D, Badura HE, El-Khattouti A, Soell M, Porzig BB, Spernger A, *et al.* Vinblastine-induced apoptosis of melanoma cells is mediated by Ras homologous A protein (Rho A) via mitochondrial and non-mitochondrial-dependent mechanisms. *Apoptosis* 2013,**18**:980-997.
201. Qi M, Elion EA. MAP kinase pathways. *J Cell Sci* 2005,**118**:3569-3572.
202. Marinissen MJ, Chiariello M, Tanos T, Bernard O, Narumiya S, Gutkind JS. The small GTP-binding protein RhoA regulates c-jun by a ROCK-JNK signaling axis. *Mol Cell* 2004,**14**:29-41.
203. Symons A, Beinke S, Ley SC. MAP kinase kinase kinases and innate immunity. *Trends Immunol* 2006,**27**:40-48.
204. Drake CG, Lipson EJ, Brahmer JR. Breathing new life into immunotherapy: review of melanoma, lung and kidney cancer. *Nat Rev Clin Oncol* 2014,**11**:24-37.
205. Hamid O, Robert C, Daud A, Hodi FS, Hwu WJ, Kefford R, *et al.* Safety and Tumor Responses with Lambrolizumab (Anti-PD-1) in Melanoma. *N Engl J Med* 2013.
206. Wolchok JD, Kluger H, Callahan MK, Postow MA, Rizvi NA, Lesokhin AM, *et al.* Nivolumab plus Ipilimumab in Advanced Melanoma. *N Engl J Med* 2013.
207. Gajewski TF, Schreiber H, Fu YX. Innate and adaptive immune cells in the tumor microenvironment. *Nat Immunol* 2013,**14**:1014-1022.
208. Zitvogel L, Galluzzi L, Smyth MJ, Kroemer G. Mechanism of action of conventional and targeted anticancer therapies: reinstating immunosurveillance. *Immunity* 2013,**39**:74-88.
209. Lutz MB, Kukutsch N, Ogilvie AL, Rossner S, Koch F, Romani N, *et al.* An advanced culture method for generating large quantities of highly pure dendritic cells from mouse bone marrow. *J Immunol Methods* 1999,**223**:77-92.
210. Elkord E, Williams PE, Kynaston H, Rowbottom AW. Human monocyte isolation methods influence cytokine production from in vitro generated dendritic cells. *Immunology* 2005,**114**:204-212.
211. Nagy LE. *Alcohol : methods and protocols*. Totowa, NJ: Humana Press; 2008.
212. Lavalette S, Raoul W, Houssier M, Camelo S, Levy O, Calippe B, *et al.* Interleukin-1beta inhibition prevents choroidal neovascularization and does not exacerbate photoreceptor degeneration. *Am J Pathol* 2011,**178**:2416-2423.
213. Jin YH, Kang HS, Mohindru M, Kim BS. Preferential induction of protective T cell responses to Theiler's virus in resistant (C57BL/6 x SJL)F1 mice. *J Virol* 2011,**85**:3033-3040.
214. Wu Q, Gardiner GJ, Berry E, Wagner SR, Lu T, Clay BS, *et al.* ICOS-expressing lymphocytes promote resolution of CD8-mediated lung injury in a mouse model of lung rejection. *PLoS One* 2013,**8**:e72955.
215. Holscher C, Atkinson RA, Arendse B, Brown N, Myburgh E, Alber G, *et al.* A protective and agonistic function of IL-12p40 in mycobacterial infection. *J Immunol* 2001,**167**:6957-6966.
216. Schmittgen TD, Livak KJ. Analyzing real-time PCR data by the comparative C(T) method. *Nat Protoc* 2008,**3**:1101-1108.
217. Steinman RM, Banchereau J. Taking dendritic cells into medicine. *Nature* 2007,**449**:419-426.
218. Idoyaga J, Moreno J, Bonifaz L. Tumor cells prevent mouse dendritic cell maturation induced by TLR ligands. *Cancer immunology, immunotherapy : CII* 2007,**56**:1237-1250.
219. Almand B, Clark JI, Nikitina E, van Beynen J, English NR, Knight SC, *et al.* Increased production of immature myeloid cells in cancer patients: a mechanism of immunosuppression in cancer. *J Immunol* 2001,**166**:678-689.
220. Ghiringhelli F, Puig PE, Roux S, Parcellier A, Schmitt E, Solary E, *et al.* Tumor cells convert immature myeloid dendritic cells into TGF-beta-secreting cells inducing CD4+CD25+ regulatory T cell proliferation. *J Exp Med* 2005,**202**:919-929.
221. Zou W. Immunosuppressive networks in the tumour environment and their therapeutic relevance. *Nat Rev Cancer* 2005,**5**:263-274.
222. Sabado RL, Bhardwaj N. Directing dendritic cell immunotherapy towards successful cancer treatment. *Immunotherapy* 2010,**2**:37-56.
223. Mizumoto N, Gao J, Matsushima H, Ogawa Y, Tanaka H, Takashima A. Discovery of novel immunostimulants by dendritic-cell-based functional screening. *Blood* 2005,**106**:3082-3089.
224. Tanaka H, Matsushima H, Mizumoto N, Takashima A. Classification of chemotherapeutic agents based on their differential in vitro effects on dendritic cells. *Cancer research* 2009,**69**:6978-6986.
225. Tanaka H, Matsushima H, Nishibu A, Clausen BE, Takashima A. Dual therapeutic efficacy of vinblastine as a unique chemotherapeutic agent capable of inducing dendritic cell maturation. *Cancer research* 2009,**69**:6987-6994.
226. Zitvogel L, Kepp O, Galluzzi L, Kroemer G. Inflammasomes in carcinogenesis and anticancer immune responses. *Nature immunology* 2012,**13**:343-351.
227. Perez EA. Microtubule inhibitors: Differentiating tubulin-inhibiting agents based on mechanisms of action, clinical activity, and resistance. *Mol Cancer Ther* 2009,**8**:2086-2095.
228. John J, Ismail M, Riley C, Askham J, Morgan R, Melcher A, *et al.* Differential effects of Paclitaxel on dendritic cell function. *BMC Immunol* 2010,**11**:14.
229. Lotze MT. Getting to the source: dendritic cells as therapeutic reagents for the treatment of patients with cancer. *Ann Surg* 1997,**226**:1-5.

230. Poppema S, Brocker EB, de Leij L, Terbrack D, Visscher T, Ter Haar A, *et al.* In situ analysis of the mononuclear cell infiltrate in primary malignant melanoma of the skin. *Clin Exp Immunol* 1983,**51**:77-82.
231. Nestor MS, Cochran AJ. Identification and quantification of subsets of mononuclear inflammatory cells in melanocytic and other human tumors. *Pigment Cell Res* 1987,**1**:22-27.
232. West MA, Wallin RP, Matthews SP, Svensson HG, Zaru R, Ljunggren HG, *et al.* Enhanced dendritic cell antigen capture via toll-like receptor-induced actin remodeling. *Science* 2004,**305**:1153-1157.
233. Savina A, Amigorena S. Phagocytosis and antigen presentation in dendritic cells. *Immunol Rev* 2007,**219**:143-156.
234. Daniels MA, Teixeiro E, Gill J, Hausmann B, Roubaty D, Holmberg K, *et al.* Thymic selection threshold defined by compartmentalization of Ras/MAPK signalling. *Nature* 2006,**444**:724-729.
235. Jung S, Unutmaz D, Wong P, Sano G, De los Santos K, Sparwasser T, *et al.* In vivo depletion of CD11c+ dendritic cells abrogates priming of CD8+ T cells by exogenous cell-associated antigens. *Immunity* 2002,**17**:211-220.
236. Hamid O, Carvajal RD. Anti-programmed death-1 and anti-programmed death-ligand 1 antibodies in cancer therapy. *Expert Opin Biol Ther* 2013,**13**:847-861.
237. Topalian SL, Drake CG, Pardoll DM. Targeting the PD-1/B7-H1(PD-L1) pathway to activate anti-tumor immunity. *Curr Opin Immunol* 2012,**24**:207-212.
238. Curran MA, Montalvo W, Yagita H, Allison JP. PD-1 and CTLA-4 combination blockade expands infiltrating T cells and reduces regulatory T and myeloid cells within B16 melanoma tumors. *Proc Natl Acad Sci U S A* 2010,**107**:4275-4280.
239. Wolchok JD, Kluger H, Callahan MK, Postow MA, Rizvi NA, Lesokhin AM, *et al.* Nivolumab plus ipilimumab in advanced melanoma. *N Engl J Med* 2013,**369**:122-133.
240. Waitz R, Solomon SB, Petre EN, Trumble AE, Fasso M, Norton L, *et al.* Potent induction of tumor immunity by combining tumor cryoablation with anti-CTLA-4 therapy. *Cancer Res* 2012,**72**:430-439.
241. Francisco JA, Cerveny CG, Meyer DL, Mixan BJ, Klussman K, Chace DF, *et al.* cAC10-vcMMAE, an anti-CD30-monomethyl auristatin E conjugate with potent and selective antitumor activity. *Blood* 2003,**102**:1458-1465.
242. Kawai T, Akira S. The role of pattern-recognition receptors in innate immunity: update on Toll-like receptors. *Nature immunology* 2010,**11**:373-384.
243. Mariathasan S, Weiss DS, Newton K, McBride J, O'Rourke K, Roose-Girma M, *et al.* Cryopyrin activates the inflammasome in response to toxins and ATP. *Nature* 2006,**440**:228-232.
244. Wallace A, LaRosa DF, Kapoor V, Sun J, Cheng G, Jassar A, *et al.* The vascular disrupting agent, DMXAA, directly activates dendritic cells through a MyD88-independent mechanism and generates antitumor cytotoxic T lymphocytes. *Cancer Res* 2007,**67**:7011-7019.
245. Roberts ZJ, Goutagny N, Perera PY, Kato H, Kumar H, Kawai T, *et al.* The chemotherapeutic agent DMXAA potently and specifically activates the TBK1-IRF-3 signaling axis. *J Exp Med* 2007,**204**:1559-1569.
246. Cheng G, Sun J, Fridlender ZG, Wang LC, Ching LM, Albelda SM. Activation of the nucleotide oligomerization domain signaling pathway by the non-bacterially derived xanthone drug 5'6-dimethylxanthenone-4-acetic acid (Vadimezan). *J Biol Chem* 2010,**285**:10553-10562.
247. Buchanan CM, Shih JH, Astin JW, Rewcastle GW, Flanagan JU, Crosier PS, *et al.* DMXAA (Vadimezan, ASA404) is a multi-kinase inhibitor targeting VEGFR2 in particular. *Clin Sci (Lond)* 2012,**122**:449-457.
248. Fan M, Chambers TC. Role of mitogen-activated protein kinases in the response of tumor cells to chemotherapy. *Drug Resist Updat* 2001,**4**:253-267.
249. Kolomeichuk SN, Terrano DT, Lyle CS, Sabapathy K, Chambers TC. Distinct signaling pathways of microtubule inhibitors--vinblastine and Taxol induce JNK-dependent cell death but through AP-1-dependent and AP-1-independent mechanisms, respectively. *FEBS J* 2008,**275**:1889-1899.
250. Chiang HS, Zhao Y, Song JH, Liu S, Wang N, Terhorst C, *et al.* GEF-H1 controls microtubule-dependent sensing of nucleic acids for antiviral host defenses. *Nat Immunol* 2014,**15**:63-71.
251. Fukazawa A, Alonso C, Kurachi K, Gupta S, Lesser CF, McCormick BA, *et al.* GEF-H1 mediated control of NOD1 dependent NF-kappaB activation by Shigella effectors. *PLoS Pathog* 2008,**4**:e1000228.
252. Zhao Y, Alonso C, Ballester I, Song JH, Chang SY, Guleng B, *et al.* Control of NOD2 and Rip2-dependent innate immune activation by GEF-H1. *Inflamm Bowel Dis* 2012,**18**:603-612.
253. Guo F, Tang J, Zhou Z, Dou Y, Van Lonkhuyzen D, Gao C, *et al.* GEF-H1-RhoA signaling pathway mediates LPS-induced NF-kappaB transactivation and IL-8 synthesis in endothelial cells. *Mol Immunol* 2012,**50**:98-107.
254. Davis RJ. Signal transduction by the JNK group of MAP kinases. *Cell* 2000,**103**:239-252.
255. Martin K, Muller P, Schreiner J, Prince SS, Lardinois D, Heinzelmann-Schwarz VA, *et al.* The microtubule-depolymerizing agent ansamitocin P3 programs dendritic cells toward enhanced anti-tumor immunity. *Cancer Immunol Immunother* 2014,**63**:925-938.

256. Muller P, Martin K, Theurich S, Schreiner J, Savic S, Terszowski G, *et al.* Microtubule-depolymerizing agents used in antibody-drug conjugates induce antitumor immunity by stimulation of dendritic cells. *Cancer Immunol Res* 2014,**2**:741-755.
257. John J, Ismail M, Riley C, Askham J, Morgan R, Melcher A, *et al.* Differential effects of Paclitaxel on dendritic cell function. *BMC immunology* 2010,**11**:14.
258. Joo HG. Altered maturation of dendritic cells by taxol, an anticancer drug. *Journal of veterinary science* 2003,**4**:229-234.
259. Ma Y, Shurin GV, Peiyuan Z, Shurin MR. Dendritic cells in the cancer microenvironment. *J Cancer* 2013,**4**:36-44.
260. Legitimo A, Consolini R, Failli A, Orsini G, Spisni R. Dendritic cell defects in the colorectal cancer. *Hum Vaccin Immunother* 2014,**10**:3224-3235.
261. Mattarollo SR, Loi S, Duret H, Ma Y, Zitvogel L, Smyth MJ. Pivotal role of innate and adaptive immunity in anthracycline chemotherapy of established tumors. *Cancer Res* 2011,**71**:4809-4820.
262. Ghiringhelli F, Apetoh L, Tesniere A, Aymeric L, Ma Y, Ortiz C, *et al.* Activation of the NLRP3 inflammasome in dendritic cells induces IL-1beta-dependent adaptive immunity against tumors. *Nat Med* 2009,**15**:1170-1178.
263. Kroemer G, Galluzzi L, Kepp O, Zitvogel L. Immunogenic cell death in cancer therapy. *Annu Rev Immunol* 2013,**31**:51-72.
264. Krysko DV, Garg AD, Kaczmarek A, Krysko O, Agostinis P, Vandenabeele P. Immunogenic cell death and DAMPs in cancer therapy. *Nat Rev Cancer* 2012,**12**:860-875.
265. Crespo J, Sun H, Welling TH, Tian Z, Zou W. T cell anergy, exhaustion, senescence, and stemness in the tumor microenvironment. *Curr Opin Immunol* 2013,**25**:214-221.
266. Pauken KE, Wherry EJ. Overcoming T cell exhaustion in infection and cancer. *Trends Immunol* 2015,**36**:265-276.
267. Baitsch L, Baumgaertner P, Devevre E, Raghav SK, Legat A, Barba L, *et al.* Exhaustion of tumor-specific CD8(+) T cells in metastases from melanoma patients. *J Clin Invest* 2011,**121**:2350-2360.
268. Curiel TJ, Wei S, Dong H, Alvarez X, Cheng P, Mottram P, *et al.* Blockade of B7-H1 improves myeloid dendritic cell-mediated antitumor immunity. *Nat Med* 2003,**9**:562-567.
269. Iwai Y, Ishida M, Tanaka Y, Okazaki T, Honjo T, Minato N. Involvement of PD-L1 on tumor cells in the escape from host immune system and tumor immunotherapy by PD-L1 blockade. *Proc Natl Acad Sci U S A* 2002,**99**:12293-12297.
270. Blank C, Brown I, Peterson AC, Spiotto M, Iwai Y, Honjo T, *et al.* PD-L1/B7H-1 inhibits the effector phase of tumor rejection by T cell receptor (TCR) transgenic CD8+ T cells. *Cancer Res* 2004,**64**:1140-1145.
271. Holmgaard RB, Zamarin D, Munn DH, Wolchok JD, Allison JP. Indoleamine 2,3-dioxygenase is a critical resistance mechanism in antitumor T cell immunotherapy targeting CTLA-4. *J Exp Med* 2013.
272. Junttila MR, de Sauvage FJ. Influence of tumour micro-environment heterogeneity on therapeutic response. *Nature* 2013,**501**:346-354.
273. DuPage M, Dooley AL, Jacks T. Conditional mouse lung cancer models using adenoviral or lentiviral delivery of Cre recombinase. *Nat Protoc* 2009,**4**:1064-1072.
274. Taneja P, Frazier DP, Kendig RD, Maglic D, Sugiyama T, Kai F, *et al.* MMTV mouse models and the diagnostic values of MMTV-like sequences in human breast cancer. *Expert Rev Mol Diagn* 2009,**9**:423-440.
275. Almand B, Resser JR, Lindman B, Nadaf S, Clark JI, Kwon ED, *et al.* Clinical significance of defective dendritic cell differentiation in cancer. *Clinical cancer research : an official journal of the American Association for Cancer Research* 2000,**6**:1755-1766.
276. Coventry BJ, Lee PL, Gibbs D, Hart DN. Dendritic cell density and activation status in human breast cancer -- CD1a, CMRF-44, CMRF-56 and CD-83 expression. *British journal of cancer* 2002,**86**:546-551.
277. Mullard A. Maturing antibody-drug conjugate pipeline hits 30. *Nat Rev Drug Discov* 2013,**12**:329-332.
278. Gopal AK, Chen R, Smith SE, Ansell SM, Rosenblatt JD, Savage KJ, *et al.* Durable remissions in a pivotal phase 2 study of brentuximab vedotin in relapsed or refractory Hodgkin lymphoma. *Blood* 2015,**125**:1236-1243.
279. Pham A, Chen R. Brentuximab vedotin for the treatment of Hodgkin's lymphoma. *Expert Rev Hematol* 2015:1-10.
280. Nicoletti R, Lopez S, Bellone S, Cocco E, Schwab CL, Black JD, *et al.* T-DM1, a novel antibody-drug conjugate, is highly effective against uterine and ovarian carcinosarcomas overexpressing HER2. *Clin Exp Metastasis* 2015,**32**:29-38.
281. Peddi PF, Hurvitz SA. Ado-trastuzumab emtansine (T-DM1) in human epidermal growth factor receptor 2 (HER2)-positive metastatic breast cancer: latest evidence and clinical potential. *Ther Adv Med Oncol* 2014,**6**:202-209.
282. Younes A, Gopal AK, Smith SE, Ansell SM, Rosenblatt JD, Savage KJ, *et al.* Results of a pivotal phase II study of brentuximab vedotin for patients with relapsed or refractory Hodgkin's lymphoma. *J Clin Oncol* 2012,**30**:2183-2189.

283. Younes A, Bartlett NL, Leonard JP, Kennedy DA, Lynch CM, Sievers EL, *et al.* Brentuximab vedotin (SGN-35) for relapsed CD30-positive lymphomas. *The New England journal of medicine* 2010,**363**:1812-1821.
284. Theurich S, Malcher J, Wennhold K, Shimabukuro-Vornhagen A, Chemnitz J, Holtick U, *et al.* Brentuximab vedotin combined with donor lymphocyte infusions for early relapse of hodgkin lymphoma after allogeneic stem-cell transplantation induces tumor-specific immunity and sustained clinical remission. *Journal of clinical oncology : official journal of the American Society of Clinical Oncology* 2013,**31**:e59-63.
285. Theurich S, Wennhold K, Wedemeyer I, Rothe A, Hubel K, Shimabukuro-Vornhagen A, *et al.* CD30-targeted therapy with brentuximab vedotin and DLI in a patient with T-cell posttransplantation lymphoma: induction of clinical remission and cellular immunity. *Transplantation* 2013,**96**:e16-18.
286. Martinon F, Gaide O, Petrilli V, Mayor A, Tschopp J. NALP inflammasomes: a central role in innate immunity. *Semin Immunopathol* 2007,**29**:213-229.
287. Zhang K, Kaufman RJ. From endoplasmic-reticulum stress to the inflammatory response. *Nature* 2008,**454**:455-462.
288. Huang Y, Fang Y, Wu J, Dziadyk JM, Zhu X, Sui M, *et al.* Regulation of Vinca alkaloid-induced apoptosis by NF-kappaB/IkappaB pathway in human tumor cells. *Mol Cancer Ther* 2004,**3**:271-277.
289. Wang TH, Wang HS, Ichijo H, Giannakakou P, Foster JS, Fojo T, *et al.* Microtubule-interfering agents activate c-Jun N-terminal kinase/stress-activated protein kinase through both Ras and apoptosis signal-regulating kinase pathways. *J Biol Chem* 1998,**273**:4928-4936.
290. Wang LG, Liu XM, Kreis W, Budman DR. The effect of antimicrotubule agents on signal transduction pathways of apoptosis: a review. *Cancer Chemother Pharmacol* 1999,**44**:355-361.
291. Jung YJ, Isaacs JS, Lee S, Trepel J, Neckers L. Microtubule disruption utilizes an NFkappa B-dependent pathway to stabilize HIF-1alpha protein. *J Biol Chem* 2003,**278**:7445-7452.
292. Wang TH, Popp DM, Wang HS, Saitoh M, Mural JG, Henley DC, *et al.* Microtubule dysfunction induced by paclitaxel initiates apoptosis through both c-Jun N-terminal kinase (JNK)-dependent and -independent pathways in ovarian cancer cells. *J Biol Chem* 1999,**274**:8208-8216.
293. Berry A, Goodwin M, Moran CL, Chambers TC. AP-1 activation and altered AP-1 composition in association with increased phosphorylation and expression of specific Jun and Fos family proteins induced by vinblastine in KB-3 cells. *Biochem Pharmacol* 2001,**62**:581-591.
294. Leppa S, Bohmann D. Diverse functions of JNK signaling and c-Jun in stress response and apoptosis. *Oncogene* 1999,**18**:6158-6162.
295. James SE, Burden H, Burgess R, Xie Y, Yang T, Massa SM, *et al.* Anti-cancer drug induced neurotoxicity and identification of Rho pathway signaling modulators as potential neuroprotectants. *Neurotoxicology* 2008,**29**:605-612.
296. Wang W, Wang YQ, Meng T, Yi JM, Huan XJ, Ma LP, *et al.* MCL-1 degradation mediated by JNK activation via MEKK1/TAK1-MKK4 contributes to anticancer activity of new tubulin inhibitor MT189. *Mol Cancer Ther* 2014,**13**:1480-1491.
297. Yujiri T, Sather S, Fanger GR, Johnson GL. Role of MEKK1 in cell survival and activation of JNK and ERK pathways defined by targeted gene disruption. *Science* 1998,**282**:1911-1914.
298. Yujiri T, Fanger GR, Garrington TP, Schlesinger TK, Gibson S, Johnson GL. MEK kinase 1 (MEKK1) transduces c-Jun NH2-terminal kinase activation in response to changes in the microtubule cytoskeleton. *J Biol Chem* 1999,**274**:12605-12610.
299. Riento K, Ridley AJ. Rocks: multifunctional kinases in cell behaviour. *Nat Rev Mol Cell Biol* 2003,**4**:446-456.
300. Eitaki M, Yamamori T, Meike S, Yasui H, Inanami O. Vincristine enhances amoeboid-like motility via GEF-H1/RhoA/ROCK/Myosin light chain signaling in MKN45 cells. *BMC Cancer* 2012,**12**:469.
301. Pollock JK, Verma NK, O'Boyle NM, Carr M, Meegan MJ, Zisterer DM. Combretastatin (CA)-4 and its novel analogue CA-432 impair T-cell migration through the Rho/ROCK signalling pathway. *Biochem Pharmacol* 2014,**92**:544-557.

10 Attachments

10.1 Materials

Chemicals and reagents	*Source*
Acetic acid	Merck
Accutase	PAA
Agarose	Sigma
BCA	Pierce
β-Mercaptoethanol	Sigma
Bovine serum albumin (BSA)	Sigma
Brefeldin A	Sigma
Ciproxin	Bayer
Collagenase IV	Worthington
Corynebacterium diphtheriae diphtheria toxin (DT)	Millipore
CpG DNA	Microsynth
D-Glu-meso-diaminopimelic acid (iE-DAP)	Adipogen
Disodium hydrogen phosphate (Na_2HPO_4)	Merck
Dimethylsulfoxide (DMSO)	Sigma
Dithiothreitol (DTT)	Sigma
DNAse type IV	Sigma
dNTPs	Roche
ECL Films	Kodak
ECL Substrate	Thermo Scientific
Ethanol, absolute	Sigma
Ethylenediamine tetraacetate sodium salt (EDTA)	Gibco
FITC-Dextran	Sigma
FoxP3-Fix/Perm-Kit	BioLegend
IC Fixation buffer	eBioscience
Glycine	Sigma
GM-CSF, recombinant human	Peprotech
GM-CSF, recombinant mouse	Peprotech
Histopaque®1077/ Histopaque®1119	Sigma
Hyaluronidase	Sigma
Hydrochloric acid	Sigma
Interleukin 4 (IL-4), recombinant human	Peprotech
Isobutanol	Merck
Isopropanol	Merck
Laemmli Buffer 2x	Bio-Rad
LPS, 026:B6 Escherichia coli	Sigma
Chemicals and reagents	*Source*
LPS, TLRpure®	Adipogen
M-CSF, recombinant mouse	Peprotech
Methanol	Merck

Monensin 1000x	Biolegend
Muramyl dipeptide (MDP)	Adipogen
Nigericin sodium salt	Adipogen
Nitrocellulose Membrane, 0.45 µm	Bio-Rad
Non-fat dry milk	Sigma
OCT Compound	Tissue-Tek
Ovalbumin, SIINFEKL peptide	Peptides & Elephants
Ovalbumin, SIITFEKL peptide (T_4)	Peptides & Elephants
Ovalbumin, ISQAVHAAHAEINEAGR peptide	Abbiotech
Ovalbumin (EndoGrade) protein	Hyglos
Paraformaldehyde	Fluka
PBS (1x and 10x)	Sigma
Permeabilzation buffer	BioLegend
Phorbol-12-myristate13-acetate (PMA)	Sigma
Poly I:C (High Molecular weight)	Adipogen
Ponceau S solution	Sigma
Potassium bicarbonate ($KHCO_3$)	Sigma
Potassium chloride (KCl)	Sigma
ProLong® Antifade Reagent Containing DAPI	Life Technologies
Protease inhibitor	Pierce
PVDF Membrane, Immun-Blot® 0.2 µm	Bio-Rad
RedSafeTM Nucleic Acid Stain Solution	Chembio
Sodium acetate (NaAc)	Fluka
Sodium azide (NaN_3)	Sigma
Sodium chloride (NaCl)	Merck
Sodium dodecylsulfate	BDH
Sodium hydroxide (NaOH)	Aldrich
TRIS (Tris(hydroxymethyl)-aminomethan	Sigma
Triton X-100	Sigma
Trypan blue	Gibco
Trypsin 0.5%	Gibco
Tween-20	Fluka

Buffers and solutions

TE Buffer (TRIS-EDTA)

10 mmol	Tris
1 mmol	EDTA
1M	HCl adjust pH to 7.5
add H_2O	

FACS-buffer

2% (v/v)	FCS
2 mmol	EDTA
0.01% (v/v)	sodium azide sol.
PBS	

ELISA washing buffer

PBS containing 0.05% Tween-20

10x TBS (TRIS buffered saline)

80 g	NaCl	Dissolve all dry reagents together
2 g	KCl	in 800 mL ddH2O
30 g	TRIS base	adjust pH to 7.4 with 32% HCl
Add ddH_2O to a final volume of 1L		

10x SDS running buffer

30 g	TRIS base	The pH of the buffer should be 8.3
144 g	Glycine	and no pH adjustment is required.
10 g	SDS	
Add ddH_2O to a final volume of 1L		

1x Transfer buffer (nitrocellulose membrane)

14.4 g	Glycine
3.02 g	TRIS base
100 mL	Methanol
Add ddH_2O to a final volume of 1L	

1x Transfer buffer (PVDF membrane)

14.4 g	Glycine
3.02 g	TRIS base
200 mL	Methanol
Add ddH_2O to a final volume of 1L	

1x Digestion mix (100 mL)

Tumor cell growth medium (DMEM + 10% FCS)	50 ml	
Accutase	50 ml	
Collagenase IV (50 mg/ml)		2 ml
Hyaluronidase (50 mg/ml)		2 ml
DNAse I; Type IV (2.5 KUnits/ml)		0.4 ml

Cell culture media and supplements

IMDM	Sigma
DMEM	Sigma
DMEM w/o phenol red	Sigma
RPMI 1640	Gibco

FCS (ES cells tested)	PAA
Sodium Pyruvat 100x	Gibco
Non-essential Amino Acids 100x	Gibco
Penicillin/Streptomycin/L-Glutamine 100x concentrated (P/S/G)	Gibco
PBS	Gibco
Trypan blue 0.4 % solution	Sigma

Freezing medium

FCS containing 10% DMSO

Reaction Kits

Kit	Source
MACS CD8 MicroBeads (positive selection; human)	Miltenyi Biotec GmbH
MACS CD14 MicroBeads (positive selection; human)	Miltenyi Biotec GmbH
Easysep $CD8a^+$ T Cell Isolation Kit II (positive selection; mouse)	Stemcell Technologies
Easysep Pan T Cell Isolation Kit II (depletion; mouse)	Stemcell Technologies
Mouse IL-1β/ IL-6/ IL-12p40 ELISA	eBiosciene/BD
Human IL-1β/ IL-6/ IL-12p40 ELISA	eBioscience/BD
Direct-zol™ RNA MiniPrep	Zymo Research
RevertAid First Strand cDNA Synthesis Kit	Thermo Scientific
GoTaq® qPCR Master Mix	Promega
Microtubules/ Tubulin In Vivo Assay Kit	Cytoskeleton, Inc.
G-LISA® RhoA Activation Assay Biochem Kit (Absorbance)	Cytoskeleton, Inc.

Antibodies and dyes

Antibody	Clone	Fluorescent label	Source
FACS antibodies			
Anti-mouse CD4	GK1.5	PE-Cy7	BioLegend
Anti-mouse CD4	RM4-5	V450	BD
Anti-mouse CD8	53-6.7	BV421	BioLegend
Anti-mouse CD8	53-6.7	PE-Cy7	BioLegend
Anti-mouse CD11b	M1/70	V450	BD
Anti-mouse CD11c	N418	FITC	BioLegend
Anti-mouse CD40	2/23	PE	BioLegend
Anti-mouse CD80	16-10A1	PE	BioLegend
Anti-mouse CD86	GL1	APC	BD
Anti-mouse/human FoxP3	150D/E4	PE	eBioscience
Anti-mouse I-E I-A	M5/114.15.2	Pacific Blue (PB)	BioLegend
Anti-mouse IFN-γ	XMG1.2	PE	BD
Anti-mouse IL-6	MP5-20F3	PE	eBioscience
Anti-mouse IL-12p40	C15.6	PE	BD
Anti-mouse IL-1β (pro-form)	NJTEN3	PE	eBioscience
Anti-mouse CD16/32 (FcR block)		-	BioLegend
Anti-human CD3	Hit3a	APC	BioLegend
Mouse IgG1 Isotype Ctrl	MOPC-21	A488	BD
Anti-human CD3	Hit3a	APC-Cy7	BioLegend
Anti-human CD4	SFCI12T4D11	ECD	Beckman Coulter
Anti-human CD4	SFCI12T4D11	PB	Beckman Coulter
Anti-human CD8	Hit8a	PE-Cy7	BioLegend
Anti-human CD8	RPA-T8	PerCP-Cy5.5	BD
Anti-human CD11b	M1/70	AF700	BD
Anti-human CD11b	ICRF44	PE-Cy7	BD
Anti-human CD11c	3.9	PE	BioLegend
Anti-human CD14	M5E2	FITC	BD
Anti-human CD16	3G8	PB	BD
Anti-human CD19	J3-119	FITC	Beckman Coulter
Anti-human CD19	HIB19	AF700	BD
Anti-CD20	2H7	PB	BioLegend
Anti-CD25	M-A251	PE-Cy7	BD
Anti-human CD40	5C3	APC	Biolegend
Anti-human CD45	HI30	Biotin	BD
Anti-human CD62L	HRL1	Biotin	BD
Anti-human CD69	FN50	APC-Cy7	BD
Anti-human CD80	L307.4	FITC	BD
Anti-human CD83	HB15e	APC	eBioscience
Anti-human CD83	HB15e	Biotin	BioLegend

Anti-human CD86	2331 (FUN-1)	PE	BD
Anti-human FoxP3	259D	AF488	BD
Anti-human HLA-DR	L243	PB	BioLegend
Anti-human HLA-A2	BB7.2	PE	BD
Anti-human CD16/32 (FcR block)	-	-	BioLegend
Streptavidin	-	BV650	Biolegend
Streptavidin	-	PE-Cy7	Biolegend
FACS dyes			
eFluor670 Proliferation Dye	-		Invitrogen
eFluor450 Proliferation Dye	-		Invitrogen
SytoxGreen® Nucleic Acid Stain	-	FITC	Life Technologies
LIVE/DEAD® Fixable Dead Cell Stain Kits	-	Near-IR (APC-Cy7)	Invitrogen
Activating antibodies			
Anti-mouse CD3	17A2	Functional grade purified	eBioscience
Anti-mouse CD28	37.51	Functional grade	eBioscience
Anti-human CD3	UCHT1	Functional grade	eBioscience
Anti-human CD28	CD28.2	Functional grade	eBioscience
Western Blot/ Immunoprecipitation/ Immunofluorescence antibodies			
c-Jun Rabbit mAb	60A8	-	Cell Signaling Technology (CST)
Phospho-c-Jun (Ser73) XP® Rabbit mAb	D47G9	-	CST
Phospho-c-Jun (Ser63) Rabbit mAb	54B3	-	CST
SAPK/JNK Rabbit mAb	9252	-	CST
Phospho-SAPK/JNK (Thr183/Tyr185) Rabbit mAb	98F2	-	CST
p38 MAPK XP® Rabbit mAb	D13E1	-	CST
Phospo-p38 MAPK (Thr180/Tyr182) XP® Rabbit mAb	D3F9	-	CST
p44/42 (ERK1/2) MAPK	137F5	-	CST
Phospho-p44/42 (ERK1/2) (Thr202/Tyr204) MAPK XP® Rabbit mAb	D13.14.4E	-	CST
NF-κB p65 XP® Rabbit mAb	D14E12	-	CST
Phospho-NF-κB p65 Rabbit mAb	93H1	-	CST

β-Actin Rabbit mAb	13E5	-	CST
lfc (GEF-H1; ARHGEF)	Polyclonal sheep	-	Exalpha Biologicals, Inc.
Phospho-lfc (GEF-H1) (Ser885)	Polyclonal rabbit	-	Abcam

Cytotoxic Compounds

Drug	Mechanism	Source
Ansamitocin P_3	Microtubule Assembly Inhibitor/ Destabilizer	National Cancer Institute (NCI)
BIBF 1120	Angiokinase Inhibitor	LC Laboratories
Celecoxib	Cyclooxygenase-2 Inhibitor	Spitalpharmazie
Combretastatin-A_4-Phosphate	Microtubule Destabilizer, Vascular-disrupting Agent	Cayman Chemical
D-64131	Tubulin Formation Inhibitor	Santa Cruz Biotechnology
DM1	Microtubule Assembly Inhibitor/ Destabilizer	Concortis
DMXAA	Vascular-disrupting Agent	Sigma
Docetaxel	Mitosis-blocking; Tubuli-stabilizing	LC Laboratories
Dolastatin 15	Microtubule Assembly Inhibitor/ Destabilizer	NCI
Dolastatin 10	Microtubule Assembly Inhibitor/ Destabilizer	NCI
Enalapril	Angiotensin-converting Enzyme	Merck
Epothilone A	Mitosis-blocking; Tubuli-stabilizing	Santa Cruz Biotechnology
Gemcitabine	DNA-replication Blocker	LC Laboratories
l-NMMA	Nitric Oxide Synthase (NOS) Inhibitor	Cayman Chemical
MMAE (monomethyl-auristatinE)	Microtubule Assembly Inhibitor/ Destabilizer	Seattle Genetics
Naproxen	Cyclooxygenase (COX) Inhibitor	Cayman Chemical
Paclitaxel	Mitosis-blocking; Tubuli-stabilizing	Cayman Chemical
Patupilone (Epothilone B)	Mitosis-blocking; Tubuli-stabilizing	LC Laboratories
SAHA	HDAC Inhibitor	Cayman Chemical
Sunitinib	Receptor Tyrosinkinase Inhibitor	Pfizer Inc.
Vinblastine	Microtubule Assembly Inhibitor	NCI
Vincristine	Microtubule Assembly Inhibitor	NCI
Vindesine	Microtubule Assembly Inhibitor	NCI
Vinflunine	Microtubule Assembly Inhibitor	NCI
Vinorelbine	Microtubule Assembly Inhibitor	NCI

Antibody-drug conjugates and therapeutic antibodies

Therapeutic Antibody	Species	Clone	Source
α-PD-1 (blocking)	Mouse (experimental)	RMP1-14	BioXCell
α-CTLA-4 (blocking)	Mouse (experimental)	9D9	BioXCell
α-CD4 (depleting)	Mouse (experimental)	GK1.5	BioXCell
α-CD8 (depleting)	Mouse (experimental)	53–6.72	BioXCell
α-IFN-γ (neutralizing)	Mouse (experimental)	XMG1.2	BioXCell

Antibody-drug conjugate	Species	Antigen	Cytotoxic payload	Source
Brentuximab Vedotin (Adcetris®)	Human (approved)	CD30	MMAE	Seattle Genetics/ Takeda
Anti-Thy1.1 MMAE	Mouse (experimental)	Thy1.1	MMAE	Seattle Genetics

Adenovirus (vaccination)

Virus (Vaccination)	Species	Protein expressed	Source
Ad5TRFOva; Adenovirus type 5 (replication deficient)	Mouse (experimental)	Chicken ovalbumin (OVA)	University of Iowa Gene Transfer Vector Core

10.2 Mammalian cell lines

Cell line	Species	Origin	Cell Type	Source
SP37A3	Mouse; B6	Spleen	Dendritic Cell	Merck
E.G7	Mouse; B6	Lymphoma cell line EL-4	T cell Lymphoma	ATCC
3LL-Thy1.1-OVA		Lung carcinoma cell line 3LL	Carcinoma	Douglas T Fearon Cancer Research UK Cambridge Institute
MC38	Mouse; B6	Colon	Adeno Carcinoma	Mark Smyth, Peter MacCallum Cancer Centre, Melbourne
RMA-Thy1.1	Mouse; B6	T cell lymphoma cell line EL-4	T cell lymphoma	Angelo Corti, San Raffaele Scientific Institute, Milan
Karpas-299	Human	T cell	Anaplastic Large Cell lymphoma	Jürg Schwaller, Department Biomedicine, Basel
L-540	Human	T cell	Hodgkin Lymphoma	Jürg Schwaller, Department Biomedicine, Basel
Ramos	Human	B cell	Burkitts Lymphoma	Jürg Schwaller, Department Biomedicine, Basel

11 Acknowledgement

At this place I would like to express my sincere gratitude to all the people that have accompanied me during the last years at the Department of Biomedicine. There surely have been times in which I was not so sure anymore whether I do the right thing here. But irrespective of all ups and downs I realize again and again and I am undoubtedly sure now that research is exactly what I want to do.

And therefore, I first of all want to thank my supervisor Alfred Zippelius, who was the one proposing to me to start a PhD when I have not even thought about it before. He gave me the confidence to choose this path for myself and I have never regretted this decision. I am especially thankful not only for the opportunity to work on this exciting project, but more importantly for his constant support and for having an open door and an open ear at all times. I am absolutely appreciating that he always gave me the freedom to take my own decisions and I want to express a special thanks for the trust he has put in my work and myself. I have been encouraged to visit other labs as well as scientific conferences in order to expand my knowledge and experience, for which I am honestly very grateful.

I want to address a special thanks to Daniela Finke and Jean Pieters who have agreed to supervise me as members of my PhD committee and greatly supported the project (and myself) with helpful discussions. Also, I want to thank Jean and his former PhD student Vincent Tchang for providing OT-II mice in times of need.

I want to thank Ed Palmer for being the chairman of my PhD defense, and more importantly for all the helpful discussions, for all kinds of OVA peptides, mice, and especially for inviting us to be part of his labmeeting at the very beginning of my PhD. I always enjoyed these meetings and learned a lot. At this point I also want to thank Simona Rossi and her lab for many discussions and their help whenever needed.

I want to thank Giulio Spagnoli, Giandomenica Iezzi and Elisabetta Padovan and all their lab members for their constant support and for setting up the Immuno-Oncology JC with us.

A special thanks goes to Daniel Speiser and Petra Baumgärtner at the Ludwig Institute for Cancer Research in Lausanne, who hosted me for two weeks, showed me how to handle human T cell clones and answered all of my questions with great patience. I am also absolutely grateful to both Freddy and Hans-Christian Reinecker for giving me the unique opportunity to visit the Massachusetts General Hospital in Boston. A very special thanks goes to Christian and his lab members Yun, Guoxing, Shan, Pankaj and Tatsushi, who helped me to get the most out of four weeks, and thanks to them the project on the molecular mechanism of DC maturation evolved up to the current state!

I want to thank Sebastian Theurich and Michael von Bergwelt-Baildon for our fruitful collaboration on brentuximab and Alexander Dalpke for taking the time to discuss my project and giving valuable advice by sharing his expertise on DC signaling.

I am absolutely happy I had the chance to learn from and work with all the great people in our group! I learned a lot from Philipp, who supervised me and developed the project with me from the very beginning on; thank you for all your support! Also, without Greg I probably would not even have made it through the Master Thesis ;o) I want to especially thank Sébastien for his (not only) scientific support, the great help with the DC immunofluorescence and the hint on GEF-H1! I am thankful that Yvonne and Béa accompanied me from the beginning on, and especially Béa helped me with the first experiments and still works with me on the last ones. Thanks to Norbert for his invaluable technical advice and patience, to Mélanie for showing me how to handle the mice and for the nice company in the mouse house, to Narasimha for being the great person he is and for discussing with me whenever I needed scientific advice or simply clear my head.

The biggest **thank you** is for Petra, who shared so much time and so many conversations with me, is always there for me and helped me through the greatest troubles!!
I am also absolutely grateful for the critical reviews of this thesis. Daniela, Franziska, Jens, Sébastien, Philipp and Christiane, I am aware it takes some time and thank you for that!
I think I am lucky to be working in this group as we generally had a lot of fun and I made some true friends. Thanks also to Matthias, Michal, Reto and Vincent for the good times and endless coffees we had together.

GRACIAS para TODO, Seba. I would not have made it, at least not so smoothly, without the endless support of my family. Only because of them I am now standing here.